NUCLEAR MAGNETIC RESONANCE STUDIES of DYNAMIC COBALT and RHODIUM CLUSTERS in SOLUTION and in the SOLID STATE

by

Edward C. Lisic, II

Dissertation submitted to the Faculty of the
Virginia Polytechnic Institute and State University
in partial fulfillment of the requirements for the degree of
Doctor of Philosophy
in
Chemistry

APPROVED:

B. E. Hanson, Chairman

P. J. Harris

J. G. Dillard

M. Hudlicky

J. Mason

May 1986

Blacksburg, Virginia

MCR
10/30/86

NUCLEAR MAGNETIC RESONANCE STUDIES of DYNAMIC COBALT and RHODIUM CLUSTERS in SOLUTION and in the SOLID STATE

by

Edward C. Lisic II

B. E. Hanson, Chairman

Chemistry

(ABSTRACT)

The intramolecular carbonyl exchange which occurs in solution for the dinuclear and tetranuclear cobalt complexes containing the bisphosphines DPM, bis(diphenylphosphino)methane; DMPM, (dimethyl-diphenylphosphino)methane; and DMM, bis(dimethylphosphino)methane is very fast at temperatures down to -80°C. For the tetranuclear clusters $Co_4(CO)_8(DPM)_2$, $Co_4(CO)_8(DMPM)_2$, $Co_4(CO)_8(DMM)_2$, and $Rh_4(CO)_8(DPM)_2$, this exchange is slow at -80°C on the NMR time scale. The postulated mechanism for carbonyl exchange is based on a previously proposed mechanism, which is the expansion of the ligand icosahedron into a cubooctohedron. Because of the constraints imposed by the bisphosphine ligands, only one ligand icosahedron can be formed that is consistent with the known structure. Racemization of enantiomers by rotation of the ligands on the apical metal atom can occur, and thus enables complete carbonyl exchange to take place.

The series of binary metal carbonyls: $Co_2(CO)_8$, $Fe_3(CO)_{12}$, $Co_4(CO)_{12}$, $Co_3Rh(CO)_{12}$, $Co_2Rh_2(CO)_{12}$ and $Rh_4(CO)_{12}$, has been studied by variable temperature MAS (magic angle spinning) ^{13}C NMR spectroscopy. All of these mo-

lecules except for $Rh_4(CO)_{12}$ show dynamic behavior as evidenced by their solid state ^{13}C NMR spectra. Since carbonyl ligands cannot move within the crystalline lattice to an extent sufficient to render bridging and terminal carbonyls equivalent, then the dynamic behavior observed for the binary metal carbonyls must be described as metal atom movement within the carbonyl cage. The tetranuclear clusters which contain rhodium show a higher coalesence temperature in their NMR spectra than $Co_4(CO)_{12}$. As the rhodium content increases the activation energy for carbonyl exchange for exchange increases. cluster $Rh_4(CO)_{12}$ does not exhibit dynamic behavior in the solid state. It is concluded that the rhodium tetrahedron is too large to move within the carbonyl cage.

The cobalt "A-Frame" complexes $Co_2(CO)_3(DPM)_2I_2$, $Co_2(CO)_3(DMM)(DPM)I_2$, and $Co_2(CO)_3(DPM)_2S$ were synthesized but show no dynamic behavior in solution. The crystal structure of $Co_2(CO)_3(DMM)(DPM)I_2$ shows that this "A-Frame" complex is coordinatively saturated around the cobalt atoms. Thus, these molecules are relatively inert, and show no evidence of carbonyl scrambling.

ACKNOWLEDGEMENTS

I am pleased to thank Professor Brian E. Hanson for his contributions to this work. His direction and encouragement in my efforts have been invaluable and personally satisfying. I would also like to thank Professor Paul Harris for his continuing assistance and attention. Of the many others who have contributed to this work, I would especially like to thank my fellow graduate students, Logan Jackson, George Wagner, Dennis Taylor and Bill Bebout.

I am grateful to the National Science Foundation, the Jeffress Trust, and the Virginia Mining and Mineral Research Resource Institute for their financial support of this work.

TABLE OF CONTENTS

LIST OF ILLUSTRATIONS

LIST OF TABLES

INTRODUCTION

Dynamic rearrangements for a wide variety of compounds of organometallic complexes in solution are well documented and have been studied for over 20 years by NMR spectroscopy.[1] In this dissertation a discussion of solution vs solid state rearrangements of some metal carbonyls is presented. Most binary metal carbonyls have been investigated for ligand fluxionality in solution thus new information in this area must be obtained from the study of substituted metal carbonyls. Therefore this exploration will, of necessity, investigate new synthetic pathways to novel metal complexes, which will be examined by NMR techniques for clues to fluxional behavior. No method of analysis illustrates or even detects fluxionality of metal carbonyls as well as solution NMR spectroscopy. The availabilty of multinuclear FT-NMR instrumentation allows chemists to routinely observe ^{13}C, ^{1}H, and ^{31}P nuclei in metal complexes. The use of solution NMR to investigate fluxional rearrangement processes is therefore essential to this study.

In 1958, the first attempt to define the structure of a metal carbonyl molecule using ^{13}C NMR spectroscopy was reported.[2] This study found only a single signal for the carbonyl carbons in the molecule $Fe(CO)_5$ as a neat liquid at ambient temperature. From consideration of the trigonal bipyramidal structure of $Fe(CO)_5$, it would be expected that two carbonyl resonances should be seen (one for the axial carbonyls and one for the equatorial carbonyls in a ratio of 2:3). More recently[3] it has been shown that even at cold temperatures of 103°K only

a sharp singlet is seen in the ^{13}C NMR spectrum of $Fe(CO)_5$ Thus, the process of ligand site exchange, or fluxionality, is very rapid at 103°K and higher temperatures.

Sterochemical nonrigidity is generally observed for pentacoordinate compounds, such as PF_5 and $(CH_2)_4PF_3$, which show ligand exchange by a Berry pseudorotation mechanism as evidenced by ^{19}F NMR spectroscopy.[4,5] The use of variable temperature ^{31}P NMR spectroscopy in the study of dynamic processes was pioneered by Meakin and Jesson.[6] They show that many of the ML_5 (L = phosphine or phosphite ligands) complexes undergo intermolecular exchange via the Berry mechanism.

Intermolecular ligand exchange can also be seen by ^{31}P NMR spectroscopy. A ^{31}P NMR study of the phosphine-catalyzed cis-trans isomerization of four-coordinate platinum (II) complexes gave direct characterization of intermediates in solution and showed that the cis-trans isomerization of PtX_2L_2 catalyzed by L (phosphines) proceeds by rapid displacement of X^- by L followed by a slow displacement of L by X^- and not by pseudorotation of a five coordinate intermediate. The fastest process observed for both triphosphine complexes $[PtCl(PMe_3)_3]^+$ and $PtI_2(PMe_3)_3$ is intermolecular phosphine exchange.[7]

To date, most of the dynamic systems studied by ^{31}P NMR spectroscopy have involved metal complexes with monophosphine ligands; however, recently a number of studies using polydentate ligands have also been reported. Polyphosphine ligands provide advantages over monodentate ligands with comparable donor groups by reducing the rates of intramolecular exchange and by limiting the number of chemically reasonable pathways for the rearrangements. These

advantages were demonstrated by Wreford et al.[8] in studying the mechanism of intramolecular exchange in seven coordinate complexes of the type $XM(CO)_2(diphos)_2^+$.

Hanson[9] used the phosphine ligand DPM, bis(diphenylphosphino) methane ($Ph_2P\text{-}CH_2\text{-}PPh_2$), to form the cluster $Ru_3(CO)_{10}$DPM. The use of the bidentate ligand enabled a mechanism to be postulated for the observed dynamic process.

This dissertation will contain the results of a study of the dynamic processes in cobalt dimers and cobalt and rhodium tetranuclear clusters which contain the bidentate phosphines: DPM; DMPM, dimethyl diphenyl phosphino methane ($Me_2P\text{-}CH_2\text{-}PPh_2$); and DMM, bis(dimethyl phosphino) methane ($Me_2P\text{-}CH_2\text{-}PMe_2$). The synthesis and characterization of cobalt carbonyl phosphine complexes and clusters is particularly addressed in Chapters 1, 2 and 4. It was anticipated that the use of bridging phosphine ligands would restrict fluxional pathways for the carbonyl ligands in the dinuclear and tetranuclear metal carbonyl complexes of Co and the tetranuclear metal carbonyl clusters of Rh. Thus, from this study, conclusions about the validity of previously postulated mechanisms for carbonyl scrambling in tetranuclear clusters of Co and Rh are discussed in this dissertation.

Magic angle spinning (MAS) NMR techniques have only recently become available for the investigation of dynamic processes in the solid state. Thus the use of magic angle spinning NMR techniques could reveal mechanisms for the fluxionality of metal carbonyl complexes in the solid state.

The use of solid state ^{13}C NMR spectroscopy to study metal carbonyls may be important in understanding the bonding and potential energy surfaces of metal

carbonyls which are themselves important in heterogeneous and homogeneous catalysis. The study of intramolecular and intermolecular CO exchange may serve, to some extent, to model the problem of CO mobility on metal surfaces. It has also been postulated that dynamic processes may dramatically affect the reactivity of some metal carbonyl catalysts.[10]

The second section of this work presented in Chapter 4 deals with the variable temperature ^{13}C NMR spectra of binary metal carbonyls in the solid state with an emphasis on cobalt and rhodium carbonyls, including some mixed metal clusters. The solid state ^{13}C NMR data for these clusters will be compared to the solution ^{13}C NMR data when available.

The problem of fluxionality for metal carbonyls in the solid state has received little attention in the literature except for $Fe_3(CO)_{12}$[11] and $Co_2(CO)_8$.[12]

CHAPTER 1. SYNTHESIS AND CHARACTERISTICS OF COBALT CARBONYL BINUCLEAR COMPLEXES

Historical

The chemistry of organocobalt compounds is very extensive and the organometallic chemistry for oxidation states from -1 to +4 is well established. Cobalt has a valence shell electron configuration of $(3d)^7$ $(4s)^2$ and, since it has an odd number of electrons, a consequence of the 18-electron rule is that compounds with even numbered oxidation states, such as Co°, are either paramagnetic, or polynuclear with metal-metal bonds. Typical of these are the two principal homoleptic carbonyls of cobalt, $Co_2(CO)_8$, and $Co_4(CO)_{12}$, which were the first organocobalt compounds to be prepared and characterized.[13] Dicobalt octacarbonyl is now of major economic importance: over 25,000 tons are employed per annum in hydroformylation synthesis.[14]

In the hydroformylation of alkenes, the use of phosphine modified cobalt catalysts, such as $[Co_2(CO)_6(PBu_3)_2]$, has been studied in detail.[15] This is due to the fact that the phosphine ligand can enhance the formation of straight chain products in hydroformylation of alkenes. The use of different alkyl and aryl tertiary phosphines, as well as amines and arsines, as ligands on cobalt carbonyls gives rise to an area of chemistry dealing with ligand substitution of cobalt carbonyls, especially the dinuclear complex, $Co_2(CO)_8$. The substitution chemistry of $Co_2(CO)_8$ has been studied with almost all phosphines that are available.

The use of bidentate or multidentate phosphines as ligands in cobalt carbonyl chemistry has developed slowly. In 1974 the synthesis of complexes of the type $Co_2(CO)_6[(R_2E)_2CH_2]$ (R = C_6H_5 ; E = Sb, As, P) was published.[16] Of interest was the fact that the methylene protons and the methyl protons in the complexes were expected to be stereochemically nonequivalent in the proposed structures but the ^1H NMR of the complexes containing $R_2Sb\text{-}CH_2\text{-}SbR_2$ (R = CH_3,p-$CH_3C_6H_4$) show only a single resonance which is unchanged even at temperatures down to -50°C. This implied that a fluxional process was taking place making the protons equivalent. However, the authors did not record the ^{13}C NMR spectrum of the cobalt carbonyl dimers to determine if carbonyl exchange was occurring. Since 1974 there have been only a few examples of $Co_2(CO)_6$(L-L) complexes in the literature.[17] Apart from the reactions of $Co_2(CO)_6$(L-L) with alkynes little of the chemistry of linked cobalt dimers had been investigated prior to 1982.

The impetus of the work in the first section of this dissertation is on the expansion of the chemistry of linked cobalt dimers. Synthetic methods for the synthesis of other bis phosphines besides DPM containing the (P-CH_2-P) moiety exist in the literature.[18] Comparison of these ligands with DPM in cobalt complexes was one of the original goals and is presented in this work. The study of cobalt carbonyl dimers linked by bridging bis phosphine ligands is not a random one. The use of DPM to form a strong stable bridge to link binuclear complexes is fast becoming a special area in organometallic and inorganic chemistry.

Even though DPM reacts with $Mo(CO)_6$, $Cr(CO)_6$ and $W(CO)_6$ to form chelated complexes of the type $M(CO)_4$DPM,[19] it does not tend to form chelated

complexes with most of the other transition metals that have been studied. In fact the tendency of DPM is to form bridged binuclear complexes. An up-to-date survey of the chemical literature on the subject shows that binuclear complexes can be synthesized with DPM containing the metals; Au-Au,[20] Pd-Pd,[21] Pt-Pt,[22] Co-Co,[16] Rh-Rh,[23] Ir-Ir, Fe-Fe,[24] Ru-Ru,[25] Mn-Mn,[26] Re-Re,[27] Cr-Cr,[28] Mo-Mo,[29] V-V,[30] and Nb-Nb.[31] These binuclear metal complexes may or may not contain a metal-metal bond, however, the tendency for most of these complexes is to have a metal-metal bond interaction.

The phosphine DMM, bis (dimethyl phosphino) methane, became available only as recently as 1977, but there are problems in the reported synthesis.[32] The synthesis involves forming $Cl_2P\text{-}CH_2\text{-}PCl_2$ from PCl_3 and Al in CH_2Cl_2, and is shown in equation 1.

$$PCl_3 + CH_2Cl_2 + Al_s \rightarrow 50\%\ Cl_2P - CH_2 - PCl_2 + AlCl_3 \quad . \qquad (1)$$

Once formed and isolated, $Cl_2P\text{-}CH_2\text{-}PCl_2$ will undergo a Grignard reaction with MeMgCl to give $Me_2P\text{-}CH_2\text{-}PMe_2$. Problems with this synthesis of DMM, however, forced us to abandon this procedure and to utilize another synthetic pathway. The Russian publication claims that an aluminum intermediate, with the formula $Cl_2Al\text{-}CH_2\text{-}AlCl_2$, forms $Cl_2P\text{-}CH_2\text{-}PCl_2$. This has since been proven to be untrue[33]; however, the actual synthesis except for this does work as described.

An alternate synthesis of DMM [18] was established by Karsch and co-workers also in 1977; this synthetic route is much cleaner and gives a product of greater purity as well as in better yield. This synthesis route can be seen in the following equations.

PMe_3 + tert-butyl Li → $Me_2P\text{-}CH_2^-Li^+$

$Me_2P\text{-}CH_2\text{-}Li^+ + Cl\text{-}PR_2 \rightarrow Me_2P\text{-}CH_2\text{-}PR_2 + LiCl$

The synthesis of not only DMM but also of other bis phosphinomethanes is possible with this synthetic route. The synthesis of the phosphine DMPM, (dimethyldiphenylphosphinomethane), is easily accomplished and this ligand is interesting for the study of fluxional processes because it is unsymmetrical. The synthesis of the three bis phosphines DPM, DMPM, and DMM are described in the experimental section of this chapter.

Since the crystal structure of $Co_2(CO)_6$DPM has never been obtained, the detailed structure is not known, however, it probably adopts a structure similar to that seen in the crystal structure of the bis arsine cobalt dimer, ($Co_2(CO)_6(C_4F_4(AsMe_2)_2)$).[34] This is in contrast to the non-bridged structure observed for the cobalt dimers $Co_2(CO)_6(PPh_3)_2$ and $Co_2(CO)_6(P\text{-}nBu_3)_2$. Structural representations of $Co_2(CO)_6(Ph_3)_2$ and $Co_2(CO)_6$(DPM) are shown below.

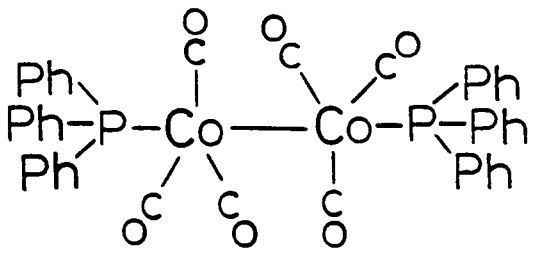

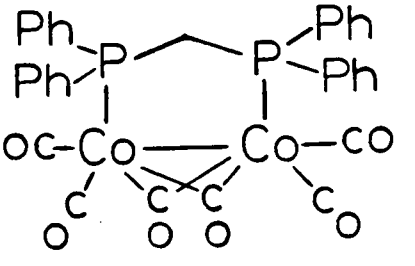

The cobalt dimer $Co_2(CO)_6(PPh_3)_2$, which has no bridging ligands, is very likely to form mononuclear products when it undergoes a chemical reaction in solution. The effect of DPM in $Co_2(CO)_6$DPM is to form a more stable metal dimer which resists the cleavage of its cobalt-cobalt metal bond. Thus, chemistry of the cobalt-cobalt metal bond can be studied under more rigorous environments than in cobalt dimers without bridging ligands. The first reactions reported for $Co_2(CO)_6$L-L molecules, including $Co_2(CO)_6$DPM were with unsaturated organic molecules such as acetylene, diphenylacetylene, etc.[35] The original goals were that a catalytic activity with these reagents might be found, however, only mono-substituted complexes were formed.

Until 1982, no other reports of the chemistry of $Co_2(CO)_6$DPM appeared in the literature. Since 1982 there have been some derivatives of $Co_2(CO)_6$DPM reported. It has been reported [36]that $Co_2(CO)_6$DPM is a somewhat worse hydroformylation catalyst than $Co_2(CO)_8$ and worse than $Co_2(CO)_6$ $[P(t\text{-butyl})_3]_2$. This is probably due to the fact that the dimer is more stable to disruption of the metal-metal bond. The reaction of $Co_2(CO)_6$DPM with molecular hydrogen at high pressure and temperature forms the oxidative addition product, $Co_2(CO)_4(\mu\text{-H})(\mu\text{-PPh}_2)$DPM, by destroying some $Co_2(CO)_6$DPM and scavenging DPM for the $(\mu\text{-PPh}_2)$ group.[37] (The scission of P-Ph bonds has been seen in other cobalt carbonyls under these type of conditions.) Other reports of fluxionality [38] in derivatives of $Co_2(CO)_6$DPM and of the unique ability of this molecule to undergo a substitution reaction with diazomethane replacing a bridging carbonyl,[39] have given reasons why interest is warranted in these type of complexes beyond hydroformylation or OXO chemistries.

In this chapter is discussed the synthesis, characteristics, and solution dynamics of the series of compounds $Co_2(CO)_6$(DPM), **1**, $Co_2(CO)_6$(DMPM), **2** and $Co_2(CO)_6$(DMM), **3**, DMM = bis(dimethylphosphine) methane, DMPM = -(dimethyl, diphenylphosphino) methane. These are shown schematically below.

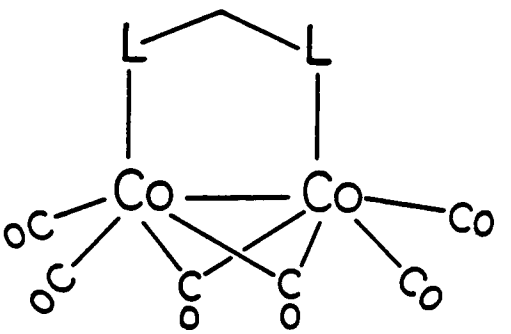

1 L^L = DPM

2 L^L = DMPM

3 L^L = DMM

Experimental

All reactions were performed under an atmosphere of dry nitrogen. Solvents were either distilled or dried over molecular sieves and purged with N_2 before use. Dicobalt octacarbonyl (STREMCHEMICALS) was purified by sublimation and used immediately. The reactions forming cobalt phosphine dimers were followed by solution infrared spectroscopy until reaction was complete (as seen by the disappearance of the band at 1890 cm^{-1} due to $Co(CO)_4$-.

Proton NMR Spectra were recorded on a Varian EM390 spectrometer. Carbon-13 and Phosphorus-31 NMR spectra were recorded on either a JEOL FX200, an IBM WP270 or an IBM WP200 NMR spectrometer. Variable temperature ^{13}C NMR spectra were recorded on an IBM WP200 NMR spectrometer

on samples enriched in ^{13}CO. All enriched compounds were synthesized from $Co_2(CO)_8$ enriched to 15% in ^{13}CO by stirring in a pentane solution of the compound under an atomsphere of 95% ^{13}CO in the presence of small amounts of Pd/C (typically 2.5mg Pd/C per gram of dicobalt octacarbonyl.

All NMR solvents were degassed prior to use. Chemical shifts in ppm are reported from TMS which was an internal standard (^1H and ^{13}C NMR spectra) or 85% aqueous H_3PO_4which was an external standard (^{31}P NMR spectra).

Infrared specta were recorded on a Perkin Elmer Infrared Spectrometer.

DPM, (Ph_2P-CH_2-PPH_2). A three-necked 500 ml flask equipped with a vacuum stopcock and an addition funnel was charged with 300 ml of liquid ammonia and placed in a dry ice/acetone bath. Small freshly cut pieces of Na metal were added to the liquid ammonia, while the flask was slowly purged with N_2, and the mixture was stirred magnetically until the Na had completely dissolved. Triphenylphosphine powder, 26 grams (0.099 moles) was added to the reaction mixture. This formed the red-orange solution of diphenyl phosphide anion. The mixture was allowed to stir for an hour. Then ammonium bromide 9.8 grams (0.100 moles) was added to the mixture and stirring was continued for an additional hour. This was followed by the dropwise addition of 3.17 ml of CH_2Cl_2 in 15 ml of diethyl ether, over a 2 hour period. This reacts to form the product DPM, bis(diphenylphosphino)methane, which is a white powder. The ammonia was then evaporated from the reaction mixture by a fast stream of dry N_2 to leave the crude product which was stored under N_2 gas. The product was recrystallized using quantities of absolute ethanol. The product DPM is a white, crystalline powder which has a melting point of 119° C. Yield 60-70%.

PMe_3. To a three-necked 1 liter flask equipped with a 1000 ml addition funnel, a sealed mechanical stirrer, and a dry ice condenser, was added 1/3 mole (45.8 g) of PCl_3 and 350 ml of anhydrous ether. The outlet of the dry-ice condensor lead to a trap containing 300 ml of a saturated KI solution which was 1.1M in AgI to prevent any loss of PMe_3. The flask was cooled to -78°C with a dry-ice acetone bath, and under a dry N_2 purge, 1 mole of a 2.2M ethereal solution of CH_3Li was added over an hour to the stirred PCl_3 solution. After addition of the CH_3Li, the reaction flask was then allowed to slowly warm to 0°C, and 300 ml of H_20 was added carefully to dissolve the white precipitate of LiCl. The water-ether mixture was separated and the water layer was removed via a stopcock on the bottom of the three-necked flask. The 300 ml of KI-AgI solution was then added to the ethereal solution. This was agitated vigorously and the white precipitate of $[AgIP(CH_3)_3]_4$ was produced. This precipitate was collected by filtration and washed with a total of 350 ml of saturated KI solution, 600 ml of H_20 and 350 ml of ether. The product was dried under vacuum at room temperature. Yield $\cong$ 60 grams. To generate free PMe_3 a 250 ml flask was charged with 22 g of the $[AgIP(CH_3)_3]_4$ and a magnetic stirring bar. The flask was equipped with a small distillation head which was connected to a trap to capture the distilled PMe_3. The flask was lowered into a silicon oil bath preheated to 250°C. The system was evacuated to approximately 1 torr and the PMe_3 trap was cooled by liquid nitrogen to -196°C. After an hour, 5 grams of pure trimethylphosphine was collected.

$(CH_3)_2P\text{-}CH_2^-Li^+$. A 200 ml flask was charged with 10 ml of distilled pentane. Then 5 grams of trimethyl phosphine (0.0657 moles) diluted with 5 mls of pentane was added to the flask. A 40 ml solution of 1.7 M tert-butyl lithium in pentane was added dropwise to the trimethyl phosphine solution over a 15 minute period. Very little heat was evolved. After 24 hours of stirring the precipitate was collected under N_2, and washed with 10 ml of dry oxygen free pentane. The precipitate was dried under vacuum at 50°C. Yield, 4.7 g ,90%.

DMM, ($Me_2P\text{-}CH_2\text{-}PMe_2$). A 100 ml flask was charged with 2.2 grams of lithiated trimethylphosphine under N_2 and 40 ml of dry ether. The resulting slurry was cooled to 0°C with an ice water bath. A solution of 2.6 grams of $(CH_3)_2PCl$ in 10 ml of pentane was then added dropwise to the slurry over a period of 10 minutes. The reaction mixture was then allowed to warm to room temperature and was stirred for an hour at that temperature. The solution was then filtered and the ether distilled off to give the bis phosphine DMM in raw form. The phosphine can be purified by distillation at 42°C at 0.2 torr. Yield (2.4 ml)$\cong$90%.

DMPM ($Ph_2P\text{-}CH_2\text{-}PMe_2$). A 100 ml flask containing a magnetic stir bar was charged with 0.56 g of Me_2PCH_2Li (6.8×10^{-3} moles). This was slurried in 10 ml freshly distilled diethyl ether and cooled in an ice/salt bath to -2°C. Dropwise addition of 1.08 ml diphenylchlorophosphine (1.33 gr, 6.8×10^{-3} moles) in 10 ml of ether resulted in the formation of LiCl. When addition was complete the reaction mixture was allowed to warm to room temperature and stirring was continued for an additional hour. The yellow solution was filtered and solvent

was removed to give the bis phosphine DMPM in raw form. The phosphine can be purified by distillation at 130°C at 0.2 torr. Yield(2.2 ml) ≅ 50%.

$Co_2(CO)_6$DPM, 1. A solution of $Co_2(CO)_8$ (3g, 8.8 × 10^{-3} mol) was prepared in 20ml of CH_2Cl_2. In a separate flask 3.4g (8.8 x 10^{-3} mol) of DPM was dissolved in 20 ml of CH_2Cl_2 and then transferred dropwise via syringe to the solution of $Co_2(CO)_8$. After evolution of CO had ceased, the reaction mixture was allowed to stir for 30 hours. The solution was filtered under N_2 and the product obtained as an orange-red, crystalline, air stable solid upon addition of hexane at -78°C. Yield 5g (80%) Anal. Calcd. for $C_{31}H_{22}Co_2O_6P_2$: C, 55.6; H, 3.29 Found: C, 55.4 H, 3.20.

$Co_2(CO)_6$(DMPM),2. A solution of $Co_2(CO)_8$ (2.5g, 7.3 × 10^{-3} mol) was prepared in CH_2Cl_2. In a separate flask a 15ml solution of DMPM (1.95g, 7.5 × 10^{-3} mol) in CH_2Cl_2 was prepared and added dropwise via syringe to the $Co_2(CO)_8$ solution. After addition the reaction mixture was allowed to stir for 4 days at which time the reaction was complete. The solution was filtered under N_2 and the product obtained as an orange brown, crystalline, slightly air sensitive solid upon addition hexane at -78°C. Yield 2g (51%). Anal. Calcd. for $C_{21}H_{18}Co_2O_6P_2$: C, 46.18; H, 3.32; P, 11.34; O, 17.56 Found: C, 45.94; H, 3.36; P, 11.47; O, 17.58.

$Co_2(CO)_6$DMM,3. A CH_2Cl_2 solution of DMM (5ml, 0.33g, 2.4 × 10^{-3} mol) was added dropwise to a 10ml solution of $Co_2(CO)_8$ When the addition was complete the mixture was allowed to stir for 8 days. This was filtered and addition of hexane at -78°C gave the product as an orange, needlelike crystalline, air

stable solid. Yield 0.73 g (72%). Anal. Calcd. for $C_{11}H_{14}Co_2O_6P_2$: C, 31.4; H, 3.32; P, 15.2; 0, 22.8; Found: C, 30.98; H, 3.46; P, 14.4; 0, 27.7.

Results and Discussion

Synthesis

It is well known that the reaction of certain phosphine and phosphite ligands with dicobalt octacarbonyl leads to rapid disproportionation.[40] Very bulky phosphines and arsine ligands react more slowly by a dissociative pathway to yield neutral dimers $Co_2(CO)_6L_2$ directly.[41] In the case of the ditertiary phosphines the addition of L-L to $Co_2(CO)_8$ gives the salt $[Co(CO)_3L\text{-}L]^+[Co(CO)_4]^-$ according to equation (4).

$$Co_2(CO)_8 + L - L \rightarrow [Co(CO)_3L - L][Co(CO)_4] \quad (4)$$

This reaction is rapid and is over in a matter of minutes as indicated by infrared spectroscopy analysis which shows the characteristic band at 1890 cm^{-1}due to the cobalt tetracarbonyl anion, $[Co(CO)_4]^-$ The reaction to form the neutral dimers, according to equation 5 is much slower, again as monitored by infrared spectroscopy of the reaction mixture, which shows the decrease of the carbonyl stretching frequency at 1890 cm^{-1} and an increase in the bridging carbonyl stretching frequencies of the dimers, which are listed in Table I.

$$[Co(CO)_3R_2P - CH_2 - PR_2]^+[Co(CO)_4]^- \rightarrow Co_2(CO)_6(R_2P - CH_2 - PR_2) + CO \quad (5)$$

With the bulky bis phosphine, DPM, the neutral dimer is seen to form quite rapidly so that it is not possible to rule out some substitution by a dissociative pathway for DPM.[41] For the ligands DPM, DMPM, and DMM, the approximate half lives for reaction with $Co_2(CO)_8$ to yield $Co_2(CO)_6$(L-L) are 5 hours, 1 day, and 4 days, respectively. As a general rule, bulky substituents on the bis phosphine favor small-ring formation,[28 42 43] and it is therefore expected that the intermediate chelate complex should be more stable when DPM is used than DMM. However, in the synthesis of $Co_2(CO)_6$L-L the ligands DMPM and especially DMM stabilize the intermediate salt. This is reasonable due to the increased basicity of these ligands. With bis(dimethyl-phosphino)methane it is possible to isolate $[Co(CO)_3DMM]^+[Co(CO)_4]^-$ as a purple crystalline solid. Although reasonably pure when first isolated, the salt slowly converts to the corresponding neutral dimer even in the solid state.

The infrared spectra of **1**, and **2**, are consistent with the number of allowed infrared bands for molecules of C_2v point group symmetry. Extra bands in **3** are due to the lower symmetry when the unsymmetrical DMPM ligand is present. The carbonyl stretching frequencies have a tendency towards lower wave number when the more basic ligands DMPM and especially DMM are present in the complex. This is consistent in that a more basic phosphine such as DMM places more electron density on the cobalt dimer which responds by backbonding more

Table I. Carbonyl Stretching Frequencies. (a)

	Terminal				Bridging	
INFRARED SPECTRA were recorded in CH_2Cl_2						
$Co_2(CO)_6DPM$	2040m,	2000s,	1984vs,		1820m,	1795m
$Co_2(CO)_6DMPM$	2040m,	2000s,	1982vs,	1960s	1815m,	1777m
$Co_2(CO)_6DMM$	2025m,	1998s,	1978vs,		1813m,	1775m
INFRARED SPECTRA were recorded in a Nujol Mull						
	Terminal				Bridging	
$Co_2(CO)_6DPM$	2042m,	2000vs,	1989vs,	1975vs,	1812m,	1799s
$Co_2(CO)_6DMPM$	2042m,	2010vs,	1990vs,	1975vs,	1810m,	1787s
$Co_2(CO)_6DMM$	2035m,	1993vs,	1976vs,	1950vs,	1805m,	1769s

(a) in cm^{-1}

Table II. ^{1}H, ^{31}P, NMR Data.

	^{1}H NMR (a)		
	φ	CH_2	CH_3
$Co_2(CO)_6DPM$	7.5 (m)	3.15 (t,10.1 Hz)	--
$Co_2(CO)_6DMPM$	7.37 (m)	2.25 (t, 9 Hz)	1.40 (d, 3.6 Hz)
$Co_2(CO)_6DMM$	--	1.77 (d, 13 Hz)	1.59 (t, 3.5 Hz)
	^{31}P NMR (b)		
	$-P\varphi_2$		$-PMe_2$
$Co_2(CO)_6DPM$	60.39		--
$Co_2(CO)_6DMPM$	60.18 (d, 210 Hz)		37.83 (d, 210 Hz)
$Co_2(CO)_6DMM$	--		39.42

(a) chemical shifts from TMS in ppm
(b) chemical shifts from 85% phosphoric acid (ext. ref.)

Table III. Coordinative Chemical Shifts. (a)

	γ_c	γ_1	γ_{ccs}
$Co_2(CO)_6DPM$	60.39	-23.0	83.39
$Co_2(CO)_6DMPM$	60.18 (b) and 37.88 (c)	-21.7 (b) and -52.6 (c)	81.88 (b) and 90.43 (c)
$Co_2(CO)_6DMM$	39.42	-55.7	95.12

(a) chemical shifts in ppm from 85% phosphoric acid (ext. ref.)
(b) reported for the diphenylphosphine portion of the DMPM ligand
(c) reported for the dimethylphosphine portion of the DMPM ligand

with the carbonyl ligands. This can be seen by the infrared stretching frequencies moving to a lower frequency, indicating a lessening of the CO bond order.

The ^{1}H NMR spectra of **1**, **2**, and **3** show this overall trend also, as can be seen in Table II. The methylene (CH_2) protons are shifted downfield when the more basic methyl phosphines are present in the metal dimer. The ^{31}P NMR spectra of **1**, **2**, and **3** show in more dramatic form the chemical character of phosphorus in these dimers. The ^{31}P NMR spectrum of **1** is a broad singlet at 60.39 ppm. This indicates that the two phosphorus nuclei are equivalent in **1** in solution, just as the free DPM ligand has phosphorus nuclei that are equivalent in solution as seen by ^{31}P NMR spectroscopy (see Table II). A large chemical shift occurs when DPM binds to $Co_2(CO)_8$ to form compound **1**. This can be assigned a mathematical expression and a definite value can be derived for this "coordinative chemical shift". This expression is given by the equation; (γc - γl) = γccs, where all γ are in parts per million in chemical shift.[44] These have been calculated and are compared in Table III for the cobalt dimers. This data indicates that the phosphine DMM is affected more by complexation than DPM, possibly because of its more basic nature. However, the effect of complexation on the ligands studied seems to be relatively the same, as evidenced by the small relative difference in the coordinative chemical shifts for these ligands.

The complex **2**, containing the unsymmetrical bisphosphine DMPM, has a ^{31}P NMR spectrum showing the chemical shifts of the two different phosphorus nuclei, which are approximately where they were predicted to be from the comparison of the ^{31}P NMR spectra of compounds **1** and **3**. Of interest is the fact

that a large coupling (d, 210 Hz) occurs between these two phosphorus nuclei through the bridging methylene group.

Figure 1 shows the variable temperature ^{13}C NMR spectrum of **1** in methylene chloride solution. As can be seen, only a single resonance at 216.24 ppm is observed at 24°C consistent with a rapid dynamic process which scrambles bridging and terminal carbonyls. The carbonyl signal is very sharp indicating that the process is at the fast exchange limit. As the temperature is decreased to -60 °C, the signal broadens, and at -90°C the signal splits into two resonances, a small signal at 236.91 ppm which is in the bridging carbonyl region, and a larger signal at 212.61 ppm which is in the terminal carbonyl region. However, these signals do not integrate exactly to 1:3 as expected for this molecule in a static condition, as the temperature is not cold enough to completely freeze out the dynamic process on the NMR time scale. With the spectrometer and the solvent system employed, temperatures lower than -90°C are not possible. Therefore, since the slow exchange limit is not reached, a reasonable mechanism for the fluxionality of these cobalt carbonyl dimers can not be postulated at. It is reasonable to assume that the dynamic process may be similar to that ascribed for $Co_2(CO)_8$. Of interest is the fact that the bis-phosphine, DPM, does slow down the fluxional process in cobalt carbonyl. Evidence can be obtained from the variable temperature ^{13}C NMR spectra of the dimer $Co_2(CO)_6$DPM that shows that the carbonyl exchange is slow at -90°C, whereas $Co_2(CO)_8$ shows only a single resonance at temperatures even lower than -90°C. Thus, the dynamic process has been hindered by the bis phosphine ligands. The dimers **2** and **3** also

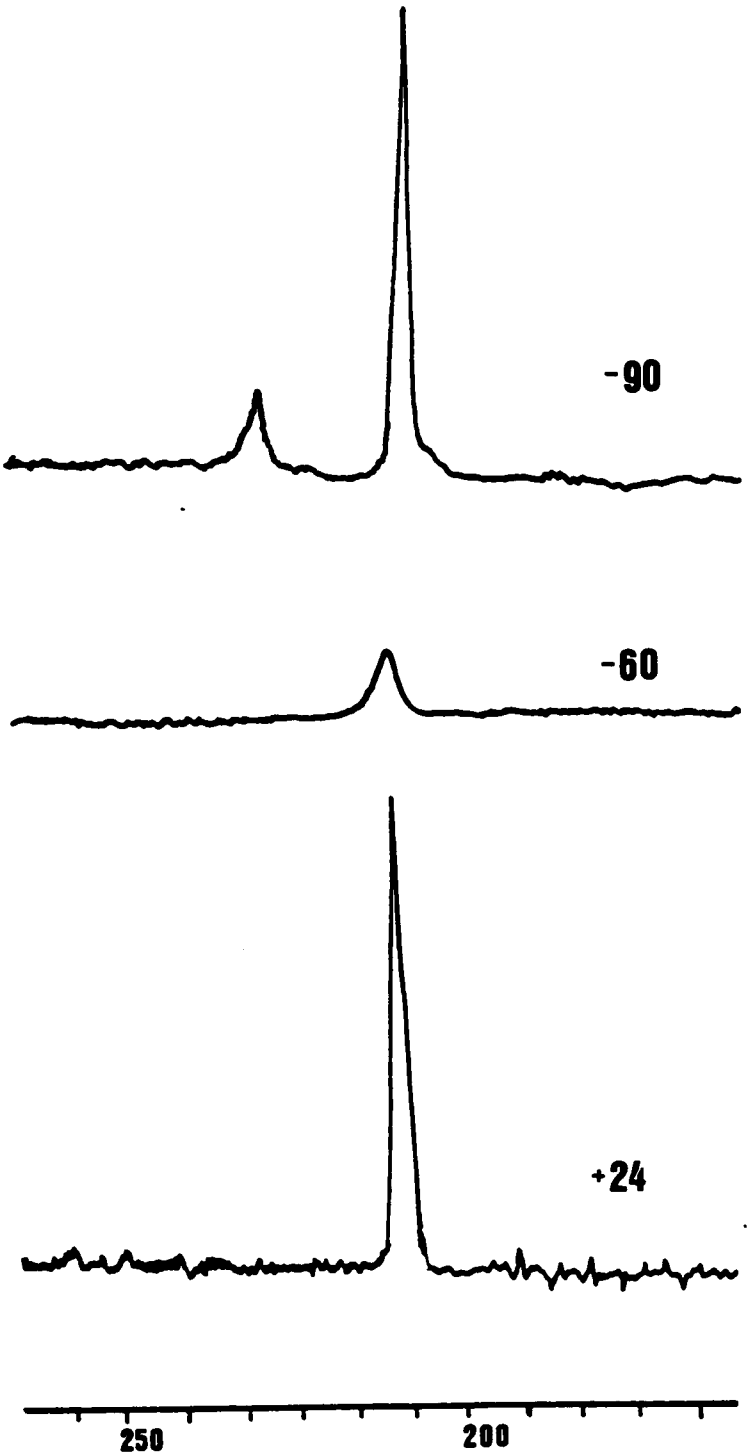

Figure 1. Variable temperature ^{13}C NMR spectra for $Co_2(CO)_6DPM$: The solvent is CD_2Cl_2, the chemical shifts are from TMS. At ambient temperature all carbonyls are equivalent. At -90°C signals corresponding to bridging and terminal carbonyls are seen; however, bridge-terminal exchange has not been completely frozen.

show only a single ^{13}C resonance down to -60°C. This was the lowest temperature reached for these molecules.

Another primary goal of synthesizing the cobalt dimers **1**, **2**, and **3** was to use them in a planned synthesis of cobalt tetranuclear complexes. The cobalt dimers **1**, **2**, and **3** also are used to form cobalt "A-Frame" complexes which are discussed in Chapter 4. The synthesis and a detailed discussion of the dynamic behavior of cobalt and rhodium tetranuclear clusters which contain the DPM ligand is found in the next chapter. It should be noted, in conclusion of this chapter, that the molecule $Co_2(CO)_6DPM$, **1**, is of prime importance in every chapter of this dissertation.

CHAPTER 2. COBALT AND RHODIUM TETRANUCLEAR CLUSTERS CONTAINING DPM, DMPM, AND DMM

At the time of discovery of $Co_2(CO)_8$, the simultaneous discovery of $Co_4(CO)_{12}$ was made and a close relationship exists between the two metal carbonyls. It is known that $Co_2(CO)_8$ slowly decomposes at ambient temperature to give $Co_4(CO)_{12}$. An efficient synthesis of $Co_4(CO)_{12}$, involves simply heating a THF or toluene solution of $Co_2(CO)_8$ to 60-70°C which yields the product $Co_4(CO)_{12}$. Thus it was natural to expect that heating the cobalt carbonyl phosphine dimers (1, 2 and 3) would yield the corresponding tetrameric cobalt carbonyls with a molecular formula of $Co_4(CO)_8(L\text{-}L)_2$.This is shown in equation 6 where L-L = DPM, L-L = DMPM, L-L = DMM.

$$2Co_2(CO)_8(L - L) \rightarrow Co_4(CO)_8(L - L)_2 + 4CO \qquad (6)$$

The red colored cobalt dimers form the black tetranuclear clusters very slowly at 60°C in solution, but at 100°C tetramer formation is fast and goes to completion in about 6 hours. This reaction is best followed by solution ^{31}P NMR spectroscopy which indicates the disappearance of the phosphine containing dimer and appearance of the phosphine containing tetramer. The chemical shifts of these tetramers, which were used for identification purposes, are listed in Table IV.

The authors of the first reports[45] of the cobalt tetramer $Co_4(CO)_8DPM_2$ identified this molecule from the close resemblance of the infrared carbonyl stretching frequencies of this molecule with that of $Rh_4(CO)_8DPM_2$. The original

Table IV. ^{31}P and ^{13}C NMR Data.

	^{31}P NMR(a)	
	$-P\varphi_2$	PMe_2
$Co_4(CO)_8(DPM)_2$	24.29	--
$Co_4(CO)_8(DMPM)_2$	20.66 27.23 (~1)b 20.0 (~6)b	7.59 (br,s) 14.75 (~2)b 7.50 (~5)b
$Co_4(CO)_8(DMM)_2$		11.80 (br, s) 12.15 (~3)b 11.10 (~1)b
	^{13}C NMR (c)	
$Co_4(CO)_8(DPM)_2$(d)	260.1, 258.2	206.9, 203.2, 201.7
$Co_4(CO)_8(DMPM)2$(d)	260.5, 259.8, 259.4, 258.1, 250.7, 250.0	210.0, 208.5, 203.8, 203.1, 201.3
$Co_4(CO)_8(DMM)_2$(d)	258.7, 249.9	199.4, 197.7

(a) chemical shifts from 85% phosphoric acid
(b) number in parenthesis refers to relative intensity
(c) chemicals shifts from TMS
(d) recorded at -80°C

synthesis of $Co_4(CO)_8DPM_2$ and $Rh_4(CO)_8DPM_2$ involved direct substitution of the dodecacarbonyls.[46] This is shown in equation 7. Infrared stretching frequencies for the cobalt clusters are given in Table V.

$$M_4(CO)_{12} + 2DPM \rightarrow \quad \text{(7)}$$

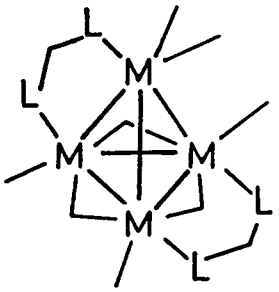

The rhodium tetramer, $Rh_4(CO)_8DPM_2$, was completely characterized by x-ray crystallography [46] and exhibits the structure shown in equation 7, which contains two bridging bidentate DPM ligands with a phosphorus atom bonded to each rhodium atom, three bridging carbonyls which lie in a basal plane of rhodium atoms, and an apical rhodium atom which contains only terminally bonded ligands.

The molecule, $Co_4(CO)_8DPM_2$, can also be directly synthesized in the manner of $Rh_4(CO)_8DPM_2$. However, the direct synthesis of $Co_4(CO)_8DPM_2$ also produces an impurity as indicated by the infrared spectrum of the isolated product, $Co_4(CO)_8DPM_2$. One impurity seems to be some form of $Co(CO)_4^-$, because it has an absorption band at 1890 cm^{-1}, which is characteristic of $Co(CO)_4^-$. Thus, the synthesis of $Co_4(CO)_8$ $(L\text{-}L)_2$ clusters developed in this study (equation 6) to yield the new series of compounds, $Co_4(CO)_8DPM_2$(4), $Co_4(CO)_8DMPM_2$(5), and $Co_4(CO)_8DMM_2$(6), is much cleaner than the previously reported synthesis (equation 7).

Table V. Carbonyl Stretching Frequencies. (a)

	Terminal	Bridging
INFRARED SPECTRA were recorded in CH_2Cl_2		
$Co_4(CO)_8(DPM)_2$	2010s, 1980vs, 1960s,	1828m, 1785s, 1770s
$Co_4(CO)_8(DMPM)_2$	2010s, 1985vs, 1955s,	1819m, 1790s, 1750m
$Co_4(CO)_8(DMM)_2$	2002s, 1969s, 1950s,	1820w, 1773s, 1760s
INFRARED SPECTRA were recorded in a Nujol Mull		
	Terminal	Bridging
$Co_4(CO)_8(DPM)_2$	2006s, 1970s, 1954vs, 1941s, 1915m,	1823m, 1780s, 1760s
$Co_4(CO)_8(DMDM)_2$	1994m, 1955vs, 1944s, 1932s,	1807m, 1770s, 1735s
$Co_4(CO)_8(DMM)_2$	1987m, 1959s, 1944vs, 1928s, 1921s,	1807m, 1771s, 1732s

(a) in cm^{-1}

Recently, the synthesis of the iridium analogue of **4** has been accomplished,[47] also by the synthesis shown in equation 7, and the schematic representation of this molecule along with the corresponding Co and Rh tetranuclear clusters are shown below:

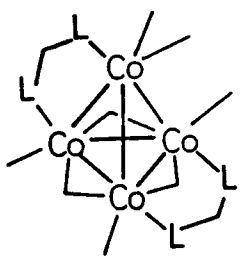

$Co_4(CO)_8DPM_2$

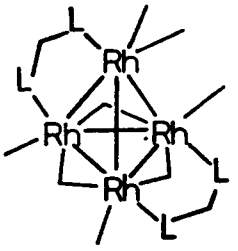

$Rh_4(CO)_8DPM_2$

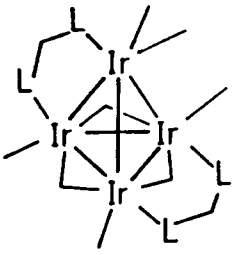

$Ir_4(CO)_8DPM_2$

This series of molecules is noteworthy in its completeness. Remarkably, when $Ir_4(CO)_{12}$, which has only terminal CO ligands, reacts with phosphine ligands to give substituted clusters, the structure exhibiting three bridging carbonyl ligands is sometimes preferred and adopted. Indeed, phosphines seem to lower the activation energy for carbonyl exchange between bridging and terminal ligands in these iridium clusters.[48]

In early studies it was shown that the tetranuclear clusters $Co_4(CO)_{12}$[49] and $Rh_4(CO)_{12}$ were fluxional in solution.[50] The fluxional behavior of these type of tetranuclear clusters is of importance in understanding the reactivity of these clusters which may be influenced by this behavior.

Experimental

Cobalt Tetramers

Approximately 0.5g of one of the cobalt dimers (**1**, **2**, or **3**) was dissolved in 30ml toluene. The solution was then heated to 110°C for 12 hours. The black solution was then filtered and concentrated. When cooled below O°C overnight the product is obtained as the pure black crystalline solid.

$Co_4(CO)_8DPM_2$, 4. Yield 0.38 g (86%) Anal. Calcd. for $C_{58}H_{44}Co_4O_8P_4$: C, 56.70; H, 3.58; P, 10.10. Found: C, 57:78; H, 3.58; P, 10.38.

$Co_4(CO)_8DMPM_2$, 5. Yield 0.32 g (72%). Anal. Calcd. for $C_{38}H_{36}Co_4O_8P_4$: C, 46.57; H, 3.67; P, 12.64; 0, 13.0 Found: C, 45.93; H, 3.65; P, 12.55; 0, 13.11.

$Co_4(CO)_8DMM_2$, 6. Yield 0.36g (84%). Anal. Calcd. for $C_{18}H_{28}Co_4O_8P_4$: C, 29.5; H, 3.82; P, 16.9; 0, 17.4. Found: C, 28.70; H, 3.80; P, 16.28; 0, 17.15.

Compound 4 may synthesized alternatively from $Co_4(CO)_{12}$ and DPM[12]. The black crystals obtained gave the same IR spectra as $Co_4(CO)_8DPM_2$ **4** synthesized as above except for an additional weak band at 1890 cm^{-1} as indicated by IR spectroscopy in both CH_2Cl_2 solution and in nujol mull. Subsequent recrystallization from toluene removed this inpurity which is tentatively assigned to $Co(CO)_4^-$.

$Rh_4(CO)_8(DPM)_2$, 8. A 100 ml flask containing a magnetic stirring bar was charged with 0.29 g (3.87×10^{-4} moles) of $Rh_4(CO)_{12}$ under an atmosphere of dry nitrogen. This was dissolved in 15 ml of degassed CH_2Cl_2. Dropwise addition of a 15 ml solution of 0.297 g (3.8×10^{-4} moles) of DPM in CH_2Cl_2 resulted

in moderate evolution of CO gas. After stirring for 2 hours, the solution was concentrated and eluted through a silica gel column with toluene. The major fraction was eluted from the column, concentrated, and the residue recrystallized from CH_2Cl_2.

Solution Structure and Dynamics

Just as the cobalt dimers, **1**, **2**, and **3** are fluxional in solution, the tetramers **4**, **5**, and **6**, undergo rapid bridge - terminal exchange in solution. For the dimers this exchange is fast at temperatures as low as -80°C. At this temperature the dimers yield a single resonance for all six carbonyl ligands, as seen by ^{13}C NMR spectroscopy. (vide supra)

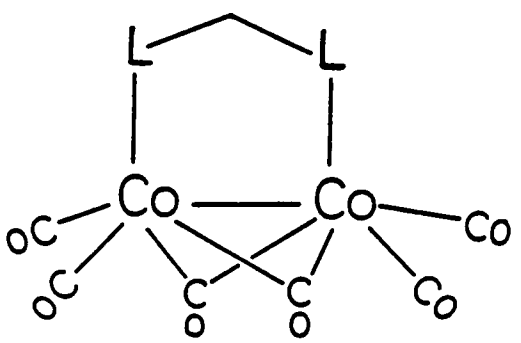

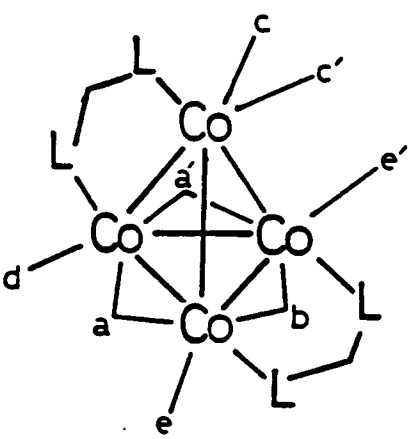

1 L^L = DPM

2 L^L = DMPM

3 L^L = DMM

4 L^L = DPM

5 L^L = DMPM

6 L^L = DMM

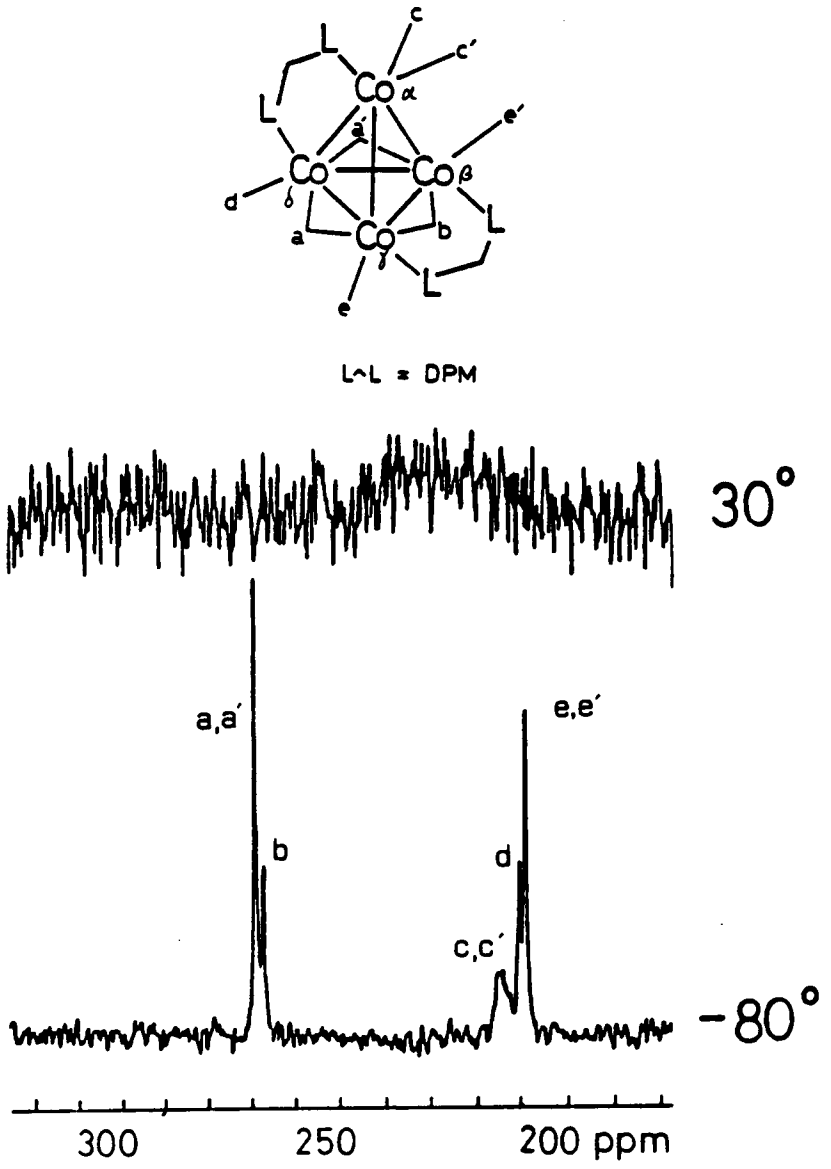

Figure 2. Carbon ^{13} C NMR spectra for $Co_4(CO)_8(DPM)_2$ at 30° and -80°C: The solvent is CD_2Cl_2, chemical shifts are from TMS. At 30°C all eight carbonyls are equivalent.

The variable temperature ^{13}C NMR spectra of the tetramers are more informative. Figure 2 shows the spectra of compound **4**, at -80°C and 25°C. At -80°C, compound **4** exhibits two bridging carbonyl resonances in a ratio of 2:1 and three terminal carbonyl resonances in a ratio of 2:1:2. This is completely consistent with the expected structure of a derivitave from C_{3v}, $Co_4(CO)_{12}$ with three bridging carbonyls in the basal plane for the cobalt tetramer $Co_4(CO)_8(DPM)_2$. Thus compound **4** adopts a structure analogous to that which has been confirmed by x-ray crystallography for $Rh_4(CO)_8DPM_2$. Other phosphine substituted derivatives of $Co_4(CO)_{12}$ exhibit similar structures.[51]

The assignment of the -80°C spectrum using the labeling scheme shown on page 26 is thus a,a'-260.1 ppm; b-258.2 ppm; c,c'-206.9 ppm; d-203.2 ppm; and e,e'-201.7 ppm. The absolute assignment of c,c' and e,e' cannot be made with certainty from the available data, however reversing the assignment does not change any of the arguments with regard to the dynamic behavior of **4**. At room temperature a single very broad resonance is observed indicating that all eight carbonyls are exchanging.

Figure 3 shows the complete set of variable temperature ^{13}C NMR spectra for compound **4** which was synthesized by the route shown in equation 7. The signal due to an impurity is designated by an asterisk in Figure 3. Comparison of Figure 2 to Figure 3 shows that there are definitely impurities and that equation 6 is a much cleaner synthetic route to compound **4** than equation 7, as mentioned previously.

The carbonyl ligands of compound **4** in Figure 3 are observed as only a broad single peak indicating carbonyl exchange. On cooling to -20°C, signals

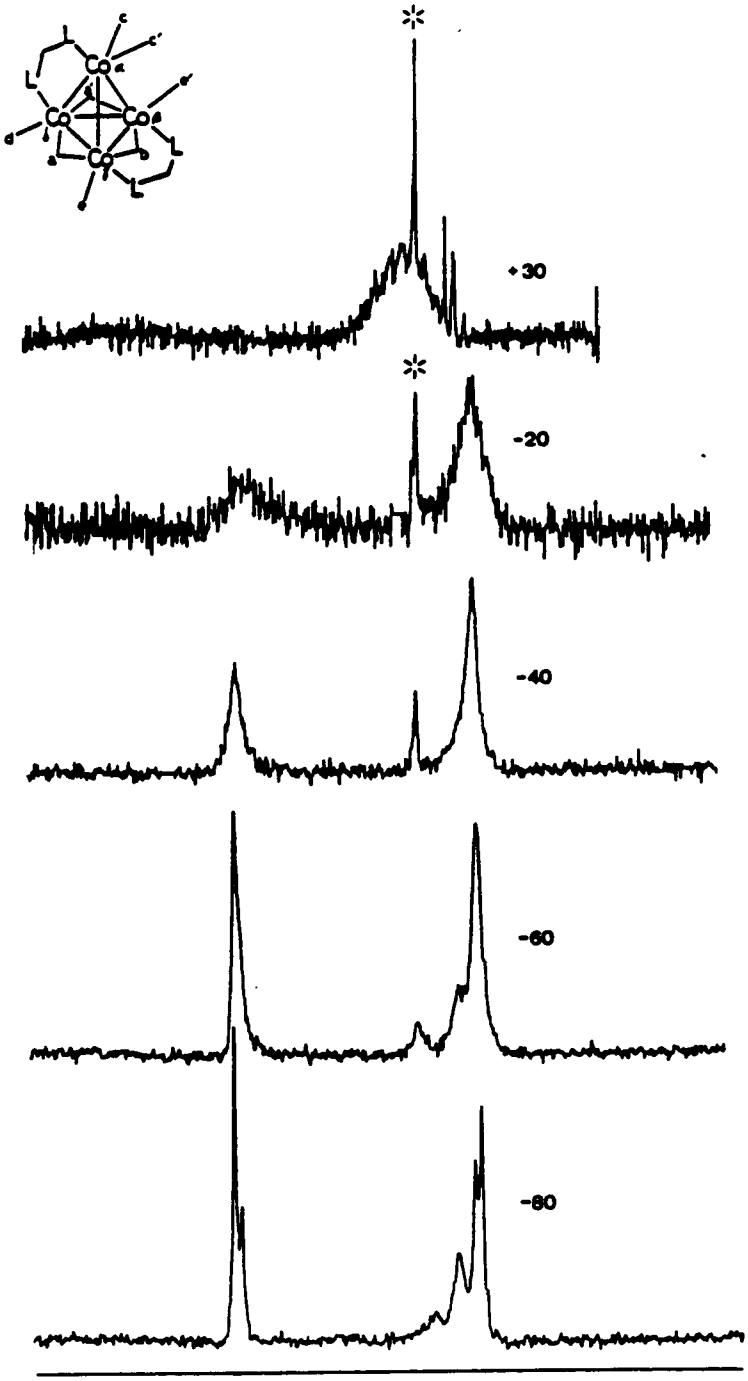

Figure 3. **Variable temperature ^{13}C NMR spectra for $Co_4(CO)_8DPM_2$:** Bridge-terminal exchange is frozen on the NMR time scale at -80°C, at 30°C, all eight carbonyls are equivalent. The signal with an asterisk indicates the impurity $Co(CO)_4^-$. The solvent is CD_2Cl_2; chemical shifts are from TMS.

corresponding to bridging and terminal carbonyls can be distinguished. This shows that the major fluxional process has slowed down on the NMR time scale. On cooling from -60°C to -80°C , the signals sharpen considerably and new bridging and terminal carbonyl signals can be distinguished. This indicates that a second low energy fluxional process may be occurring at very low temperatures. This low energy process will be mentioned throughout this chapter.

When the unsymmetrical ditertiary phosphine, DMPM, is used to form **5** two isomers are possible in solution. (In the solid state four isomers may be expected from consideration of the structure of $Rh_4(CO)_8DPM_2$[46]; however, in solution pairs of the structures should be identical.) Low temperature ^{31}P and ^{13}C NMR spectroscopy confirm the existence of isomers of **5**. Figure 4 shows the ^{13}C NMR spectrum of $Co_4(CO)_8(DMPM)_2$ at -80°C. The isomers are best resolved in the bridging carbonyl region of the ^{13}C NMR spectrum where six resonances, three for each isomer, are observed. In the schematic representation a and a′ are no longer equivalent when L-L is unsymmetrical. One possible assignment is indicated in Figure 4. Clearly the isomers are not present in equal quantities. In the terminal carbonyl region of the ^{13}C NMR spectrum the resonances due to the isomers overlap to give a complicated pattern. The total integration of bridging to terminal carbonyls is 3:5 as expected. Significantly, there is no evidence for isomers at room temperature by ^{31}P and ^{13}C NMR spectroscopy. Thus the fluxional process must interchange the two isomers.

An indication of the more stable isomer can be obtained from analysis of the ^{31}P NMR spectra. The ^{31}P NMR data are presented in Table IV. First, phosphorus bonded to the axial cobalt is distinguishable from phosphorus bonded to

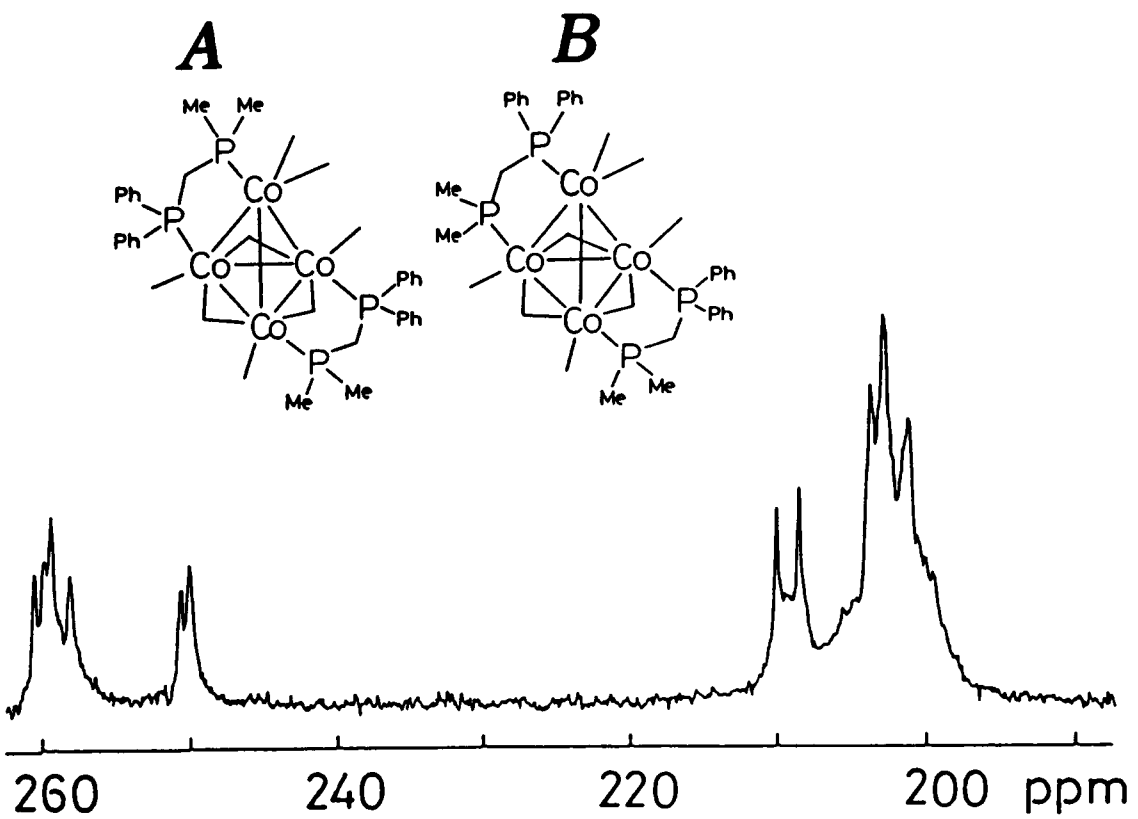

Figure 4. Low temperature ^{13}C NMR of $Co_4(CO)_8(DMPM)_2$: The spectrum is consistent with the presence of two isomers as shown schematically.

basal cobalts by ^{31}P NMR spectroscopy, but within the basal plane all three phosphorus atoms give the same chemical shift.

The two isomers of **5** are shown schematically in Figure 4. In isomer A the $-PMe_2$ groups are distinguishable by ^{31}P NMR spectroscopy. However the basal $-PMe_2$ group in A overlaps with the $-PMe_2$ groups in isomer B. Likewise the $-PPh_2$ groups in A overlap with the basal $-PPh_2$ group in B. Thus at low temperature four signals are observed in the ^{31}P NMR spectrum. These are the axial $-PMe_2$ on A; the axial $-PPh_2$ on B; the basal $-PPh_2$ on A and B; and the basal $-PMe_2$ on A and B. By comparison of the ^{31}P NMR spectra of **5** with that of **4** and **6**, the $-PPh_2$ and $-PMe_2$ groups can be assigned definitively. Also it can be estimated from Figure 4 that the relative abundance of the two isomers is approximately 1:2. Thus the weakest signal in the low temperature ^{31}P NMR spectrum of **5** will be the $-PR_2$ group bonded to the axial cobalt in the least abundant isomer. From the table this is clearly a $-PPh_2$ group. Thus isomer B shown schematically in Figure 4 is less abundant in solution at low temperature than isomer A.

The variable temperature ^{13}C NMR spectra for $Co_4(CO)_8(DMM)_2$, **6**, are shown in Figure 5. At 30°C only a single very broad resonance (at 214 ppm) is observed, just as with compounds **4** and **5**, indicating that all eight carbonyls are exchanging simultaneously, and that the fluxional process is fast on the NMR time scale at ambient temperature. As the temperature is lowered to -15°C bridging and terminal carbonyl signals can be distinguished in the spectrum. Again, this shows that the major fluxional process has slowed down on the NMR time scale at this temperature. Upon cooling the sample down to -80°C bridging

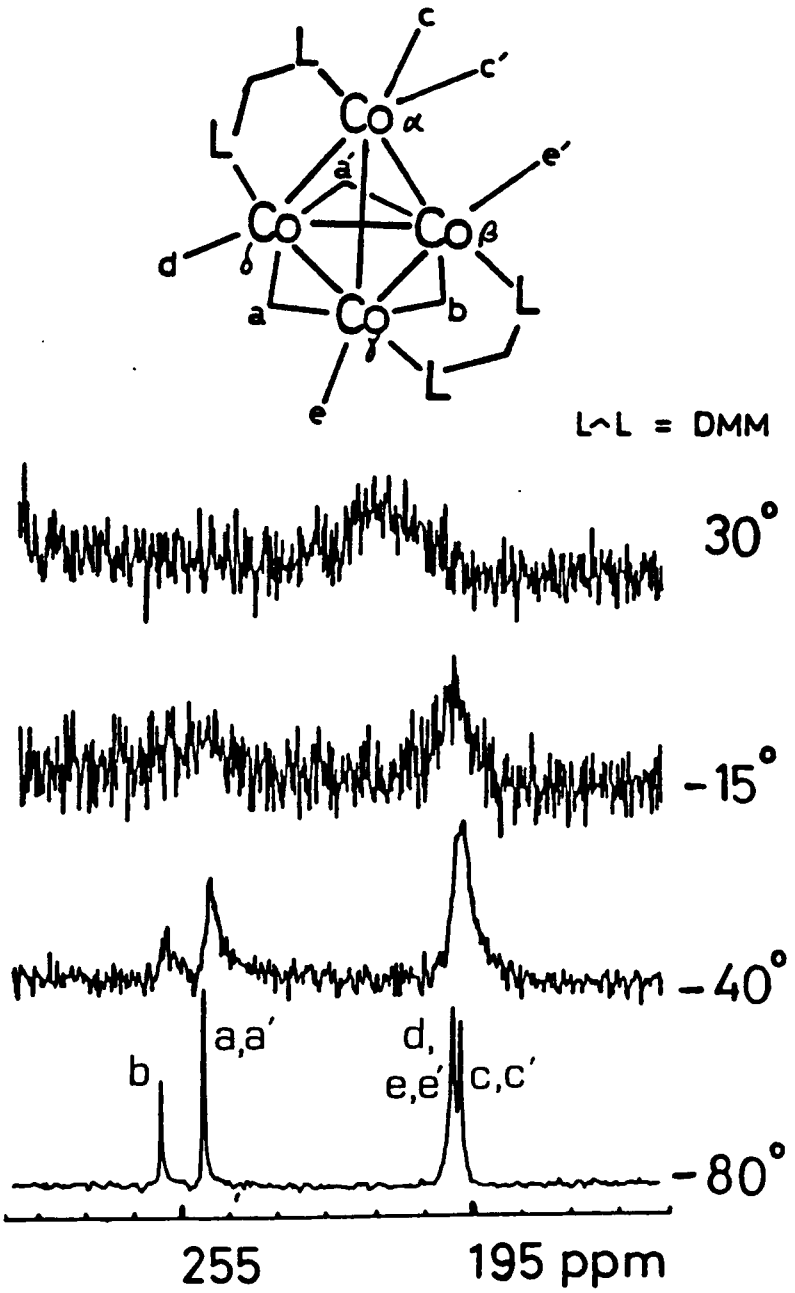

Figure 5. Variable temperature ^{13}C NMR spectra for $Co_4(CO)_8(DMM)_2$ from -80° to +30°C: Bridge-terminal exchange is frozen on the NMR time scale at -80°C.. All eight carbonyls broaden at the same rate as the temperature is raised.

and terminal carbonyl resonances sharpen dramatically. At -80°C, the spectrum of **6** exhibits two bridging peaks at 258.7 ppm and 249.9 ppm, with a ratio of 1:2, and also two terminal carbonyl peaks at 199.4 ppm and 197.7 ppm, with a ratio of 3:2.. The observation of only two terminal carbonyl resonances seems to indicate an accidental degeneracy of chemical shifts. A straightforward assignment of chemical shifts to carbonyls is then as follows: a,a′-249.9 ppm; b-257.7 ppm; c,c′-197.7 ppm; and d and e,e′-199.4 ppm. Upon comparing the -80°C spectra for compounds **4** and **6**, one sees that all of the terminal carbonyl resonances expected are seen for compound **4** and not for compound **6**. Since DPM is much more bulky than DMM, it is reasonable to assume that the low energy fluxional process is still be fast at -80°C for compound **6**. This is more circumstantial evidence for a low energy fluxional process. The nature of this process will be discussed with the mechanism for fluxionality in these complexes at the end of this chapter.

It is apparent from the spectra in Figures 2 and 5 that only a very broad carbonyl resonance is observed for compounds **4** and **6** at ambient temperature. A similar result is obtained for compound **5**. The broad peaks are centered at the weighted average position of the carbonyl resonances observed at low temperature.

In addition to ^{13}C NMR spectroscopy, ^{31}P NMR spectroscopy may also be used to examine fluxional and dynamic processes in these tetranuclear clusters as discussed earlier for compound **5**, since phosphorus is present in these clusters. One would expect that for compounds **4** and **6** that all of the phosphorus nuclei would be equivalent at ambient temperature if a dynamic process is exchanging

all eight of the carbonyl ligands. In fact this is the case as can be seen from the ^{31}P NMR data of these compounds listed in Table IV.

Figure 6 shows the variable temperature ^{31}P NMR spectra of $Co_4(CO)_8(DPM)_2$, **4**. (At 0 ppm the chemical shift reference, which is 85% H_3PO_4 placed in a capillary tube, can be seen. This freezes by -60°C and is not observed in the ^{31}P NMR spectra recorded at temperatures lower than -60°C.) At 25°C a single broad resonance at 24.29 ppm indicates that the dynamic process makes all phosphorus nuclei equivalent. Upon cooling the sample to -20°C the signal shifts downfield and broadens considerably, indicating that the coalescence temperature has been reached.

At -40°C, three signals are seen. The most downfield signal is a doublet with the most intense peak at 30.55 ppm. Because it has a relative intensity of two compared to the next most downfield signal at 24.30 ppm, which has a relative intensity ratio of one, then this most downfield signal can be assigned to the two basal phosphorus nuclei in the same DPM ligand. The peak at 24.30 ppm is then assigned to the basal phosphorus nuclei in the DPM ligand attached to both basal and apical sites. The extremely broad signal centered about 16 ppm is assigned to the apical phosphorus nuclei. If the low temperature process corresponds to movement of the ligands bound to the apical cobalt, then this would explain the weak relative intensity of this signal and also the broadness that it exhibits.

Figure 7 shows the variable temperature ^{31}P spectra of $Rh_4(CO)_8(DPM)_2$, **7**. At 23°C, the ^{31}P NMR spectrum of **7** is observed as a double multiplet with the largest coupling, 171 Hz, assigned to ^{103}Rh-^{31}P coupling. Since ^{103}Rh has a spin of I = ½ one would expect to get a doublet if all four phosphorus nuclei

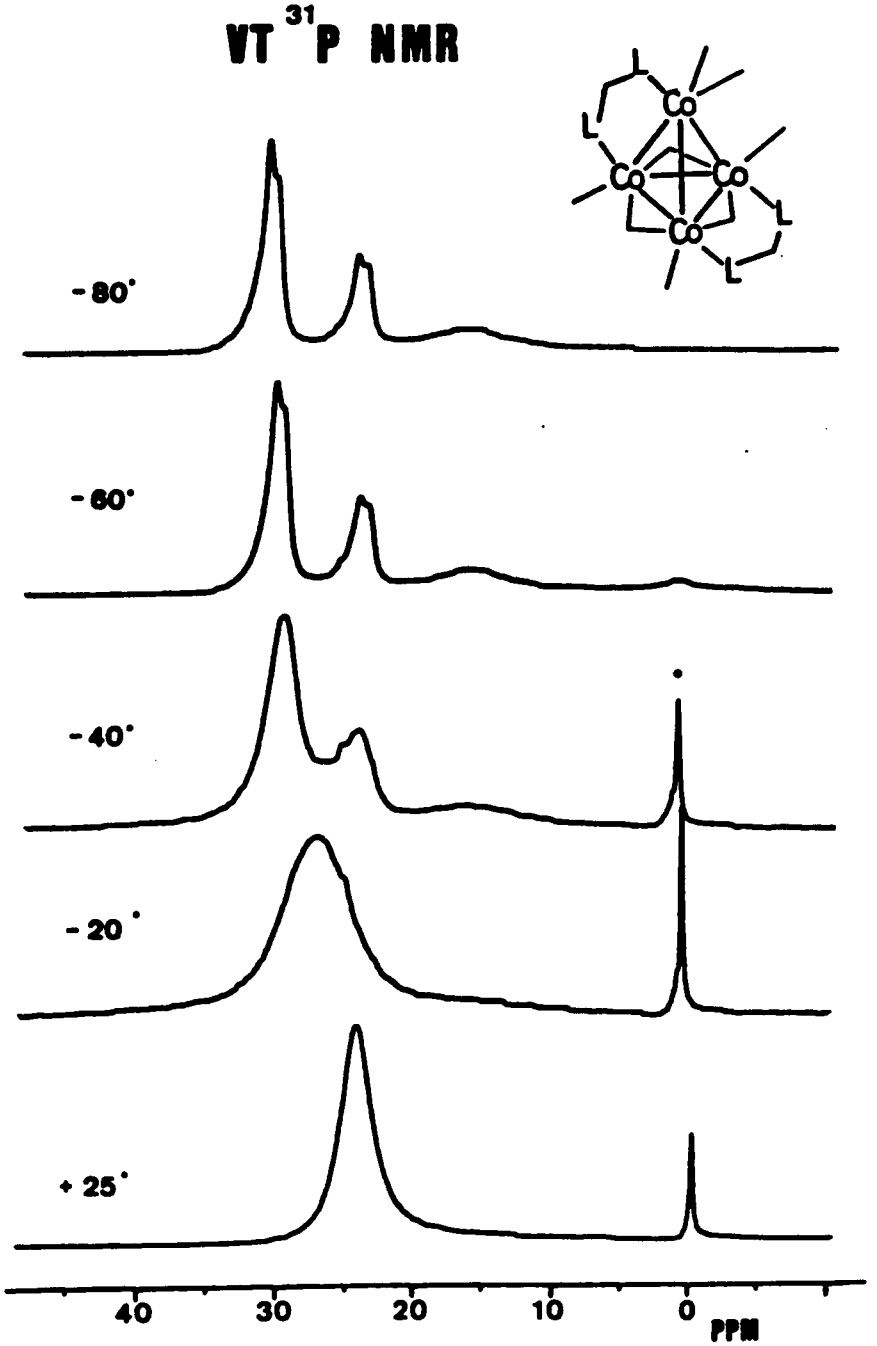

Figure 6. Variable temperature ^{31}P NMR spectra for $Co_4(CO)_8DPM_2$: The solvent is CD_2Cl_2; the internal reference for chemical shifts is 85% H_3PO_4. At 30°C all phosphorus nuclei are equivalent. At -80°C, basal and apical phosphorus nuclei can be distinguished.

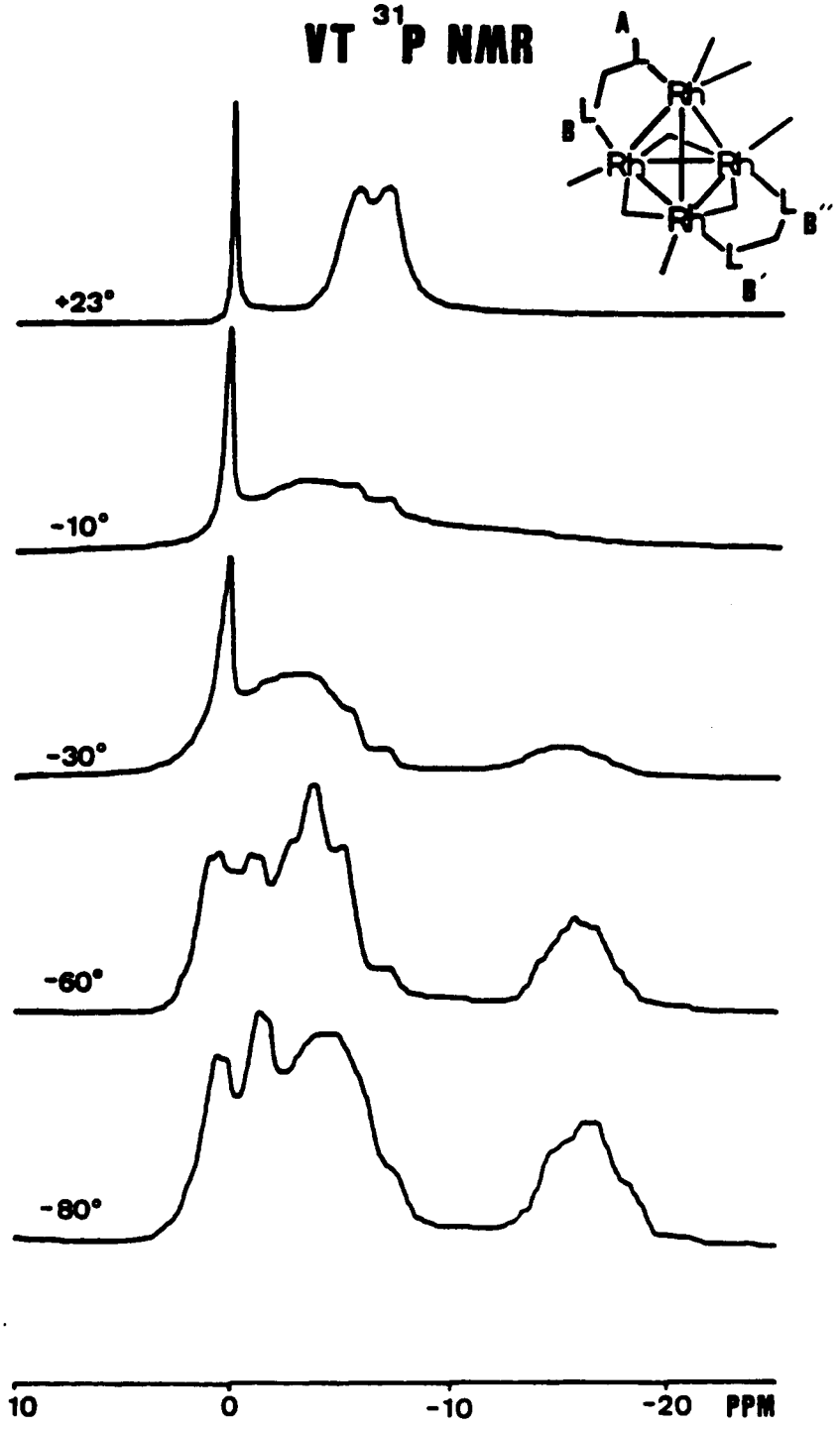

Figure 7. Variable temperature ^{31}P NMR spectra for $Rh_4(CO)_8DPM_2$: The solvent is CD_2Cl_2; the internal reference for chemical shifts is 85% H_3PO_4. At 23°C all phosphorus nuclei are equivalent, giving the observed doublet. H_3PO_4 is designated with an asterisk, and it freezes out completely at -60°C.

were magnetically equivalent and coupled to rhodium in the same way. The double multiplet has smaller couplings, evident in the larger reproduction of the 23°C spectrum in Figure 7, which indicate ^{31}P-Rh-^{103}Rh coupling occurs through a rhodium atom.

These facts indicate that compound 7, like $Co_4(CO)_8(DPM)_2$ and $Ir_4(CO)_8(DPM)_2$,[38] is at or near the fast exchange limit at room temperature and that all four phosphorus nuclei are magnetically equivalent on the NMR time scale via a fluxional or dynamic process or processes.

At -10°C the ^{31}P NMR signal of compound 7, as seen in Figure 7, broadens and moves downfield as the fluxional process reaches its coalescence temperature. At -30°C, the signal has divided into two signals with an approximate intensity ratio of 3:1. Since the lowered temperature favors the static structure seen in the crystal structure and shown in the structural representation in Figure 7, then the most upfield signal with an intensity ratio of 1 can be assigned to the phosphorus nuclei labeled A which is the phosphine nuclei bound to the apical rhodium atom. The other three phosphorus nuclei, labelled B, B′, and B″, are all in the basal plane of the rhodium tetrahedron and would therefore have approximately the same chemical shift value even though they are not magnetically equivalent. They are assigned to the very broad signal at approximately 2 ppm with an intensity ratio of 3.

At -60°C, the spectrum has sharper signals and the basal phosphines give two signals with an approximate ratio of 1:2, which are assigned to B for the most downfield double doublet of intensity ratio 1, and to B′ and B″ for the largest signal with intensity 2 at 3.5 ppm. This signal is a triplet or multiplet with a

coupling of ~100 Hz. The signal for the phosphorus nuclei B′ and B″ is seen as a sharp multiplet at -60°C, but at -80°C the signal has changed and is seen as a very broad peak with no structure evident. The signal for the apical phosphine A at -80°C and -60°C shows only a broad signal at 16 ppm, unlike the signal for the phosphorus nuclei B, which shows a much sharper signal and evidence for ^{103}Rh-^{31}P and ^{31}P-CH_2-^{31}P coupling. These facts indicate that another dynamic process may be occuring in solution. A mechanism that could explain this would be rotation by 120° of the ligands on the face of the icosahedron which are bound terminally to the apical rhodium atom containing the phosphorus nucleus designated A. The change in the variable temperature ^{31}P NMR spectra of compound 7 between -60° to -80°C shows evidence of this. At -60°C, the "face rotation" is in the fast exchange limit and the two phosphorus nuclei B′ and B″ are magnetically equivalent and couple to ^{103}Rh to give a defined signal. When cooled to -80°C the process seems to be at the coalescence point as the signals for B′ and B″ become non-equivalent as the "face rotation" becomes slow on the NMR time scale. The "face rotation" of the ligands can be thought of also as a rocking motion of the apical phosphine A between two positions separated by 120°.

Proposed Mechanism for Carbonyl Exchange

Intramolecular rearrangement of carbonyl groups in metal carbonyls is a common occurrence and has been recognized as such for almost 20 years. The first proposal of how this might take place was discussed in 1966 in an attempt to explain the anomalous IR spectrum of $Co_4(CO)_{12}$.[52] Cotton proposed that this

molecule underwent intramolecular reactions in solution and existed as a tautomeric mixture of C_{3v} and D_{2d} forms which could freely interconvert via an unbridged intermediate of T_d symmetry by means of concerted motions of the carbonyl ligands. This process is shown schematically below:

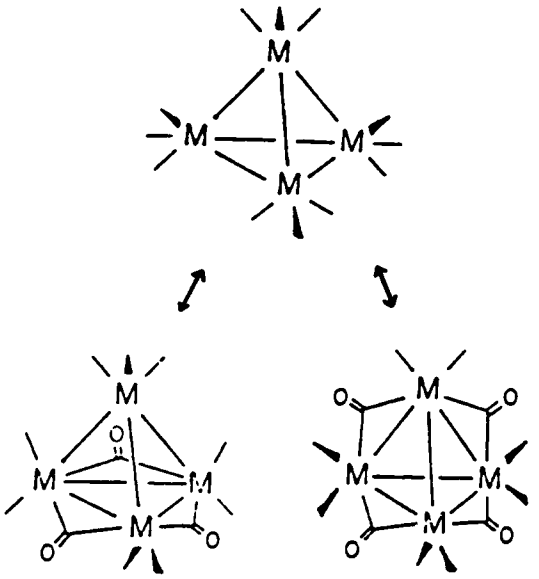

With the advent of ^{13}C NMR as a method of investigation of fluxional behavior of metal carbonyls in solution, experiments have been carried out to test this hypothesis. The low temperature (-100°C) ^{13}C NMR spectrum of $Co_4(CO)_{12}$ in CD_2Cl_2 solution shows three resonances of equal intensity, one in the bridging and two in the terminal carbonyl region.[49]

At higher temperature these signals broaden (-20°C), collapse at 10°C, and the 40°C spectrum shows an absence of carbonyl resonances. This is indicative of carbonyl scrambling and is consistent with the mechanism proposed by Cotton, involving an unbridged T_d intermediate. Even though the crystal structure determination of $Co_4(CO)_{12}$ presented problems, as will be discussed in chapter

4 of this dissertation, it has been proven that solid $Co_4(CO)_{12}$ does exhibit a C_{3v} structure.[15]

In $Rh_4(CO)_{12}$, the low temperature (-65°C) ^{13}C NMR spectrum does show 4 resonances, consistent with the C_{3v} structure. At 50°C the fast exchange limit is reached, a 1:4:6:4:1 quintet with ^1J(Rh-C) 17.1 Hz. This unequivocally shows that the carbonyl ligands are scrambling rapidly over the four metal atoms by an intramolecular exchange mechanism.

It is well known that $Co_4(CO)_{12}$,$Rh_4(CO)_{12}$, and their phosphine derivatives have structures that may be described as distorted icosahedra. The problem of ligand exchange in M_4L_{12} molecules has most recently been described in terms of a polytopal rearrangement of the icosahedral array of ligands.[53] The icosahedron is considered to open to form a cubo-octahedron; formation of a new icosahedral arrangement of ligands then exchanges ligands. When considering an isolated icosahedron there are five degenerate ways of forming a cubo-octahedron. This degeneracy is lifted when a tetrahedron of metal atoms is placed within the icosahedron (as discussed by Johnson and Benfield). Further restrictions are placed on the arrangement when the molecules **4**,**5**, and **6** are considered.

In Figure 8, structure A is a representation of the ligand icosahedron in **4** or **6** where positions 2 and 11, and 8 and 9 are occupied by the ditertiary phosphines. There is only one way to place the Co_4 tetrahedron within this framework to yield the observed structure. Thus the face defined by 4, 5, and 9 has all terminal ligands bonded to the axial cobalt (α). The basal plane cobalts (β, γ, and δ) are directed at edges 1,2; 10,11; and 7,8. Finally the positions 3, 6, and 12

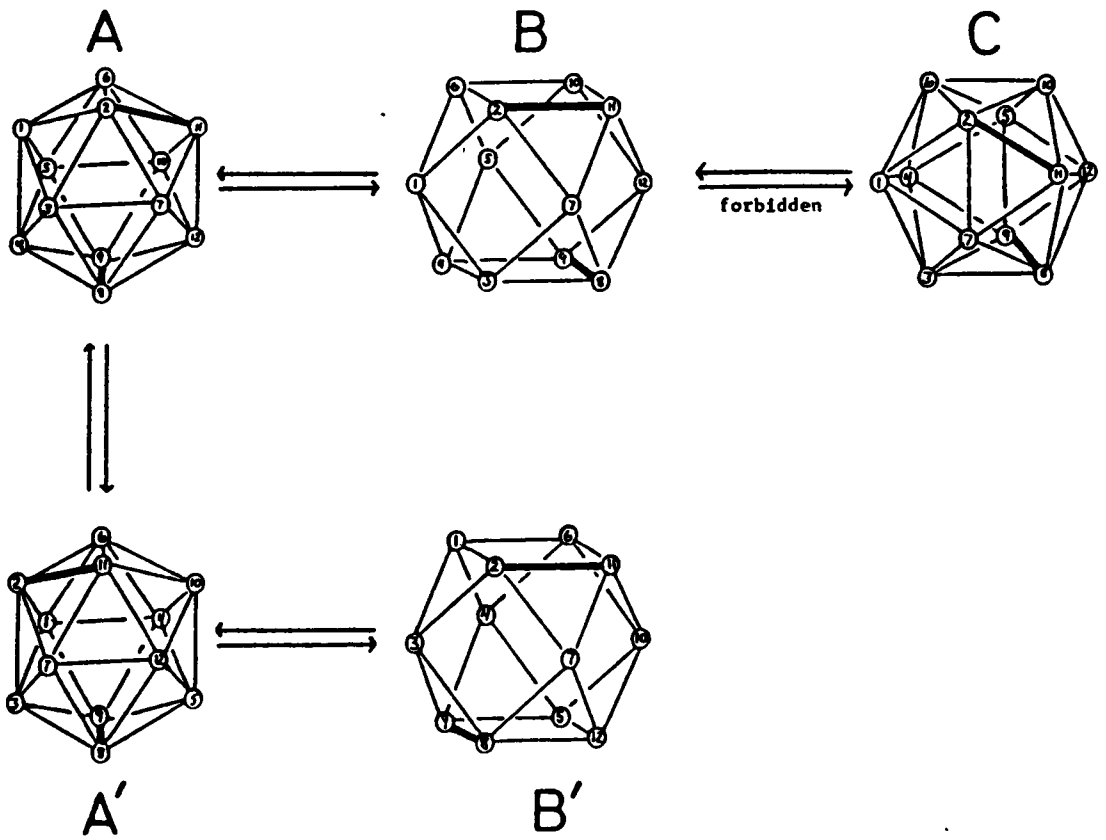

Figure 8. Schematic representation of the fluxional pathways in 4, 5, and 6: The numbering scheme is consistent with Johnson and Benfield.[53]. Icosahedron A opens to cubo-octahedron B by cleaving edges as described in the text. A goes to its mirror image A′ by rotating the face 4,5,9. The representation A′ is drawn to emphasize the mirror relationship with A.′ In A′ the α cobalt is directed to the face 4,5,9 while the basal cobalts, βγδ, are directed at the edges 1,2; 7,8; 10,11. The bridging carbonyls are 3,6,12. The structure B′ is the mirror image of B. In B and B′ the cobalts are directed at the faces 4,5,9; 3,7,8; 10,11,12; and 1,2,6. Only one orientation of B′ is shown in which 2,11 are superposable. Rotation by 180° superposes 8,9.

define bridging carbonyls. This numbering scheme is identical to that used by Johnson and Benfield. It should be further noted that A is chiral and its mirror image is also possible (A′). Also all eight carbonyls are unique in A, however rapid racemization generates a time averaged mirror plane. This accounts for the observed low temperature spectra for **4**, **5**, and **6**. Structure A may open to give a cubo-octahedral structure, B. There is only one pathway for this to occur which satisfies the following criteria: (1) each cobalt is bonded to just one phosphorus atom in B, (2) all cobalts in B have three terminally bonded ligands, and (3) L-L does not span the diagonal of a square face. These conditions are satisfied only if edges 4-8; 1,5; 2,3; 7-12; 6-11; and 9,10 in A are opened. Structure B in Figure 8 thus represents an all terminal, $Ir_4(CO)_{12}$ type structure. The cobalts are directed towards faces 4,5,9; 3,7,8; 1,2.6; and 10,11,12.

Closing opposite vertices on the square faces in B to go to structure C is not possible as this places the phosphines in unrealistic positions. Thus A and B and their mirror images are the only structures that may interconvert. In transforming A to B a slight reorientation of the cobalt tetrahedron is necessary. Although structure B has 2-fold symmetry this is not sufficient to make all eight carbonyls equivalent.

The pathway represented by the interconversion of A and B results in the exchange of the three bridging carbonyl positions, 3, 6, 12, with three terminal carbonyl positions 10,4,7. Carbonyl positions 1 and 5 are exchanged but represent terminal sites. This a direct result of the fact that the 2-fold axis in B relates positions 3,10; 6,4; 12,7; 1,5; 2,9; 8,11.

The key to complete carbonyl exchange is the racemization of A. If A is in equilibrium with its mirror image A′ and also in equilibrium with B, then B is in equilibrium with its mirror image B′. This is shown schematically in Figure 8. If all of these processes are fast on the NMR time scale then B is in rapid equilibrium with B′. This generates a time averaged D_{2d} structure in which all eight carbonyls are equivalent.

A realistic model for racemization is simply rotation of a triangular face in structure A. The only face that may be rotated that doesn't either place phosphine in a bridging position or place two phosphines on a single cobalt is face 4,5,9. This is the face of all terminal ligands on the axial cobalt, α. Structure A′ in Figure 8 is numbered to represent the result of rotation of face 4,5,9 and oriented to emphasize its mirror relationship with A. The pathway represented by A′ to B′ now allows the terminal carbonyls 1 and 5 to occupy bridging positions.

In summary then carbonyl exchange involves rapid racemization and icosahedral - cubo-octahedral rearrangements. The racemization involves a partial rotation of the three ligands bonded to the axial cobalt. Rotation of the triangular face thus represents the low energy dynamic process observed in the $M_4(CO)_{12}L\text{-}L_2$ molecules. The polytopal rearrangement corresponds closely to simple bridge terminal exchange as originally proposed by Cotton.

An interesting series of compounds has been made and studied for further understanding the dynamics of tetranuclear carbonyl clusters by Osborn et al.[54] In this series the triangular faces of the tetranuclear clusters $Co_4(CO)_{12}$, $Co_2Rh_2(Co)_{12}$, $Rh_4(CO)_{12}$, $Ir_4(CO)_{12}$ and $HFe\ Co_3(CO)_{12}$ are capped with the tripod ligand $HC(PPh_2)_3$ to give the series of compounds $M_4(CO)_9$(tripod) and

$HM_4(CO)_9$(tripod). The phosphine tripod ligand skeleton is compared to that of DPM below.

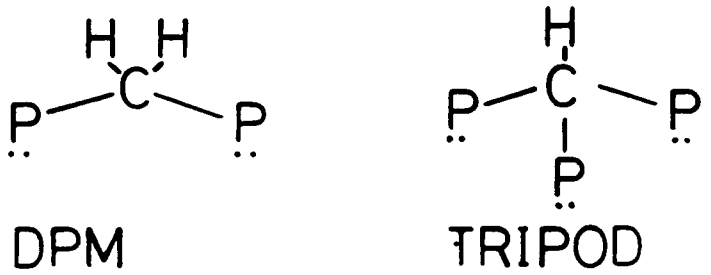

These show that the molecules are closely related. The phosphine substituted tetranuclear clusters produced by Osborn and co-workers are not fluxional in the basal plane of metals. A schematic of these molecules is shown below.

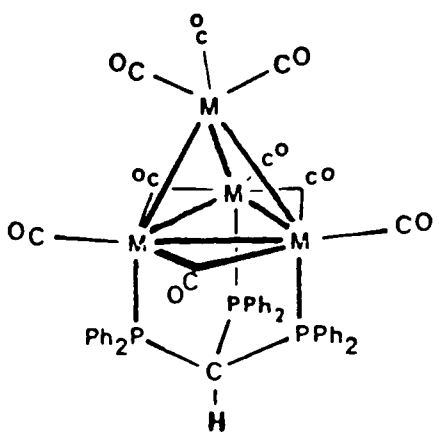

The complex has a basal plane of three metal atoms which have three bridging and three terminal carbonyl ligands and an apical metal atom with three terminal carbonyl ligands. The fact that the $M_4(CO)_9$ (tripod) molecules exhibit carbonyl exchange at the apical metal atom with its three carbonyl ligands, yet do not ex-

change bridging and terminal carbonyls in the basal plane, is in direct contrast with the fact that the molecules $M_4(CO)_8(DPM)_2$, where M = Co, Rh, Ir, are fluxional at room temperature and all carbonyls exchange. Evidence suggests that rotation and carbonyl exchange of $M(CO)_3$ faces in metal carbonyl clusters is a general phenomenon.

It seems then, that the tripod ligand effectively "locks" the ligand polyhedron bound to the basal plane of cobalts. The tripod ligand may then resist expansion of the distorted icosahedron of ligands to the cuboctahedron array of ligands. It is also possible that the metal tetrahedron itself may have to undergo a dynamic process before fluxionality can occur in the tetranuclear clusters. The tripod ligand could inhibit fluxionality by simply keeping any of the basal metal atoms from becoming an apical type metal atom, with no bridging carbonyl ligands.

This proposition is dealt with in the following chapter by the timely use of solid state NMR techniques. The assumption that the carbonyl ligands in metal carbonyls are forced to stay locked in position in the crystal lattice of a solid compound leads to the conclusion that polyhedron, or polytopol, expansion can not happen under this set of conditions. Since dynamic processes do occur in metal carbonyls in the solid state, as evidenced by MAS NMR spectroscopy, then it is reasonable to suspect that metal atom movement may be a contributing factor to the study of fluxionality of metal carbonyls.

CHAPTER 3. VARIABLE TEMPERATURE IN THE SOLID STATE ^{13}C NMR OF BINARY METAL CARBONYLS

This chapter is a discussion of the problem of the fluxional behavior of metal carbonyl clusters $M_x(CO)_y$ in the solid state.

The real excitement of studying metal carbonyl clusters with y = 12 in the solid state lies in the fact that the proposed mechanisms to explain the solution dynamics involve expansion of the ligand icosahedron to a cubooctahedron,[44] and this clearly cannot occur in the solid because of the constraints imposed by the crystal lattice.

The study of cross polarization magic angle spinning (CP-MAS) NMR spectroscopy has progressed to the stage at which commercial instrumentation is widely available. The theory and technology of CP-MAS NMR have been well reviewed in the literature.[55] For the purpose of this chapter, it is sufficient to realize that, to a first approximation, CP-MAS NMR of low abundant spins such as ^{13}C gives high resolution "liquid-like" spectra for powdered samples in which very broad lines are encountered under normal acquisition conditions in the spectra.

For samples which contain protons, ^{13}C - ^{1}H dipolar coupling is a major source of linebroadening in the ^{13}C NMR spectrum. It is possible to remove the dipolar coupling by simple high power proton decoupling; however in practice it is generally removed by a proton spin locking experiment. Obviously dipolar coupling is not a problem for binary metal carbonyls which do not contain pro-

tons. Thus a simple MAS NMR experiment was performed for the binary carbonyls studied in this section. In the absence of ^{1}H-^{13}C dipolar broadening, magic angle spinning alone is sufficient to to give narrow lines by removing the chemical shift anisotropy.

The room temperature MAS ^{13}C NMR spectra of $Co_2(CO)_8$[56] and $Fe_3(CO)_{12}$[11] have previously been published and these spectra indicated that a fluxional or dynamic process occurs in the solid state for these compounds. These involve the intramolecular exchange of carbonyl ligands.

Experimental Section

Dicobalt octacarbonyl (STREM CHEMICALS) was enriched in ^{13}CO by stirring a pentane solution of $Co_2(CO)_8$ under an atmosphere of enriched carbon monoxide in the presence of 5-10 mg 5% Pd/C. The level of enrichment was determined by mass spectroscopy to be 15-25% in different samples. The $Co_2(CO)_8$ was recrystallized from pentane prior to use. Enriched $Co_2(CO)_8$ was used to form enriched $Co_4(CO)_{12}$ and also the mixed tetranuclear clusters $Co_3Rh(CO)_{12}$and $Co_2Rh_2(CO)_{12}$.

Triirondodecacarbonyl (Pressure Chemicals) was enriched in ^{13}CO by stirring a methylene chloride solution of $Fe_3(CO)_{12}$ under an atmosphere of enriched carbon monoxide in the presence of 10mg 5% Pd/C. The level of enrichment was determined by mass spectroscopy to be 18%. The enriched $Fe_3(CO)_{12}$ was recrystallized from pentane prior to use.

All magic angle spinning NMR spectra were recorded at 22.6 MHz using the following instrumentation; a Chemagnetics superconducting magnetic at a field of 2.12 T, a Chemagnetics variable temperature ^{13}C probe tuned to 22.6 MHz, and a Chemagnetics variable temperature controller. The magnet is interfaced to a JEOL FX60Q console. All RF conversions were made locally at VPI & SU by Mr. Gennaro Iannaccone and Mr. Larry Jackson of the Analytical Services and the Electronics shop respectively.

Estimates of the ^{13}C T_1 for $Fe_3(CO)_{12}$ were made by the progressive saturation technique. The spectra at 21°C and 31°C consist of 30 $\pi/2$ pulses with a pulse delay of 4 minutes. At -11 and -30°C five $\pi/2$ pulses were recorded also with a pulse delay of 4 minutes. The spectra at -55°C and below were recorded using a single $\pi/2$ pulse on a sample that had been cooled directly to the desired temperature without experiencing an RF pulse. The temperatures reported are those given by the thermocouple of the Chemagnetics temperature controller. This thermocouple is placed in the spinner air steam immediately before the sample. Prior to recording NMR spectra samples were equilibrated for 10 minutes at the reported temperatures, furthermore temperatures did not fluctuate more than ± 2°C at any temperature setting.

$Co_4(CO)_{12}$. A 100 ml flask was charged with 3.6 g (1.05×10^{-2} moles) of $Co_2(CO)_8$ enriched with ^{13}CO. The flask was equipped with a reflux condenser and the cobalt carbonyl dissolved in 20 ml of distilled THF. The solution was heated to 60°C-70°C for 2 hours. The black solution was filtered after it had been cooled to room temperature to give black crystals of pure $Co_4(CO)_{12}$. Yield, 2.8 g (4.89×10^{-3} moles), 93%.

$Co_3Rh(CO)_{12}$. A 250 ml flask was charged with 2 g (0.05 moles) of NaOH powder that had been pulverized and degassed. A separate flask was charged with 4 g (0.011 moles) of $Co_2(CO)_8$ which had been enriched in ^{13}CO and dissolved in 30 ml of THF. The NaOH powder was slurried in 20 ml THF and the 30 ml solution of $Co_2(CO)_8$ was slowly added by dropwise addition. After two hours the yellow solution was filtered and the purple residue of cobalt salts was extracted with 30 ml of THF and the extracts were combined. The yellow THF solution of Na $[Co(CO)_4]$ was dried of solvent to give the white crystalline salt. Yield, 1.02 g (0.005 moles), 86%. This salt was then dissolved in 20 ml of degassed water. To this was added 0.37 g (0.0014 moles) of $RhCl_3 \times 3\ H_20$ dissolved in 30 ml of water by a slow dropwise addition over a period of an hour. This slow addition assured complete reaction of $RhCl_3$ to give the correct product. The reaction occurred immediately to give the brown $Co_3Rh(CO)_{12}$. After stirring for an hour after addition was complete, the solution was filtered, and the product was then dried under vacuum. The product was dissolved in pentane (the solution IR spectrum was identical with that reported by Chini) and recrystallized when cooled on dry ice. Yield, 0.06 g (9.7×10^{-4} moles), 69%.

$Co_2Rh_2(CO)_{12}$. A 100 ml flask was charged with 0.48 g (1.23×10^{-3} moles) of $Rh_2(CO)_4Cl_2$ which had been freshly sublimed. To this was added 0.63 g (1.85×10^{-3} moles) of $Co_2(CO)_8$ crystals which had been enriched with ^{13}CO. This mixture was dissolved in 25 ml of pentane and allowed to stir for three days. Evolution of CO gas could be seen through an attached oil bubbler; a pinkish-white precipitate of $CoCl_2$ could also be seen. The solution was filtered under N_2 and the solid was extracted with 60 ml of pentane and the washings were com-

bined. The solution IR spectrum was identical with that reported by Chini. The solution was placed on dry ice and beautiful reddish black crystals of $Co_2Rh_2(CO)_{12}$ were obtained. Yield, 0.37 g (5.65×10^{-4} moles), 45.9%.

Solid State ^{13}C NMR of $Co_2(CO)_8$

It was stated in a survey of ^{13}C NMR spectra of metal carbonyls in the solid state that the spectrum of $Co_2(CO)_8$ consisted of a single resonance.[56] This peak is at 205 ppm, approximately at the average position for two bridging and six terminal carbonyls. It can be concluded from this spectrum that rapid bridge-terminal exchange occurs in solid crystalline $Co_2(CO)_8$. Low temperature MAS ^{13}C NMR spectroscopy confirmed this implied dynamic behavior.[2]

The variable temperature ^{13}C NMR spectra for $Co_2(CO)_8$ at 50 MHz were recorded but were complicated by a large number of overlapping spinning sidebands.[12] Thus the authors used a TOSS pulse sequence (Total Sideband Suppression) to alleviate some of this problem. The sideband problem originated from spinning rates that were slow (about 2.5kHz at -1.34°C) with respect to the chemical shift anisotropy. In the TOSS spectrum, however, it was apparent that peaks at 182 and 234 ppm at -134°C, corresponding to terminal and bridging carbonyls respectively, are present. These shifts are comparable with assignments previously made for other metal carbonyls in solution.

As an introduction into solid state ^{13}C NMR spectroscopy of metal carbonyls it was decided that a reproduction of the above work was needed. This

would enable one to compare the previously reported data at 50 MHz to a lower field (i.e.,22.6 MHz).

Figure 9 shows the variable temperature ^{13}C NMR spectra of $Co_2(CO)_8$ in the solid state at 22.6 MHz. The spectra in Figure 9 were recorded at spinning rates in the range of 2.5 kHz(-121°C) to 3.6kHz(40°C) thus all spectra are in the fast spinning regime (above 2.5 kHz) so the centerbands are easily distinguished.

The metal carbonyl undergoes a complex series of changes from +40°C to -44°C and subtle changes are still occurring down to -121°C as evidenced by the spectral data. The spectrum at 40°C shows only a single resonance at 205.5 ppm indicating the dynamic carbonyl exchange process is in the fast exchange limit. This average peak agrees well with previously reported values.[12] The low temperature NMR spectra are uncomplicated by spinning side bands, yet the center bands are very complicated. This may be due to ^{59}Co - ^{13}CO dipolar and quadrupolar couplings which are not eliminated by magic angle spinning. Line shape analysis of spin 1/2-spin 7/2 systems have been studied in detail and it has been shown that these lead to multi-lined spectra.[57]

Figure 9 contains several unusual and as yet unexplained features. First, there is an apparent upfield shift of the signal as the temperature is decreased. This may be due, in part, to the fact that the downfield components lose more intensity due to spinning sideband formation. It is unusual for the downfield peaks to show a greater chemical shift anisotropy (as demonstrated by variable spinning rate experiments) than the upfield peaks if the former are due to bridging carbonyls and the latter are due to terminal carbonyls. Just the opposite is true for $Rh_6(CO)_{16}$ and $(C_5H_5)_2Fe_2(CO)_4$.[62] Finally, the chemical shifts of some

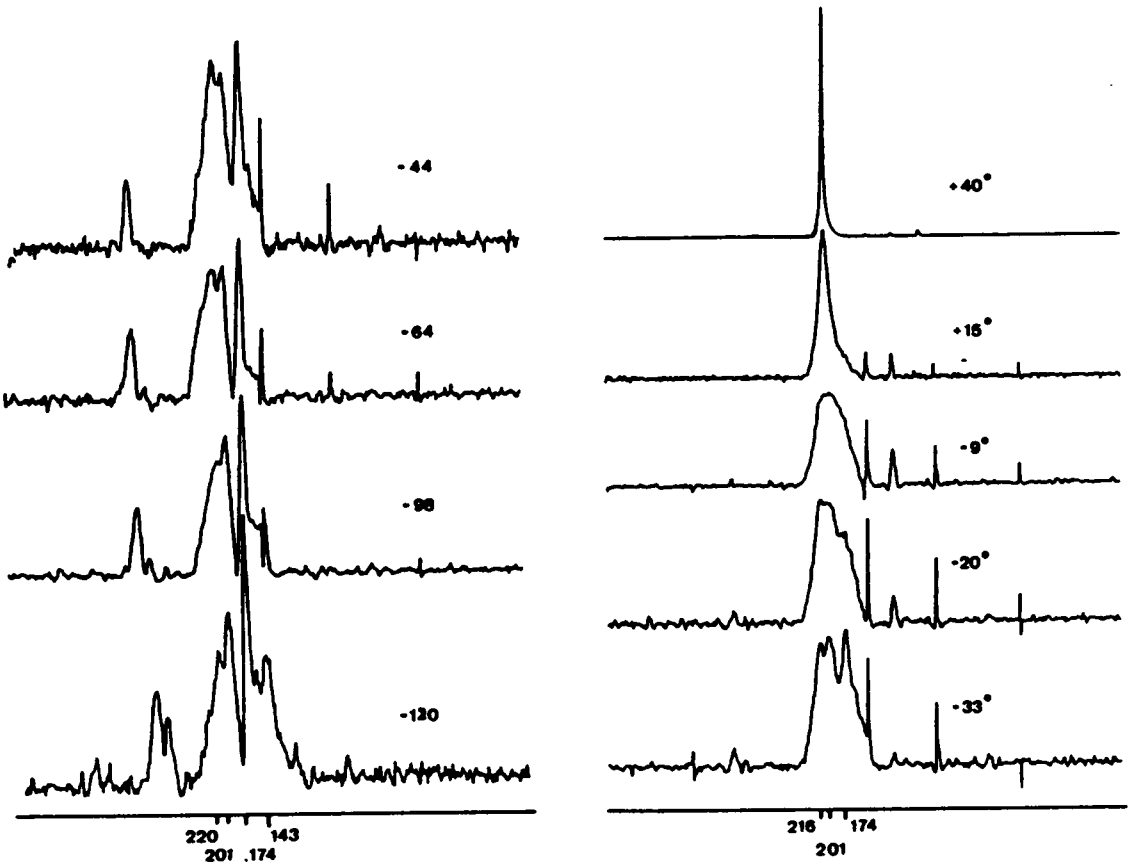

Figure 9. Variable temperature MAS ^{13}C NMR for solid $Co_2(CO)_8$: The chemical shift reference material is hexamethyl benzene. At 40°C all carbonyls are equivalent in a fast exchange limit domain on the NMR time scale.

of the peaks are anomalous. The most downfield peak in the -121°C spectrum (220.3 ppm) is out of the typical bridging carbonyl region for cobalt carbonyls which is from 235 to 260 ppm. Also the intense peak at 174 ppm is significantly upfield (15 ppm) from typical terminal carbonyls in cobalt carbonyl compounds.

The low temperature TOSS spectrum of $Co_2(CO)_8$ does show, however, that terminal and bridging carbonyls are distinguishable in approximately a 3:1 ratio at 182 ppm and 234 ppm respectively.[12] The activation energy for exchange was estimated to be 11.7 Kcal/mol from the data in the fast exchange limit.

Solid State ^{13}C NMR of $Fe_3(CO)_{12}$

Several years ago Hanson, et al, reported that the room temperature MAS ^{13}C NMR spectrum of solid $Fe_3(CO)_{12}$ is consistent with rapid bridge terminal exchange of carbonyls occurring in the solid state.[11] Broadline NMR results for $Fe_3(CO)_{12}$ were also reported to be consistent with a dynamic process in the solid state. The MAS ^{13}C NMR spectra for $Fe_3(CO)_{12}$ at temperatures down to -93°C have now been obtained. These show, for the first time, a spectrum consistent with the static structure of $Fe_3(CO)_{12}$.

The dominant spin lattice relaxation mechanism for metal carbonyls appears to be chemical shift anisotropy (CSA). Consistent with this, solid $Fe_3(CO)_{12}$ shows a small field dependence in T_1; T_1 = 80s at 15 MHz and ca 50s at 22.6 MHz at 25°C. It should be emphasized that these values are estimates obtained by the progressive saturation technique and are not very precise. The values

however are consistent with a major contribution of the CSA mechanism to the overall T_1 value.

The T_1 for solid $Fe_3(CO)_{12}$ is strongly dependent on temperature. In one experiment at -121°C the T_1 was estimated to be greater than 1h by progressive saturation. In view of the exceptionally long T_1 value at low temperature all spectra below -55°C were recorded on a sample that had been cooled directly to the appropriate temperature without experiencing an RF pulse. The long T_1 observed at low temperature is consistent with very slow molecular motions.

Variable temperature MAS ^{13}C NMR spectra for solid $Fe_3(CO)_{12}$ from 31 to -93°C are shown in Figure 10. The spectrum at 30°C agrees well with the spectrum previously reported at 24°C for $Fe_3(CO)_{12}$ at 15 MHz. At a comparable temperature (21°C) in the present study the line widths are much broader than obtained previously. This is due to the field dependence of the lineshape for a dynamic molecule, i.e., at the higher field higher temperatures are required to obtain coalescence of signals.

The most important feature apparent in these spectra is that the two resonances at 224.5 and 226.1 ppm change as the temperature is lowered. All peaks broaden as the temperature is lowered to -55° and finally at -93°C they begin to sharpen again as motions become slow on the NMR time scale. (At -121°C no further resolution of the signal is observed.) The peaks at 224.5 and 226.1 ppm are no longer present at -93°C; however, new peaks at 238.8 and 236.5 ppm appear in this spectrum. These represent bridging carbonyls and agree well with the value observed for solid $Fe_2(CO)_9$.[11] (The resolution perhaps is not sufficient to assign two discrete signals in the bridging region. However, collectively the 238.8

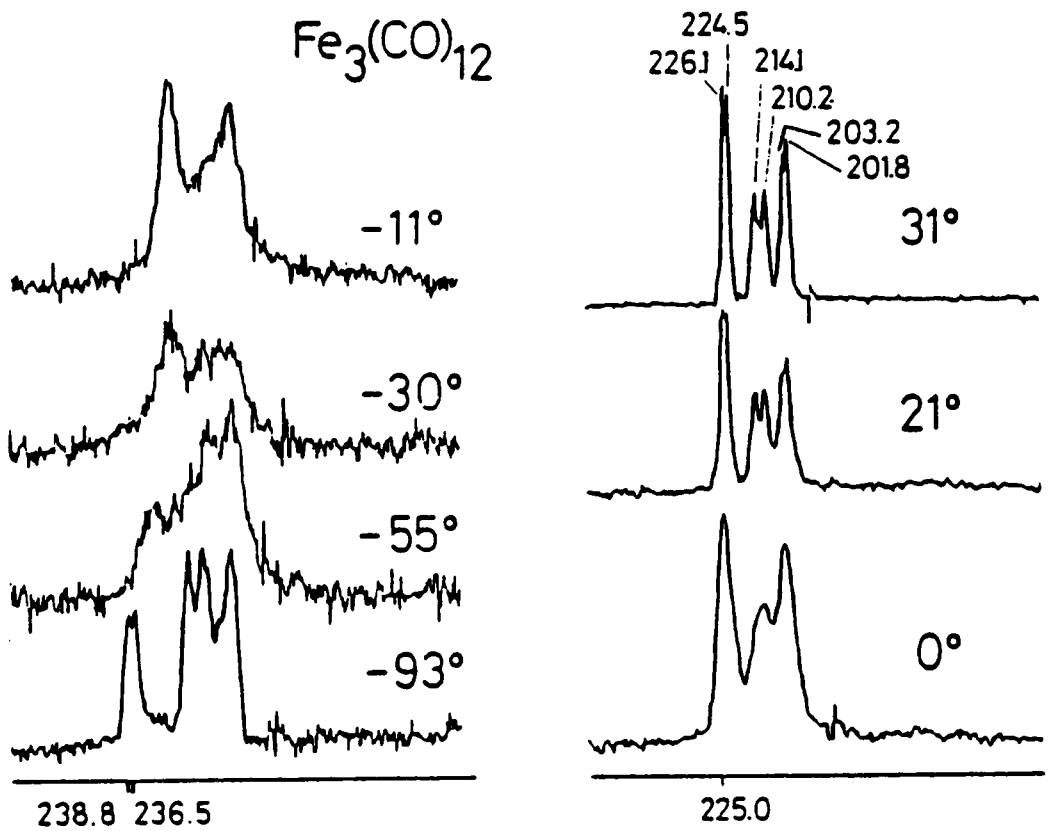

Figure 10. **Variable temperature MAS ^{13}C NMR for solid $Fe_3(CO)_{12}$:** At -93°C bridging carbonyls are observed at 238.8 and 236.5 ppm. In the terminal region three broad resonances at 216.0, 209.5, and 198.3 are observed. The integration of bridging to terminal carbonyls is 2:10, and within the terminal region the approximate relative intensities are 2:4:4. This indicates some accidental degeneracy of signals in the terminal region.

and 236.5 ppm signals integrate for two carbonyls. The integration, combined with the chemical shift, allows the assignment of these peaks to bridging carbonyls.) The integrated intensity of the bridging carbonyl peaks to all of the terminal carbonyl peaks (i.e., those from 198 to 216 ppm) is 2:10 consistent with the molecular structure for $Fe_3(CO)_{12}$ as determined by X-ray crystallography.[59] It is clear in Figure 10 that $Fe_3(CO)_{12}$ is fluxional in the solid state on the NMR time scale and that the dynamic process exchanges bridging and terminal carbonyls.

The linewidths in the low temperature spectra are very much broader than observed in the fast exchange limit. This may be due to ^{13}C-^{13}C dipolar interactions in the slow exchange limit. The sample used to obtain these spectra was enriched to 18% in ^{13}CO.

As previously proposed, the mechanism which best accounts for bridge-terminal exchange as well as exchanging terminal carbonyls in pairs of two to give the six line spectrum observed at high temperature, involves rotation of the iron triangle within the polyhedron defined by the carbonyl ligands. For clarity this is shown again in Figure 11. It has been noted that the 12 carbonyls of $Fe_3(CO)_{12}$ define a distorted icosahedron in the solid state.[60] In Figure 11 triirondodecacarbonyl is represented as an idealized icosahedron.

The cluster $Fe_3(CO)_{12}$ crystallizes in the space group $P2_1/n$ with 2 molecules per unit cell. The cluster occupies a site with inversion symmetry and therefore is disordered in the solid state. The X-ray crystal structure shows the space average of two orientations related by the inversion center, these are designated A and A′ in Figure 11. Rotation of the iron triangle by 60° interchanges A and A′

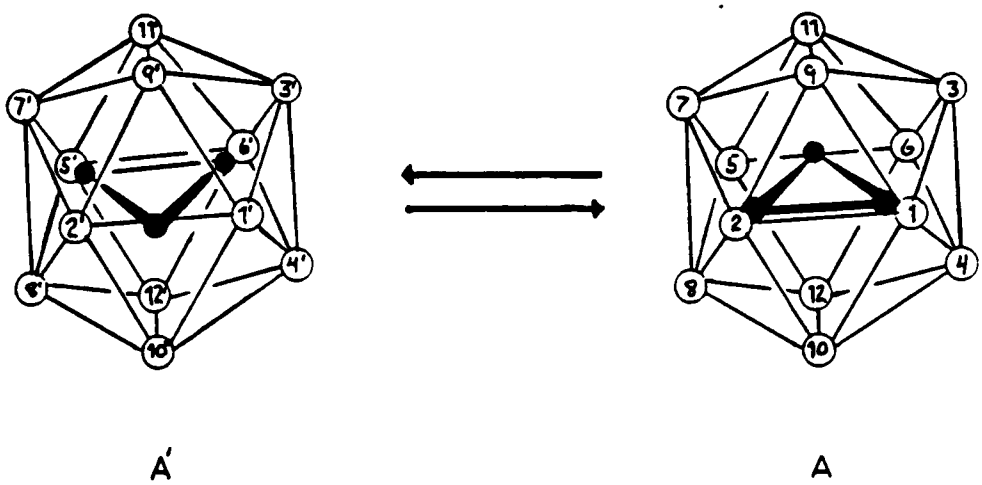

Figure 11. **Idealized representation of the structure of $Fe_3(CO)_{12}$:** The numbering scheme is the same as previously reported. Vertices 9 and 10 represent bridging carbonyls in A; 9′ and 10′ are in terminal positions in A′. The crystal structure shows the space average of these two orientations. The room temperature NMR spectrum is consistent with the time average of both orientations. Thus the motion involves rotation of the iron triangle within the polyhedron of carbonyls.

and interchanges the chemical shifts of 6 pairs of CO's; 1,5; 2,6; 3,4; 7,8; 9,12; and 10,11. These are the positions that are related by the crystallographic inversion center. The high temperature NMR spectrum therefore has 6 carbonyl peaks as required for the time average of the two orientations. The peaks at 226.1 and 224.5 pm at 31°C are assigned to carbonyls 9,10,11,12. At -93° the two orientations are equivalent in the NMR yet are not exchanging rapidly. Thus the peaks at 238.8 and 236.5 ppm are assigned to carbonyls 9 and 10 (Figure 10). An activation energy of 9.1 kcal mole^{-1} is estimated from the approximate coalescence temperature -55°C for bridge terminal exchange.

Rotation of the iron triangle in $Fe_3(CO)_{12}$ confirms, in part, the ideas originally proposed by Johnson to explain the fluxional behavior of this molecule.[53]

Solid State ^{13}C NMR of $Co_4(CO)_{12}$

The structure of $Co_4(CO)_{12}$[15] is closely related to that of $Fe_3(CO)_{12}$[59 60] both are defined by a nearly icosahedral arrangement of carbonyls with the metal cluster located inside. Tetracobaltdodecacarbonyl also exhibits a crystallographic disorder with two orientations of the Co_4 tetrahedron within the icosahedron of carbonyls. In light of the behavior of $Fe_3(CO)_{12}$ it seems likely that a similar reorientation is possible for $Co_4(CO)_{12}$.

Figure 12 shows the variable temperature ^{13}C NMR spectra for solid $Co_4(CO)_{12}$ from 24°C to 75°C at a spinning rate of 2.6 kHz. This is somewhat similar to the set of spectra obtained for $Co_2(CO)_8$ except that the signals for $Co_4(CO)_{12}$ are much broader. The line shape changes are completely reversible.

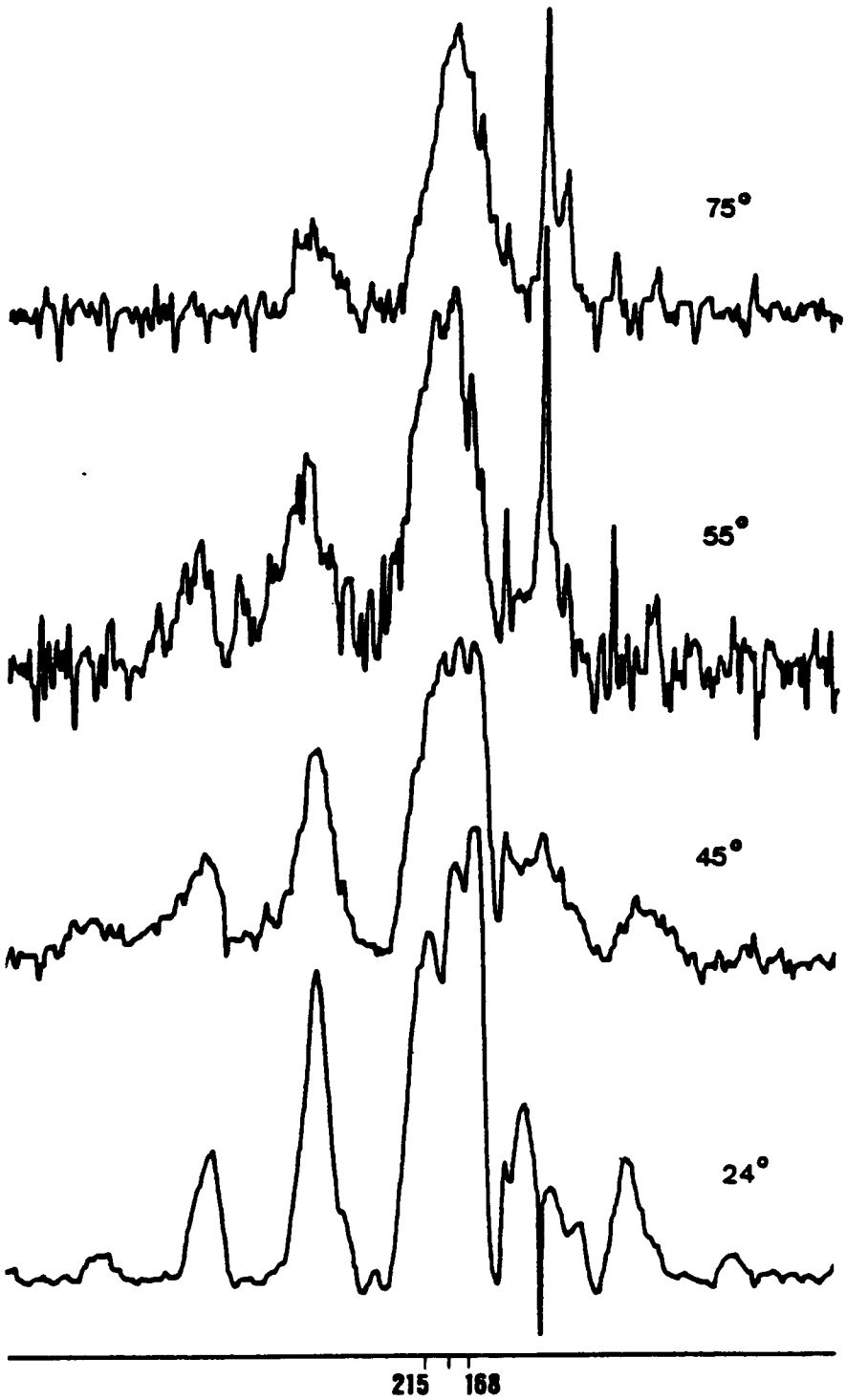

Figure 12. Variable temperature MAS ^{13}C NMR for solid $Co_4(CO_{12}$: The chemical shift reference is Delrin, the rotor material. The spinning rate is 2.6 kHz.

The spectrum at 75°C, shows that carbonyl exchange becomes rapid on the NMR time scale, as the temperature is raised. The spinning side bands, indicated with an asterisk in Figure 12, are very large in the 24°C spectrum. Figure 12 shows that a spin rate of only 2.6 kHz is not a fast enough spin rate to eliminate completely the effects of chemical shift anisotropy of the metal carbonyl signals. Thus, the experiment was repeated at a much higher spin rate.

The MAS ^{13}C NMR spectra for $Co_4(CO)_{12}$ are shown in Figure 13 from -62° to 63°C. The spectrum at 35° was obtained with proton decoupling to allow the observation of the rotor material, delrin, which served as a chemical shift reference. Spinning sidebands are designated by asterisks; the spinning rate varied from 3.7 kHz at -62 to 4.4 kHz at 25°C and above.

In Figure 13 the spectrum at 63°C shows that a a single broad line is observed at 202.8 ppm. This is similar to the room temperature spectrum of $Co_2(CO)_8$ and is consistent with all 12 carbonyls in $Co_4(CO)_{12}$ becoming equivalent on the NMR time scale. The line shape changes from 63 to -62°C are completely reversible; however, above 65°C considerable decomposition occurs during the NMR experiment so further line narrowing could not be observed. The chemical shift observed at 63°C in a highly viscous solvent (206.1 ppm) is very close to the chemical shift observed at 63°C (202.8 ppm) in the solid state.[58]

As the sample is cooled to 24°C three peaks are observed. Only one set of spinning sidebands is seen at all temperatures. In the 24°C spectrum and at all lower temperatures the spinning sidebands are associated with the peak at ca 213 ppm. This can be seen in Figure 13 but was also confirmed by variable spinning rate experiments (vide infra).

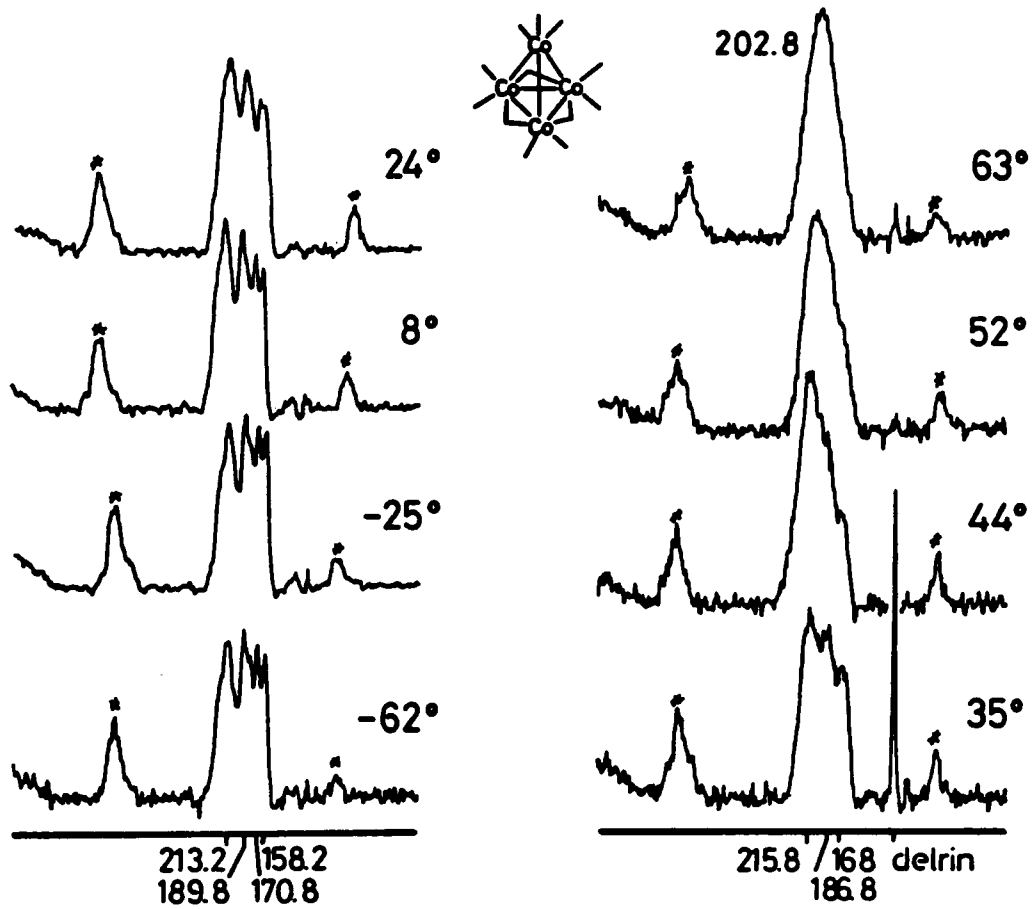

Figure 13. Variable temperature ^{13}C NMR spectra from -62° to 63°C of $Co_4(CO)_{12}$: These were recorded at 22.6 MHz using a Chemagnetics superconducting magnet and probe interfaced to a JEOL PX60QS spectrometer. Proton decoupling was used to record the spectrum at 35°C to give the delrin signal as a chemical shift reference.

When the sample is cooled further four lines appear in the spectrum at 213.2, 189.8, 170.8, and 158.2 ppm. These are quite anomalous for bridging and terminal carbonyls in neutral cobalt carbonyl derivatives. Also the signals in the NMR spectrum shift distinctly upfield as the sample is cooled. In solution the bridging CO's are observed at 243.1 ppm while the terminal CO's resonate at 195.9 and 181.98 ppm. One complicating factor in interpreting the low temperature spectra is ^{59}Co-^{13}C dipolar coupling. Using a Co-C distance of 1.83 A for a terminal carbonyl a calculated dipolar coupling of 2.56 kHz can be determined. Spinning rates of 3.7 kHz at the magic angle may not be sufficient to completely average the ^{59}Co-^{13}C dipolar interactions. Thus the spectra at temperatures -62° to 24°C probably exhibit some dipolar broadening.

Although the spectra below 24°C appear to be consistent with a static molecule there is not a satisfactory explanation for the chemical shifts at this time. It is clear that above 24°C chemical shift differences as well as dipolar couplings are lost as the signals broaden and finally coalesce at about 52°C. This can only be explained by a reorientation of the molecule.

In Figure 14 the effect of two different spin rates on the same sample of $Co_4(CO)_{12}$ is shown. The three signals exhibited by $Co_4(CO)_{12}$ at ambient temperature in the solid state have different intensity ratios due to the different spin rates. Thus it is evident that caution must be used in interpreting the intensity ratios of carbonyl resonances in solid cobalt carbonyls.

The nearly spherical icosahedra of carbonyls in $Co_4(CO)_{12}$ pack very efficiently in the solid. The carbonyl ligands mesh to some extent and the closest contact between adjacent molecules is between carbonyl oxygens at 2.86 A. Thus

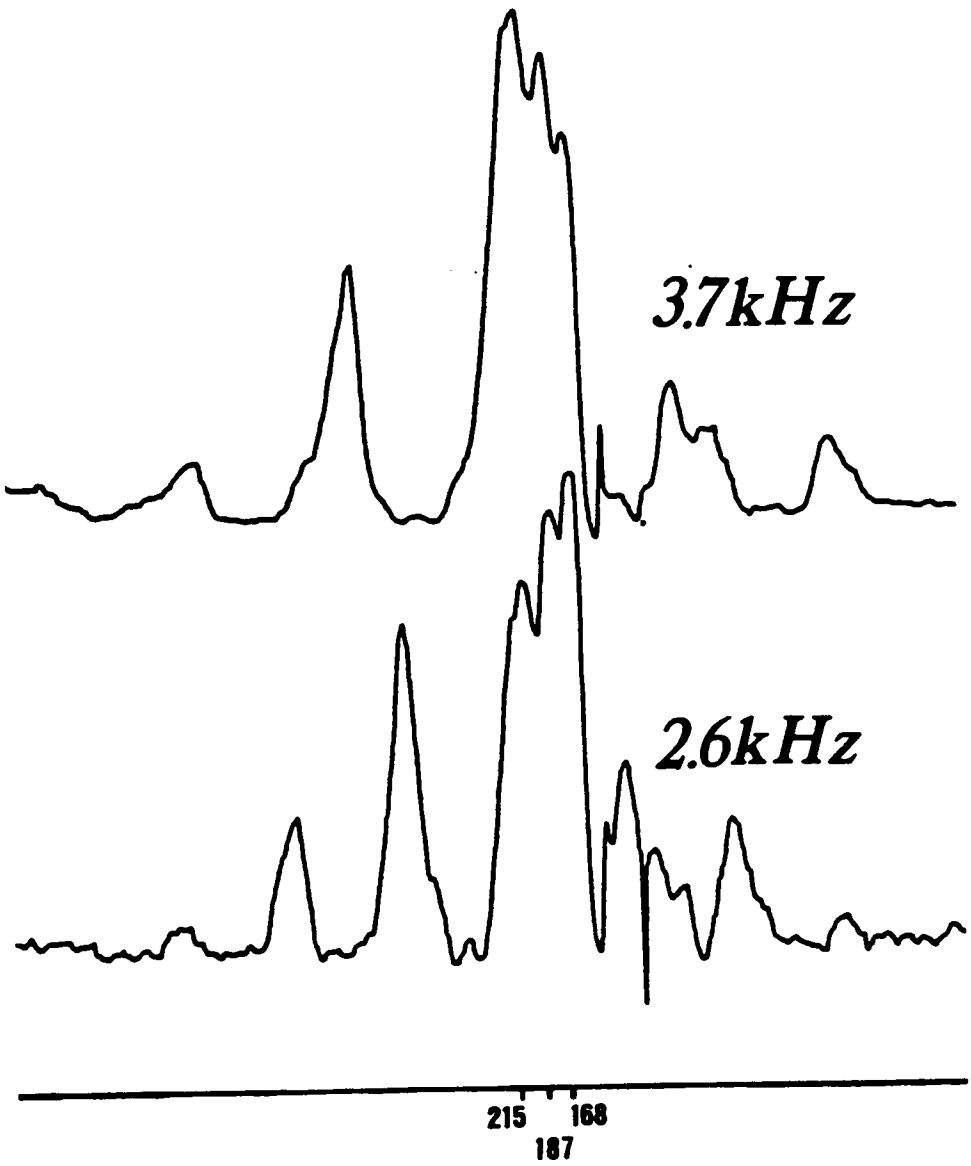

Figure 14. Ambient temperature MAS ^{13}C NMR spectra for solid $Co_4(CO)_{12}$: The spin rates are designated above. This figure illustrates the effect of spin rate on chemical shift intensities.

it seems unlikely that the reorientation involves the rotation of the entire icosahedron. Furthermore rotation of the entire icosahedron will not make all twelve carbonyl ligands equivalent.

Figure 15 shows a schematic representation of the molecular structure of $Co_4(CO)_{12}$. The numbering scheme is consistent with that given by Johnson and Benfield[53] who have considered polytopal rearrangements of $Co_4(CO)_{12}$ and its derivatives in solution. In structure A of Figure 15 the cobalt labeled α represents the apical cobalt and is directed at face 4,5,9. Cobalts β, γ, and δ are directed at edges 7,8; 10,11; and 1,2, respectively. The bridging carbonyls are represented by the vertices 3, 6, and 12. Crystallographically the molecule occupies a site of two-fold symmetry. This gives rise to the disorder of the Co_4 tetrahedron. In Figure 15 the observed two-fold axis is designated a; structures A and B are related by the two-fold axis and represent half molecules in the crystal structure.

The result of the two-fold rotation is to interchange carbonyls 1,2; 9,12; 4,11; 5,7; 8,10; and 3,6. Therefore this rotation is not sufficient to interchange all carbonyls sites. However at the temperatures reached in recording the NMR spectra (63°C) it is possible that all possible orientations of the cobalt tetrahedron are observed, or, in other words, the apical cobalt, α, may be directed at any triangular face in the ligand icosahedron. Reorientation of the tetrahedron to point at an adjacent face requires a rotation of 30°. Adjacent faces, for example, are represented by 4,5,9 and 4,9,8 in structure A.

The activation energy for exchange in the solid estimated from the apparent coalescence temperature of ~52°C, is not significantly greater than observed in solution, where the coalescence temperature was estimated to be 30°C. Thus it

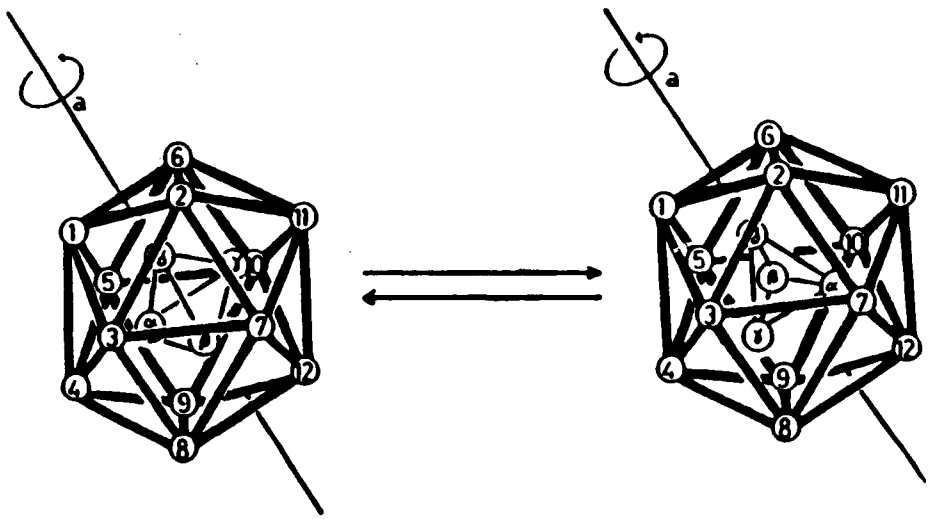

Figure 15. Schematic representation of the structure of $Co_4(CO)_{12}$ showing the twofold disorder observed crystallographically.: Rotation of the cobalt tetrahedron about the two-fold axis, a, is not sufficient to exchange all 12 carbonyls.

appears that the intramolecular motion described here is only a slightly higher energy process than the fluxional process observed in solution. Also it should be noted that the proposed mechanism to explain the solution dynamics involves expansion of the ligand icosahedron to a cubooctahedron and this clearly cannot occur in the solid because of the constraints imposed by the lattice.

Solid State ^{13}C NMR of $Co_3Rh(CO)_{12}$

Figure 16 shows the variable temperature magic angle spinning ^{13}C NMR spectra of $Co_3Rh(CO)_{12}$ in the solid state with proton decoupling. Proton decoupling, of course does not affect metal carbonyl signals; however, it does enhance the delrin signal at 89.3 ppm which is the rotor material and which served as the chemical shift standard during the variable temperature experiment. The signal due to delrin is designated with an asterisk in Figure 16 in the 80° spectrum.

The carbonyl signals are centered around 200 ppm, as can be seen in Figure 16, and spinning sidebands from these peaks were observed at approximately 0 and 400 ppm. In the 25°C spectrum the carbonyl signals are observed as two sets of peaks with approximate ratios of 1 to 3. The downfield set of peaks with an intensity of one, is very broad and has a maximum at 215.8 ppm with a definite shoulder at 223.6 ppm. These signals are assigned to the three bridging carbonyls of $Co_3Rh(CO)_{12}$. The terminal carbonyls are assigned to the upfield set of peaks with an intensity of three which are broad but narrower than the bridging car-

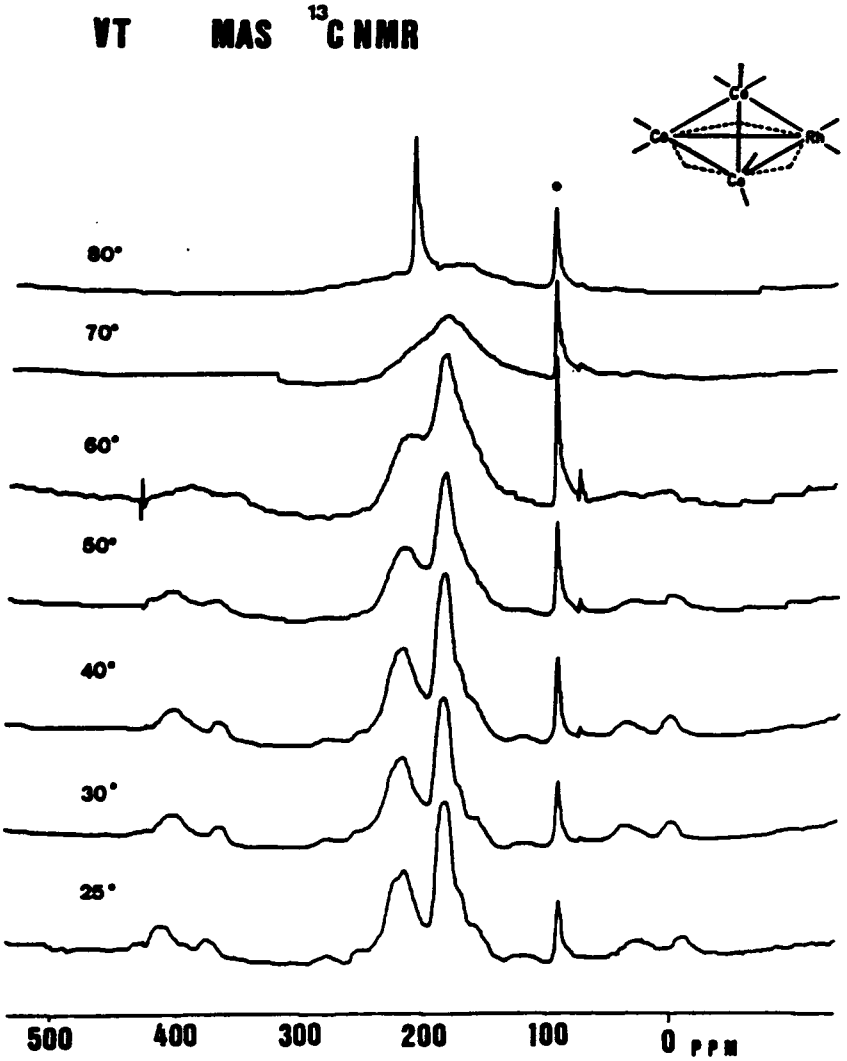

Figure 16. **Variable temperature ^{13}C NMR for solid $Co_3Rh(CO)_{12}$:** The asterisk designates the rotor material and the chemical shift reference, delrin. At 25°C signals for bridging and terminal carbonyls, centered around 200 ppm, are seen. At 80°C a single resonance is seen showing all carbonyls are equivalent.

bonyl peaks. The terminal carbonyl signals are observed as a sharp, intense signal with a maximum at 185.1 ppm with a definite shoulder at 180.2 ppm.

As the temperature is increased, the signals broaden further, until at 60°C the peaks combine. At 70°C a single very broad peak is observed indicating that the coalescence point has been reached. At a higher temperature of 80°C, the broad peak has collapsed almost completely into the baseline, and a single very sharp peak at 203.0 ppm, corresponding to a fast exchange process, has emerged.

Solid State ^{13}C NMR of $Co_2Rh_2(CO)_{12}$

Figure 17 shows the variable temperature magic angle spinning ^{13}C NMR spectra of solid crystalline $Co_2Rh_2(CO)_{12}$. Again, proton decoupling was used to enhance the delrin signal.

At 25°C the set of peaks observed in the spectrum of $Co_2Rh_2(CO)_{12}$ in Figure 17 is very similar to that seen for $Co_3Rh(CO)_{12}$ under the same conditions, as seen in Figure 16. Assigning bridging and terminal carbonyl signals also seems to be straightforward, with the downfield set of peaks at 227.5 ppm and 225.4 ppm being assigned to bridging carbonyls and with the upfield set of peaks at 189.0 ppm and 178.0 ppm being assigned to terminal carbonyls.

At 61°C, the bridging and terminal signals combine, and at 69°C the signals have coalesced. Further increase in temperature to 85°C only decreases the signal Unlike $Co_3Rh(CO)_{12}$, the fast exchange spectrum of $Co_2Rh_2(CO)_{12}$ could not be attained due to sample decomposition at temperatures greater than 85°C. The the spectral changes with temperature in Figure 17 are completely reversible.

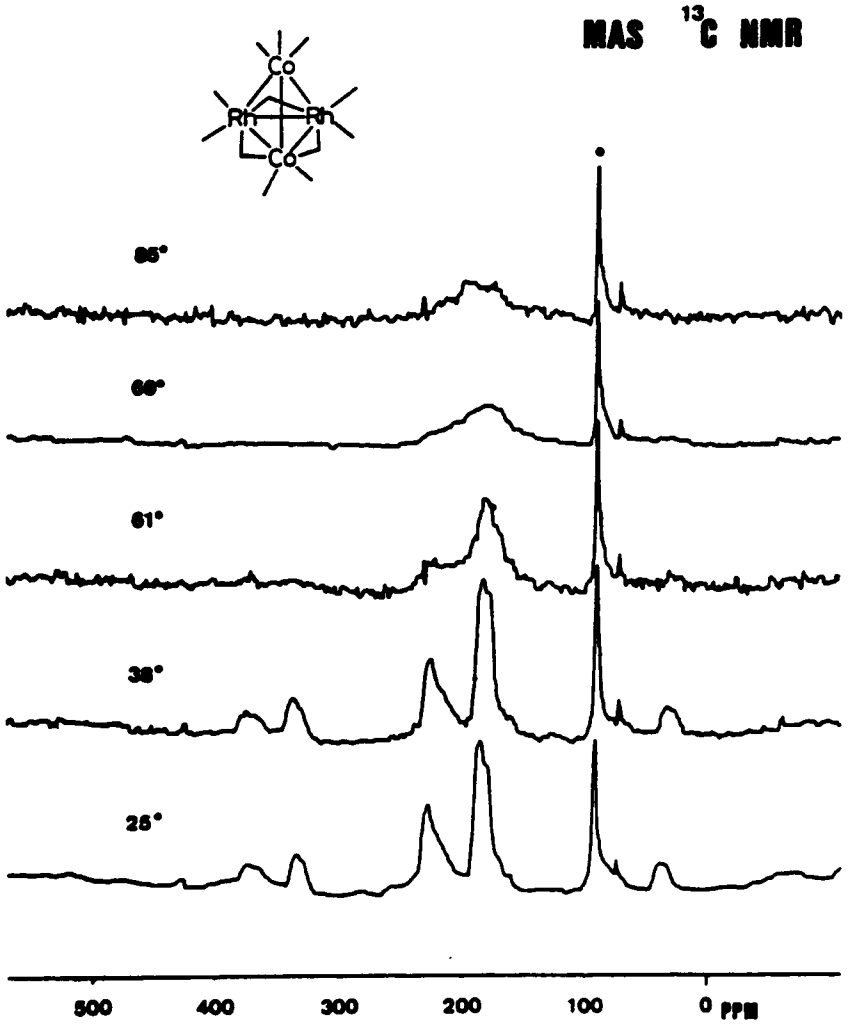

Figure 17. Variable temperature ^{13}C NMR for solid $Co_2Rh_2(CO)_{12}$: The asterisk designates the rotor material and the chemical shift reference, delrin. At 25°C signals for bridging and terminal carbonyls, centered around 200 ppm, are seen. At 69°C and 85°C the signals have collapsed, indicating carbonyl exchange is occurring.

The spinning sidebands are at approximately 350 ppm and 50 ppm, indicating a spin rate of 3.5 KHz. These also disappear at 61°C indicating that the chemical shift anisotropy of the carbonyls is removed by a dynamic process.

Solid State ^{13}C NMR of $Rh_4(CO)_{12}$

The variable temperature solid state ^{13}C NMR spectra of crystalline $Rh_4(CO)_{12}$ is shown in Figure 18. Proton decoupling was not used in the set of spectra shown here, but it was used in a spectrum that is not shown to observe the resonance for the external reference material delrin.

At 25°C the set of peaks observed in the spectrum of $Rh_4(CO)_{12}$ is very similar to those observed in both $Co_3Rh(CO)_{12}$ and $Co_2Rh_2(CO)_{12}$. The carbonyl resonances as seen by solid state NMR spectroscopy are extremely close to the values found by solution ^{13}C NMR spectroscopy for $Rh_4(CO)_{12}$, and exhibit the best correlation of solid and solution ^{13}C NMR resonances in the samples of tetranuclear metal carbonyls that we have studied. The solution and solid ^{13}C NMR data are given in Table VI for the selected Co and Rh tetranuclear clusters.

Differences in the solution and solid state ^{13}C NMR spectra of $Rh_4(CO)_{12}$ are evident however. With the instrumentation available, it is not possible to distinguish ^{103}Rh-^{13}C coupling with solid state ^{13}C NMR spectroscopy even though this coupling is routinely seen with solution ^{13}C NMR spectroscopy. The relative intensities of the carbonyl signals are not a close match with those obtained by solution NMR either, and the upfield peaks at 178.6 ppm and at 175.5 ppm, are not as intense as the terminal carbonyl resonance at 182.9 ppm. In so-

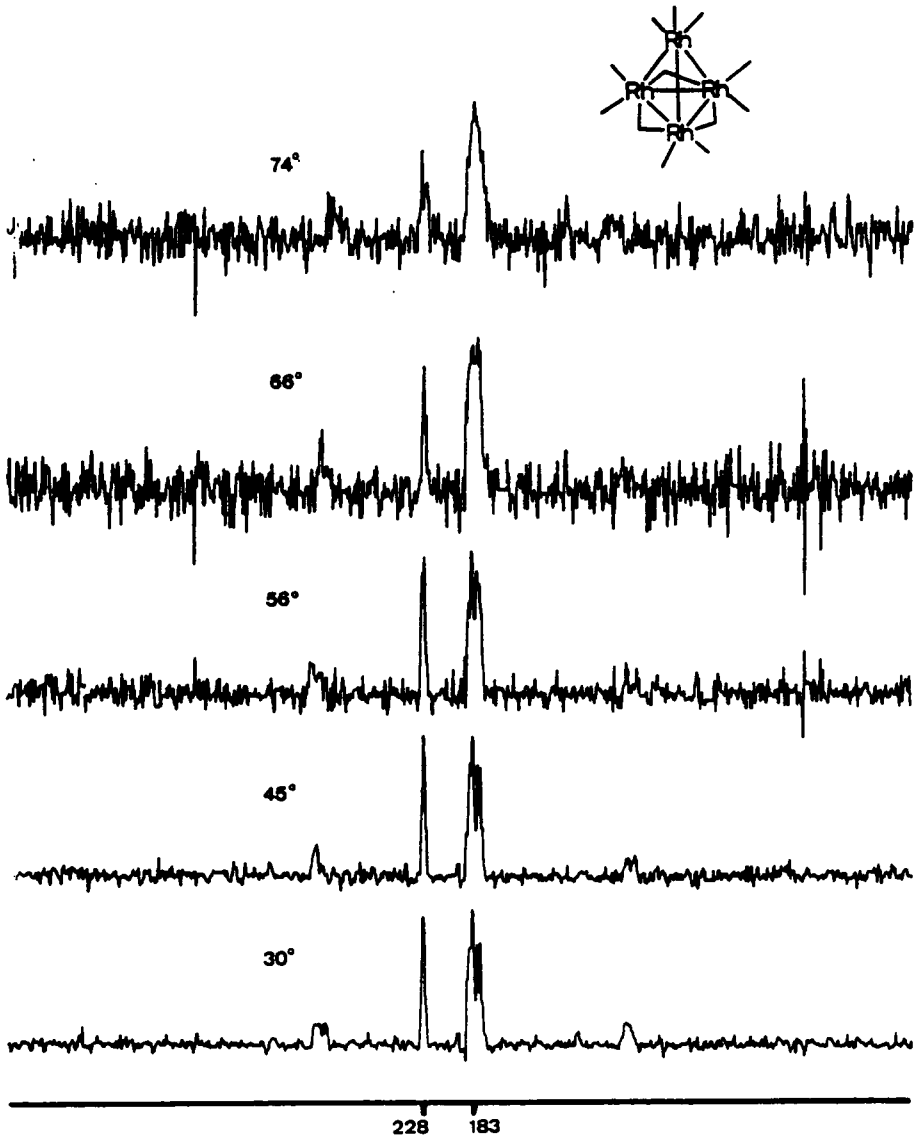

Figure 18. Variable temperature ^{13}C NMR for solid $Rh_4(CO)_{12}$: At 30°C signals for bridging and terminal carbonyls are seen. At temperatures up to 74°C, bridge-terminal carbonyl exchange does not occur.

Table VI. ^{13}C NMR Data.

	^{13}C NMR Solution Data (a), (b)	
	Bridging	Terminal
$Co_4(CO)_{12}$	243.1	195.9, 191.4
$Co_3Rh(CO)_{12}$	251.3, 238.3	201.1, 200.1, 195.5, 188.2, 183.1
$Rh_4(CO)_{12}$	228.8	183.4, 181.8, 175.5

	^{13}C NMR Solid Data (c)	
	Bridging	Terminal
$Co_4(CO)_{12}$	215.8	186.8, 168.0
$Co_3Rh(CO)_{12}$	223.6, 215.8	185.1, 180.2
$Co_2Rh_2(CO)_{12}$	227.5, 225.4	185.1, 178.1
$Rh_4(CO)_{12}$	228.4	182.9, 178.6, 175.5

(a) chemical shifts in ppm from TMS

(b) reference 48

(c) chemical shifts from delrin (89.3 ppm ext. ref.)

lution NMR spectroscopy, the corresponding signals are all of equal intensities. The bridging and terminal carbonyl resonances, however, do have an overall relative intensity ratio of approximately 1:3 as expected.

Significantly, it can be seen in Figure 18 that no observable dynamic process is occuring in solid $Rh_4(CO)_{12}$. This is evident by the fact that the bridging and terminal carbonyl signals do not merge or coalesce, but stay at the same chemical shift positions even at higher temperatures of up to 74°C. At this temperature all of the cobalt containing tetranuclear clusters exhibit a dynamic process.

Figure 19 shows the room temperature MAS ^{13}C NMR spectra of the four tetranuclear clusters discussed in this chapter: $Co_4(CO)_{12}$, the mixed metal clusters $Co_3Rh(CO)_{12}$ and $Co_2Rh_2(CO)_{12}$, and $Rh_4(CO)_{12}$. The asterisked peak indicates the signal for the rotor material and chemical shift reference, delrin.

Several important features are evident in Figure 19 which compares the solid state ^{13}C NMR spectra for this series of clusters. First, it can be seen that as cobalt replaces rhodium in the tetranuclear cluster the carbonyl signals become broader. Thus, $Co_2Rh_2(CO)_{12}$ has sharper signals than $Co_3Rh(CO)_{12}$ and both have sharper signals than $Co_4(CO)_{12}$. The signals from $Rh_4(CO)_{12}$, which has no cobalt nuclei present, are the sharpest of all. These results can readily be explained by the fact that the ^{59}Co nucleus is quadrupolar (a spin of 7/2) which couples to ^{13}C to give broad signals. Secondly, there seems to be a trend in the chemical shift values for these clusters. Figure 19 shows that on going through the series from $Rh_4(CO)_{12}$ to $Co_4(CO)_{12}$, that the values shift upfield. Possibly the most important feature evident is that the rhodium containing clusters exhibit

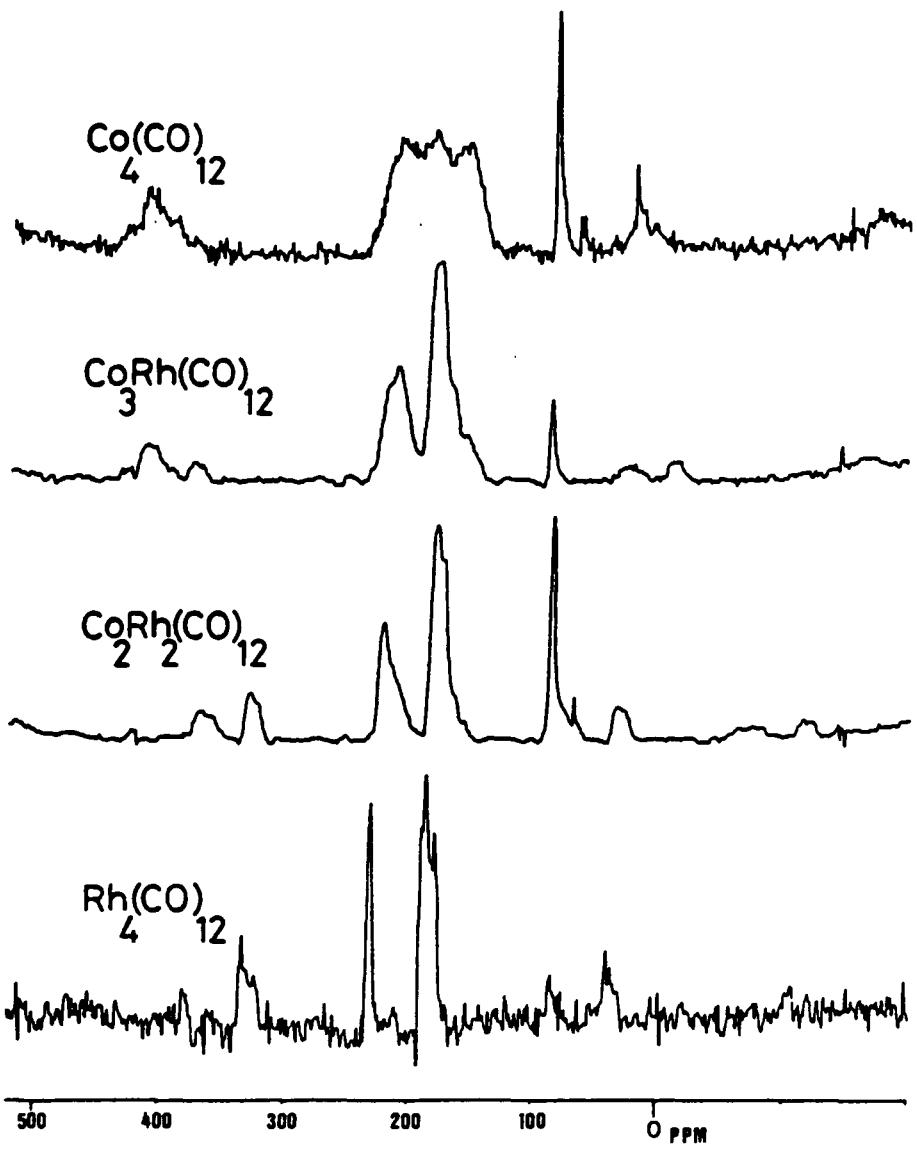

Figure 19. Ambient temperature ^{13}C NMR spectra for the tetranuclear clusters: The asterisk indicates the rotor material and the chemical shift reference, delrin. All spectra were observed with proton decoupling.

distinguishable bridging and terminal carbonyl signals, but $Co_4(CO)_{12}$ has anomalous carbonyl signals.

To determine if intermolecular or intramolecular exchange was the mechanism responsible for the carbonyl exchange observed by MAS NMR spectroscopy, an experiment using mass spectrometry was undertaken. A sample of ^{13}CO enriched $Co_4(CO)_{12}$ was examined by mass spectrometry. This indicated an enrichment of approximately 34% in ^{13}CO. An isotopically normal sample of $Co_3Rh(CO)_{12}$ (1:1 $\%^{13}CO$) was also examined by mass spectroscopy. A 1:1 mixture of the two solids was prepared by pulverizing and mixing in a mortar.

Two portions were taken from this mixture. These two portions, plus samples of the enriched $Co_4(CO)_{12}$ and of the $Co_3Rh(CO)_{12}$, were placed in separate sealed capillary tubes under N_2. The samples of pure $Co_4(CO)_{12}$ and $Co_3Rh(CO)_{12}$ did not melt at temperatures in excess of 75°C in the melting point apparatus. One of the samples of the 1:1 mixture was placed in the melting point apparatus and heated to 75°C for 1/2 hour.

Both of the samples of the 1:1 mixture (the one which had been heated to 75°C and the one which had not) were analyzed by mass spectrometry. The sample of the 1:1 mixture that had not been heated showed an enrichment of 1.9% in $Co_3Rh(CO)_{12}$, showing that the mass spec. experiment allows some intermolecular exchange during the electron impact ionization of the clusters in the spectrometer. The sample of the 1:1 mixture that had experienced the 75°C temperature showed a total enrichment of 2.6% ^{13}CO in $Co_3Rh(CO)_{12}$, which was significantly more than in isotopically normal $Co_3Rh(CO)_{12}$.

Significantly, the level of enrichment of $Co_3Rh(CO)_{12}$ in the heated 1:1 mixture was not as high as would be expected, if equilibration of carbonyls, as observed by ^{13}C MAS NMR spectroscopy at 75°C for both clusters, was occurring by intermolecular exchange. The enrichment level of ^{13}CO in $Co_3Rh(CO)_{12}$ was only 2.6%, and the expected value should be in the 10-20% enrichment level range. The ^{13}CO enrichment level of 2.6% in this sample does show that some intermolecular exchange is occuring at elevated temperatures, but that intermolecular exchange is not the process observed by ^{13}C MAS NMR spectroscopy. Thus the carbonyl exchange process must be due to intramolecular exchange.

Mechanism for Dynamic Behavior in the Solid State

Significantly, $Co_2(CO)_8$ is fluxional in the solid state at ambient temperature. Any proposed mechanism for carbonyl exchange must be consistent with the observed crystal structure. Importantly, there is no disorder in the x-ray crystal structure of $Co_2(CO)_8$.[61] It is not known if vibrations of metal atoms can occur so as not to be revealed by x-ray crystallography. Also it is not known if it is possible for carbonyl ligands to exchange between crystallographically observed sites even though this seems highly unlikely.

For the molecule $Fe_3(CO)_{12}$, however, evidence confirms that it is the movement of the Fe triangle within the carbonyl ligand cage that is the mechanism which exchanges carbonyls.[11 62] Since there is no crystal structure disorder observed for $Co_2(CO)_8$, our results seem to support the theory of ligand movement instead as the exchange mechanism in $Co_2(CO)_8$. This may be false.

The x-ray crystal structure of $Co_4(CO)_{12}$ exhibits a disorder as discussed previously, and the molecule does have dynamic behavior in the solid state. Significantly, $Rh_4(CO)_{12}$, does not exhibit dynamic behavior in the solid state, and neither does it have an x-ray crystal structure disorder.[63] Upon comparing the solid state NMR spectra at variable temperatures of the entire series of tetranuclear clusters, it can be noticed that the more rhodium nuclei in the cluster, then the higher the temperature must be, to see the fast exchange spectrum. The carbonyl fast exchange spectrum of $Co_4(CO)_{12}$ is at 63°C, for $Co_3Rh(CO)_{12}$ at 80°C, $Co_2Rh_2(CO)_{12}$ shows collapse of the carbonyl signals at 61°C but a fast exchange spectrum can not be reached, and finally, $Rh_4(CO)_{12}$ shows no dynamic behavior. Thus this trend could also be interpreted and explained by the fact that rhodium nuclei are larger and are harder to move in the crystal lattice than the much smaller cobalt and iron nuclei.

As discussed in each subsection of this chapter, it has been noticed that solution dynamics do not correspond to dynamic mechanisms possible in the solid state. Carbonyl exchange in solution has been postulated to be due to ligand polytopal (or polyhedron) expansion or by rotation of faces of these polyhedrons corresponding to rotation of ligands on an $M(CO)_3$ group. It is significant that the mechanisms in solution do, however, imply that concomitant movement of the metal atoms in the cluster does occur. This is true except for processes such as face rotation where only a single metal is involved.

Figure 20 shows the ambient temperature ^{13}C CP-MAS NMR spectrum of $Co_2(CO)_6DPM$, which had been enriched in ^{13}CO. The large central spike is the signal for the rotor material and external chemical shift standard delrin, at 89.3

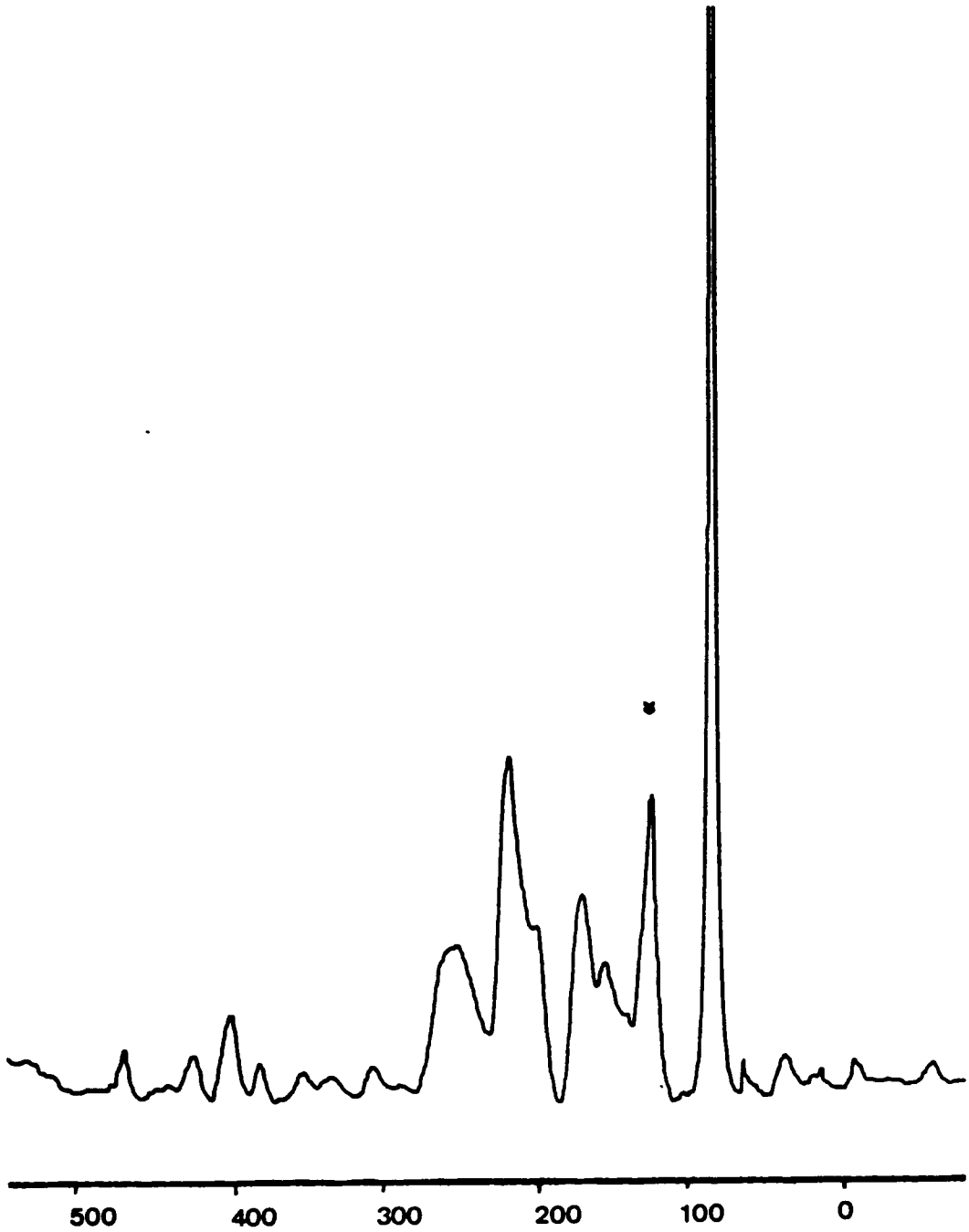

Figure 20. Solid state ^{13}C NMR of $Co_2(CO)_6DPM$: This spectrum was taken at ambient temperature and shows a bridging carbonyl resonance at 261 ppm. The chemical shift reference is delrin; the asterisk designates aromatic carbons.

ppm. The next most downfield signal at 130.5 ppm is assigned to the aromatic carbons of the DPM ligand which possesses four phenyl rings. All of the rest of the signals, except for the spinning side bands, are assigned to the six carbonyl ligands in $Co_2(CO)_6DPM$. The largest of these peaks, and only second to the delrin signal in intensity overall, is the signal at 223.9 ppm. This is obviously a terminal carbonyl signal, as well as the signal at 205.4 ppm, which is a shoulder on this intense signal. The signals at 176.6 ppm and 162.4 ppm seem anomalous as far as solution NMR spectroscopy is concerned, but it seems to be a trend in cobalt carbonyls in the solid state to give signals anomalously upfield in ^{13}C MAS NMR spectroscopy, just as exemplified by $Co_2(CO)_8$ and $Co_4(CO)_{12}$. Possibly these may be explained by a ^{59}Co-^{13}C coupling which form a complex ^{13}C NMR signal pattern, confused even further and broadened by more than one ^{59}Co nucleus.

Of extreme interest, however, is the presence of the broad signal at 261.8 ppm which is one of the first conclusive pieces of evidence for a bridging carbonyl in any cobalt carbonyl as detected by solid state ^{13}C MAS NMR spectroscopy. This fact alone may have implications in the correct postulation of a fluxional process for the carbonyl exchange as seen by solid state NMR spectroscopy. The bridging carbonyl signals have a ratio of approximately 1:3 with the observed terminal carbonyl signals from 223.9 ppm to 162.4 ppm. The spinning rate, as determined by the distance from the most intense signal at 223.9 ppm to the largest spinning side band at 404.3 ppm, is 4.1 KHz.

The question inevitably arises "why does $Co_2(CO)_6DPM$ exhibit bridging carbonyl signals at 260 ppm, but $Co_2(CO)_8$ and $Co_4(CO)_{12}$, which have been

shown to have bridging carbonyls by x-ray crystallography and IR spectral data, show no true evidence for bridging carbonyls with their most downfield signals at 213 ppm and 220 ppm respectively?" The answer may be simply that $Co_2(CO)_6DPM$ is static in the solid state, and even more so at ambient temperature than $Co_2(CO)_8$ and $Co_4(CO)_{12}$ are at low temperatures. This is due to the bis phosphine bridge, which serves to lock the cobalt-cobalt bond into place in the rigid crystalline lattice.

Thus, in $Co_2(CO)_6DPM$ the bridging bidentate phosphine DPM stops Co-Co metal atom movement, and in the binary metal carbonyls, such as $Co_2(CO)_8$ and $Co_4(CO)_{12}$, the metal cluster seems to be free to move or vibrate in the strictly carbonyl cage. This dynamic movement may or may not be indicated by x-ray crystallography.

To determine if intramolecular or intermolecular carbonyl exchange was the dominant mechanism involved in this carbonyl exchange in tetranuclear clusters, a mass spectroscopy experiment was attempted. This experiment showed that intermolecular exchange can and does occur at slightly elevated temperatures for $Co_4(CO)_{12}$ and $Co_3Rh(CO)_{12}$ at least, if not $Co_2Rh_2(CO)_{12}$, and $Rh_4(CO)_{12}$, which were not examined in this experiment. Since the expected enrichment of approximately 10-15% of $Co_3Rh(CO)_{12}$ did not occur, but only an enrichment level of 2.6% was attained, then the equilibration of the carbonyls of $Co_3Rh(CO)_{12}$ and $Co_4(CO)_{12}$ did not occur at 75°C. in a half hour. Thus the carbonyl exchange mechanism observed and detected by solid state ^{13}C NMR spectroscopy must be intramolecular exchange. Even so, at higher temperatures (above 40°C) $Rh_4(CO)_{12}$ does show loss of a signal resolution as can be seen in

Figure 18, where at these higher temperatures the fine signal structure is replaced by a broad signal. This may be due, in fact to intermolecular exchange.

A carbonyl ligand can bind to a cluster in many ways with a smooth variation from the terminal mode, to semibridging, to asymmetric bridging to symmetric bridging. With such a variable system no atom by atom assignment of bonds can be meaningful. More meaningful is a simple assumption that the CO ligands are bonded not to a single metal atom but to the metal core of the compound as a whole.

Lauher has developed and improved the surface force field model for the simulation of ligand structures in transition metal carbonyl clusters.[64] The model is actually a molecular mechanics simulation of ligand structures, but significant structures are still obtained. Preferred bonding of a carbonyl ligand to a metal atom was modeled in part by defining a sphere about the metal atom with a radius equal to the minimum of the potential well corresponding to the bond between the metal atom and the carbon atom of the carbonyl ligand (1.75A°). In this model a single carbonyl would be free to move about the surface of the sphere with no change in energy, but movements perpendicular to the surface of the sphere would require energy.

The global minimum in the $M_4(CO)_{12}$ system, as described by Lauher,[64] appears to correspond to a third isomer that has not been observed experimentally. This isomer has T symmetry and can be constructed by taking the Td isomer and by rotating or twisting in a concerted manner each $M(CO)_3$ unit about the local threefold axis. The T isomer has never been found experimentally for a $M_4(CO)_{12}$ compound, but is should be noted that the crystal structure of

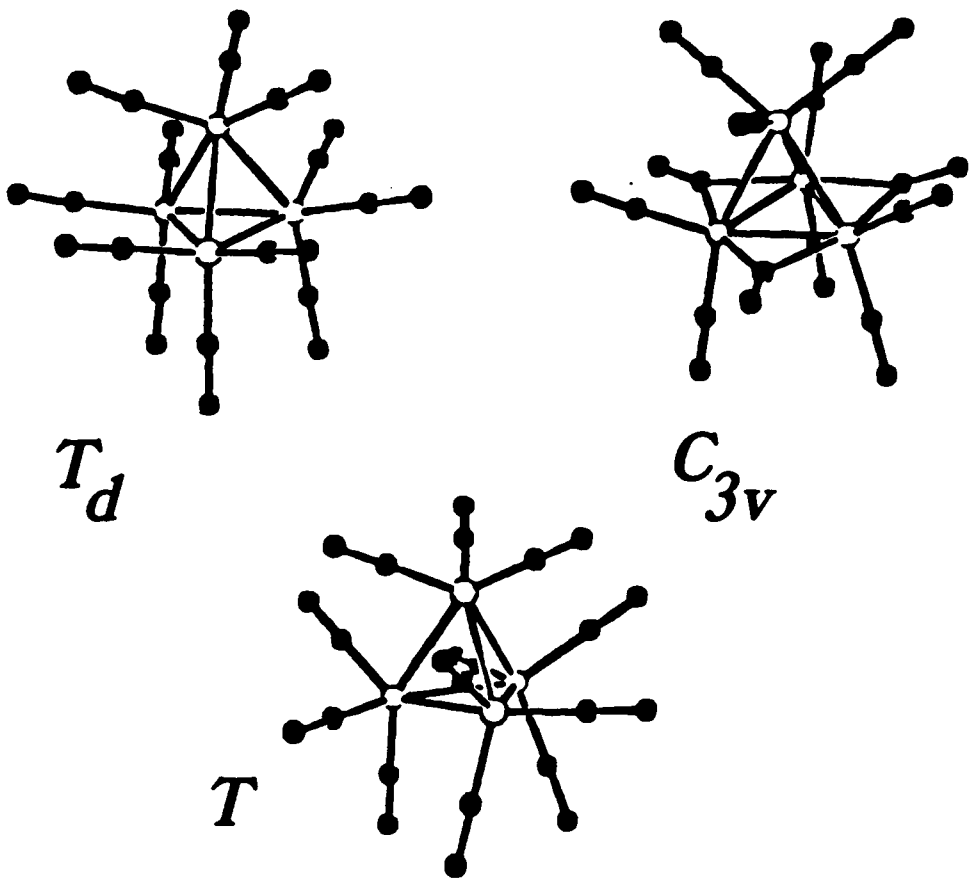

Figure 21. **Structural isomers for $M_4(CO)_{12}$:** The representations of the structural isomers of C_{3v}, T, and T_d symmetry are shown here. Carbonyl scrambling may occur via the T isomer in fluxional processes for $M_4(CO)_{12}$.

$Ir_4(CO)_{12}$, normally quoted as having Td symmetry, actually shows a slightly twisted molecule with C_3 site symmetry.

The carbonyl packing in the calculated T isomer corresponds to a distorted icosahedron and the C_3v isomer can be converted into the T isomer by a rotation of about 12° of the M_4 metal core within the carbonyl polyhedron. These isomers can be seen in Figure 21.

Carbonyl scrambling in $Co_4(CO)_{12}$ has been hypothesized to proceed via an intermediate with Td symmetry, but an interconversion via the T isomer would require less movement of the carbonyls and would seem to be a lower energy pathway. Also, $Co_4(CO)_{12}$ has the shortest metal-metal bonds and the lowest calculated steric energies of all the clusters studied by Lauher.

Johnson has also proposed that a mechanism similar to that of $Fe_3(CO)_{12}$ (Fe triangle migration within the ligand polyhedron) could be considered for $Rh_4(CO)_{12}$.[53] The Rh_4 tetrahedron could be considered to "wobble" within the icosahedron to produce a species with no CO bridges but retaining an icosahedral arrangement of ligands, and therefore different to the $Ir_4(CO)_{12}$ type of polyhedron.

In the next chapter of this dissertation the study of cobalt dimers, the "A-Frame" complexes, is presented. The goal of that work was to show the role of DPM in the fluxional behavior of cobalt carbonyls. The purpose was to ascertain the fact that DPM forces the cobalt clusters and dimers to become more rigid and presumably stop metal atom movement even in solution.

CHAPTER 4. SYNTHESIS AND REACTIVITY OF COBALT "A-FRAME" TYPE DIMERS

This chapter contains a discussion of the chemistry of cobalt carbonyl dimers which contain not one, but two bisphosphine ligands. As discussed in Chapter 1, cobalt carbonyl dimers containing a single bisphosphine ligand are fluxional on the NMR time scale, but the dynamic process is so fast that cooling these molecules down to low temperature (-80°C) does not freeze out a static structure. Further substitution of carbonyl ligands by phosphines may slow down the dynamic process and give clues to fluxional behavior in cobalt carbonyl dimers. This search for clues was the goal of examining the fluxional behavior of the more highly substituted cobalt dimers.

The cobalt carbonyl phosphine dimer **1** was studied to see if further substitution could be accomplished by using phosphine and phosphite ligands. Experiments showed that substitution by monodentate phosphine and phosphites could not be achieved. Further substitution does not occur possibly because the DPM ligand donates so much electron density to the metal atoms that replacement of any more carbonyl ligands, which act to reduce electron density on metal atoms by backbonding, is not favored.

It was found previously[37] that addition of I_2 to compound **1**, in an attempt to form a simple oxidation product, gave a compound of molecular formula $Co_2(CO)_3(DPM)_2I_2$. This compound contained bridging and terminal carbonyls and was postulated to have the structure shown schematically below.

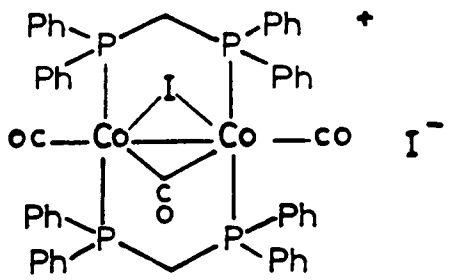

The presence of bridging and terminal carbonyl ligands indicated that fluxional behavior could possibly occur in this molecule. The presence of two bridging bidentate ligands would place restrictions on fluxional behavior that the original dimers $Co_2(CO)_6DPM$ and $Co_2(CO)_8$ do not have. Therefore, this chapter is a discussion of the synthesis and characterization of cobalt carbonyl dimers containing two bridging bidentate ligands and includes an investigation into the possible fluxional behavior of this new type of cobalt complex.

Historical

Transition metal dimers linked by two or more bridging bidentate ligands are a large and important class of molecules.[28] Compounds that fit into this class include multiply bonded dimers such as $Re_2Cl_4DPM_2$,[65] and $Mo_2Cl_4DPM_2$,[66] and "A-frame" molecules of Rh, Ir, Pd, Pt containing the $M_2(\mu\text{-}X)L_2$ moiety such as $[Rh_2(CO)_2(DPM)_2Cl]^+$,[67] $Rh(CO)_2(DPM)_2S$,[68] and $[Pd_2(DPM)_2Me_2Cl]^+$.[69] The A-frame molecules of Rh, Ir, are well known to coordinate reversibly small molecules in a bridging position. Also, the reactivity of certain complexes may

serve as models for the water-gas shift reaction.[70] The use of the ligand DPM has played an important role in the development of this chemistry. Important features of the DPM ligand are its availability and stability which make it ideal for exploratory syntheses. More recently reports of work have appeared using the methyl derivatives of DPM, namely bis(dimethyl)phosphinomethane, DMM[71] and dimethylphosphino-diphenylphosphinomethane, DMPM.[72]

Incorporation of two or more bridging bis phosphines into a cobalt carbonyl dimer is not an easy task and with the ligands used in this study, direct reaction of $Co_2(CO)_8$ or $Co_2(CO)_6$(L-L) with bis phosphines at ambient temperature does not lead to any binuclear products containing two of the bidentate ligands. For DPM, this lack of reactivity may be due in part to the steric bulk of the phosphine; however, the same result is obtained for DMM, which has a smaller steric bulk due to the smaller methyl substituents. King et al.[73] have synthesized dimers with the formula $Co_2(L\text{-}L)_5$ and $Co_2(L\text{-}L)_3(CO)_2$ (where L-L = F_2PNRPF_2). However, fluorophosphine ligands are more reactive towards metal carbonyls than DPM or DMM and thus yield the more substituted products; e.g., $Co_2(CO)_2(L\text{-}L)_3$.

It is interesting to note that the molecules $Co_2(CO)_4$(μ-acetylene) DPM can accept another DPM ligand to give analogs of $Co_2(CO)_2$(μ-acetylene) $(L\text{-}L)_2$ (where L-L = DPM, DAM) in which two bridging phosphine ligands are present.[35] Thus it seems that for Co° dimers a bridging acetylene type ligand can absorb a greater amount of donated ligand electron density from backbonding than can two bridging carbonyl ligands. Because of the great steric bulk and

unavailability of empty coordination sites, the molecules $Co_2(CO)_2(\mu\text{-acetylene})(L\text{-}L)_2$ are static in solution.

Experimental

All reactions were performed under an atmosphere of dry nitrogen. Solvents were either distilled from NaK benzophenone or dried over molecular series and purged with N_2 before use. Dicobalt octacarbonyl was purified by sublimation and used immediately. Carbon-13 and phosphorous-31 NMR spectra were recorded on an IBM WP200. All ^{13}C enriched compounds were synthesized from $Co_2(CO)_8$ enriched to 15-18% in ^{13}CO.

$[Co_2(CO)_2(\mu\text{-CO})(\mu\text{-I})(DPM)]^+I^-$, 8. A solution of 5.05g (7.5×10^{-3}mol) of $Co_2(CO)_6$ DPM and 2.93g (7.6×10^{-3}mol) DPM in 20ml of dry THF was treated dropwise with a solution of 1.9g (7.5×10^{-3}mol) of I_2 in 20 ml of THF. Evolution of CO gas was vigorous. When the addition was complete and evolution of CO gas barely noticeable, the flask containing the reaction mixture was equipped with a reflux condenser under slow N_2 purge and lowered into an oil bath. When heated to 70-80°C more CO gas was produced as well as the red precipitate of product. After 12 hours at 80°C the solution was cooled. The product was filtered and washed twice with 15 ml of hexane. The reddish brown microcrystalline powder was dried under vacuum and stored under N_2 (Yield 7.5g, 81.3%).

$Co_2(CO)_2(\mu\text{-CO})(\mu\text{-I})(DMM)(DMM)]^+I^-$, 9. A solution of 1.0g (2.37×10^{-3}mol) of $Co_2(CO)_6$ DMM and 0.91g (2.38×10^{-3}mol) of DPM in 20 ml of dry

THF was treated dropwise with stirring with a solution of 0.60g (2.37×10^{-3}mol)of I_2 in 2 ml of THF. When evolution of CO gas had ceased, the flask was equipped with a reflux condenser and heated with an oil bath at 85°C for 12 hours. The solution was allowed to cool under N_2 and then 30ml of toluene was added to the solution. The mixture was cooled to 0°C for a few hours and the product obtained upon filtration. The red brown crystalline product was washed with pentane, dried under vacuum and stored under N_2 (Yield 1.34g, 58.33%).

$Co_2(CO)_2(\mu\text{-}CO)(\mu\text{-}S)(DPM)_2$, 10. A solution of 0.437g (6.5×10^{-4} mol) of $Co_2(CO)_6(DPM)$, 0.250g (6.5×10^{-4}mol) of DPM, and 0.21g (6.5×10^{-4}mol) of elemental S in 30 ml of 1:1 THF/Benzene was heated to 65°C for 2½ hours. The solution was cooled and filtered at ambient temperature. Then 20 ml of pentane was added to the solution which was then cooled at 0° overnight. The solution formed dark red crystals of the product which were filtered, washed with a small amount of cold pentane and dried under vacuum. (Yield 0.47g, 72%). Anal. Calcd. for $C_{43}H_{44}Co_2O_3P_4S$: C, 63.48; H, 4.42; P, 12.35; 0, 4.78; S, 3.19. Found C, 63.60; H, 4.44; P, 12.29; O, 4.79; S, 3.22.

X-ray structure determination of 9. Crystals of **9** suitable for an x-ray structure determination were obtained by recrystallization from a methylene chloride solution. Data collection and structure refinement were performed by the Molecular Structure Corporation. Relevant experimental data are given in Appendix 1.

$Co_2(CO)_3DPM_2$,11 by reduction with Zn. A 100 ml flask was charged with mossy Zn, 1 g of $Co_2(CO)_3DPM_2I_2$ powder and a magnetic stir bar. This was placed under nitrogen followed by addition of 300 ml of distilled acetonitrile which formed a slurry. After approximately an hour, the reaction mixture exhibited a

yellow-green color as the microcrystalline $Co_2(CO)_3DPM_2I_2$ reacted. After 2 days of stirring the green microcrystalline powdery product was filtered off. The powder was washed with pentane and dried under vacuum. The particles of Zn are virtually impossible to separate from the green product except manually, as the green product is insoluble except in THF, and CH_2Cl_2 in which it decomposes rapidly. Yield ≅ 50-60%.

$Co_2(CO)_3DPM_2$,11 by reduction with Na/Hg amalgam. In order to produce the green dimer without the presence of Zn this reaction was attempted. In a 100 ml flask was placed 2 ml of Hg and 0.04 g (1.74×10^{-3} moles) of Na metal and a stir bar. When amalgamation was complete, 1 g of $Co_2(CO)_3DPM_2I_2$(4.1×10^{-4} moles) was placed on the amalgam under N_2 atmosphere. To this was added 20 ml of dry THF which formed a slurry with the cobalt dimer. Within 15 minutes the stirred solution-slurry turned a green color. After 30 minutes the green powder could be seen in the flask. The solution was filtered at this point to obtain the green product. Yield ≅10%. Anal. Calcd. for $C_{53}H_{44}Co_2O_3P_4$: C, 65.58; H, 4.53; P, 12.77. Found: C, 63.42; H, 4.98; P, 10.56.

Reaction of 11 with CO. In a 100 ml flask was placed 0.3 grams of compound **11** under N_2 This was slurried in 15 ml of dry THF. Through a serum stopper a long needle connected to a carbon monoxide source was placed in the flask. The flask was also connected to an oil bubbler to monitor the carbon monoxide flow. After 10 minutes, the slurry had changed into a reddish colored solution with some evidence of metallic particles. The solution was filtered under N_2 and analysis by ^{31}P NMR spectroscopy and infrared spectroscopy confirmed the presence of $Co_2(CO)_6$ DPM, as well as the anion $Co(CO)_4^-$. Infrared spectros-

copy also showed the presence of a small amount of an unidentified complex with a carbonyl stretching frequency at 1740 cm^{-1}.

Results and Discussion

The synthesis of the compounds $Co_2(CO)_3DPM_2I_2$,**8**, $Co_2(CO)_3(DMM)(DPM)I_2$,**9**, and $Co_2(CO)_3$ DPM_2S,**10**, is best described as an oxidative trapping reaction. It was noted previously that compound **8** could be synthesized in low yield from the reaction of $Co_2(CO)_6(DPM)$ with I_2. The presence of two equivalents of DPM in the product suggested that some $Co_2(CO)_6(DPM)$ is sacrificed in this reaction and that the liberated DPM traps and stabilizes the cobalt (I) dimer. Indeed, if the reaction is performed in the presence of free DPM, yields of greater than 70% are routinely obtained. The dimer $Co_2(CO)_6DMM$ may also be oxidized in this fashion to introduce the second phosphine.

$$Co_2(CO)_6(L - L) + I_2 + DPM \rightarrow [Co_2(CO)_3(L - L)(DPM)I]I \qquad (8)$$

L - L = DPM 8

L - L = DMM 9

Conductivity measurements, infrared spectroscopy, as seen in Table VII, elemental analysis, and comparison with known rhodium analogs led to the assignment of an A-frame type structure for compound **8** with a neutral ligand, in this case CO, occupying the second bridging site.[37]

Table VII. Infrared Carbonyl Stretching Frequencies. (a)

Complex	Terminal CO	Bridging CO
$Co_2(CO)_3(DPM)_2I^+I^-$	1988(s), 1944(vs)	1816(m)
$Co_2(CO)_3(DMM)(DPM)I^+I^-$	1972(s); 1950(vs)	1812(m)
$Co_2(CO)_3(DPM)_2S$	1959(s), 1948(vs)	1779(m)
$Co_2(CO)_3(DPM)_2$	1935(s), 1900(vs)	1750(s)
$Rh_2(CO)_3(DPM)_2Cl^+BPh_4^-$(b)	1992(s), 1977(vs)	1863(s)
$Rh_2(CO)_3(DPM)_2$(c)	1940, 1920	1835

(a) in cm^{-1}

(b) Reference 35

(c) Reference 74

(d) intensities are (s) strong, (vs) very strong, (m) medium

It should be noted that DPM has been the only effective trapping ligand. The bridging bidentate ligand, DMM, the chelating ligand $Ph_2PCH_2CH_2PPh_2$(diphos), and triphenylphosphine all do not react to yield an isolable product when used in place of DPM in equation 8. Thus the synthetic route taken must have as variables either L-L, or the oxidant, which in equation 8 is I_2.

Other reagents such as Br_2 or Cl_2 are more powerful oxidants than I_2 and attack the original dimer **8** to give Co^{2+}salts. Sulfur, selenium and tellurium seem to be ideal candidates for this oxidation process for several reasons. First, they are not as electrophilic as are the halogens. Secondly it is easier to work with elemental S, Se, and Te as compared to elemental Cl_2 or Br_2. Lastly, the product molecules if formed, would be neutral and not salts if the reaction were 1:1 between the cobalt dimer and the chalcogen used.

In addition to the oxidation of $Co_2(CO)_6$DPM by I_2, it is also possible to effect an oxidation by elemental sulfur in the presence of DPM as a trapping agent. Elemental analysis and spectroscopic data are consistent with the following formulation for this compound, $Co_2(CO)_2(\mu\text{-}CO)(\mu\text{-}S)(DPM)_2$. Tables VII and VIII compare the relevant spectroscopic data for compounds **8-10**. A bridging carbonyl is observed by infrared spectroscopy for compound **10**(υCO = 1772 cm^{-1}).

Table VIII. ^{13}C and ^{31}P NMR Data.

	^{13}C (a)		^{31}P (b)
Complex	Bridging CO	Terminal CO	
$Co_2(CO)_3(DPM)_2I^+I^-$	239.46	199.35	51.5
$Co_2(CO)_3(DMM)(DPM)I^+I^-$	239.77	202.50	46,41
$Co_2(CO)_3(DPM)_2S$	249.22	211.83	48.3
$Co_2(CO)_3(DPM)_2$	--	--	36.95

(a) chemical shifts in ppm from TMS

(b) chemical shifts in ppm from 85% phosphoric acid (ext. ref.)

The synthesis is shown below in equation 9.

$Co_2(CO)_6DPM + DPM + S \rightarrow$ 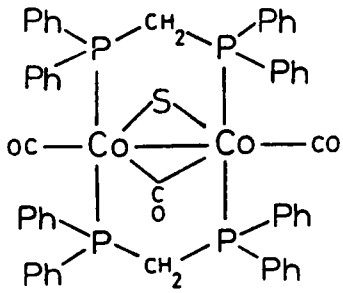 (9)

Thus the Co^{1+} complex $Co_2(CO)_3DPM_2S$,**10** is in very good yield. Synthesis of the complexes containing Se or Te were not attempted.

Unlike compounds **8** and **9** which are 1:1 salts, compound **10** is neutral due to the presence of S^{2-} in place of I^-. It is proposed that compound **10** has a structure similar to compound **9**, as shown schematically. Compound **10** is a neutral complex and is therefore more readily soluble in organic solvents such as $CHCl_3$, THF, as well as benzene, in which the analogous salts are not soluble.

In the ^{31}P NMR spectrum of compound **10**, the signal at 48.3 ppm is more upfield than the signal of compound **8**, and the CO stretching frequencies of the carbonyls of compound **10** are lower than those of compound **8**. This indicates greater electron density on the cobalt atoms of compound **10** due to the greater donating ability of the sulfido group (S^{2-}) in compound **10** over that of the iodo group (I^-) in compound **8**.

Crystal Structure of $[Co_2(CO)_3(DMM)(DPM)I]^+$, 9

X-ray diffraction quality crystals of **9** were obtained by slow evaporation of a concentrated methylene chloride solution under a nitrogen atmosphere. The relevant crystallographic data for this compound is summarized in Appendix Table I. A perspective drawing of the molecule along with the numbering scheme employed is shown in Figure 22. Atomic coordinates and selected bond distances and angles are listed in Appendix Tables 2 and 3.

The crystal structure for **9** confirms the trans-bisphosphine arrangement as previously postulated. Also the Co-Co distance, 2.555(2) A, is consistent with a single bond between the metals. This is only slightly longer than observed in $Co_2(CO)_8$, 2.525 A.[74 75] Simple electron counting arguments, of course, predict a bond order of one for both $Co_2(CO)_8$ and compounds **8** and **9**. The molecular structure of **9** is thus very similar to that of the related rhodium complex $[Rh_2(CO)_3(DPM)_2Cl]^+$.[23]

As seen from the data in Appendix Table 3, the Co_2I moiety forms a nearly equilateral triangle (the internal angles are 57.8, 61.3, and 60.9°). All three carbonyl ligands lie essentially in the same plane as the Co_2I triangle. The terminal carbonyls are bent just very slightly away from the bridging iodide; the average Co-Co-CO angle is 166.1°.

The Co-P bond distances for the DPM ligand are 2.241(3) and 2.236(3)A. These are significantly longer than the Co-P bond distances for the DMM ligand; i.e., 2.219(3) and 2.217(3)A. The bis phosphine, DMM, thus forms the stronger bond to the cobalt atoms in this complex.

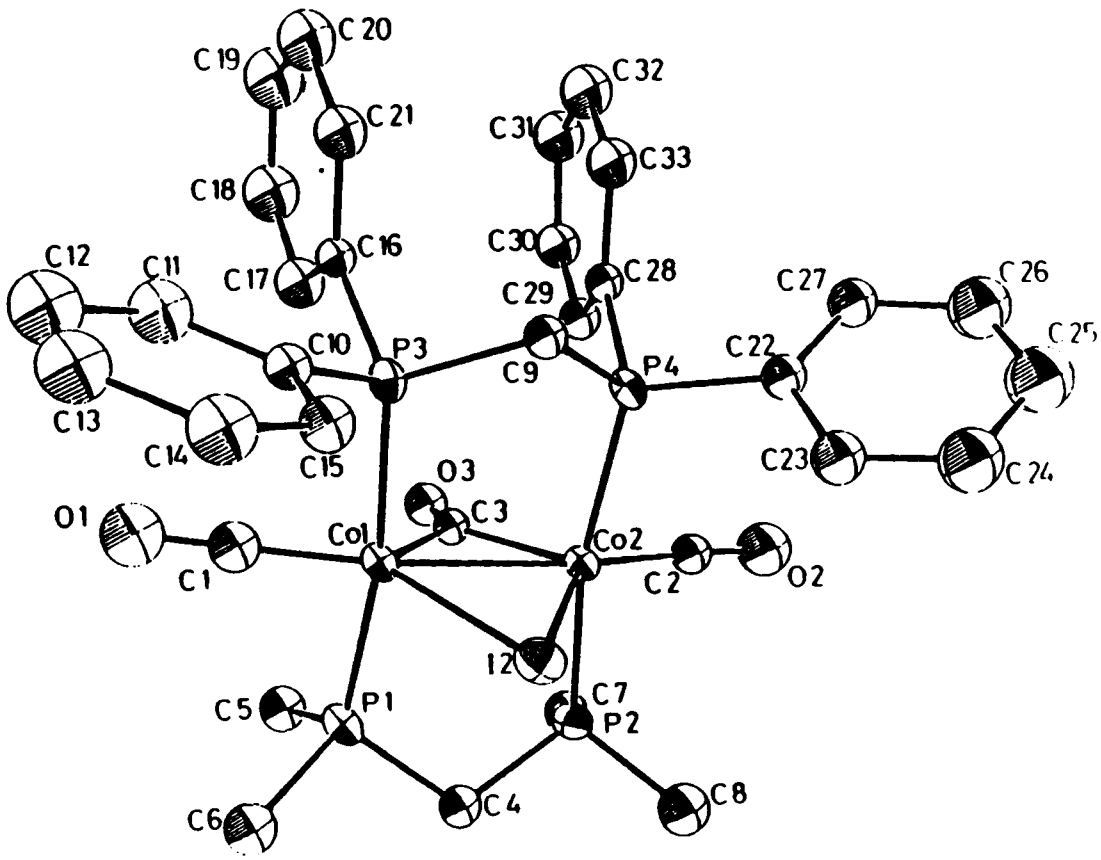

Figure 22. X-ray crystal structure of $Co_2(CO)_3(\mu\text{-}I)(DMM)(DPM)^+$: The perspective drawing and numbering scheme are shown.

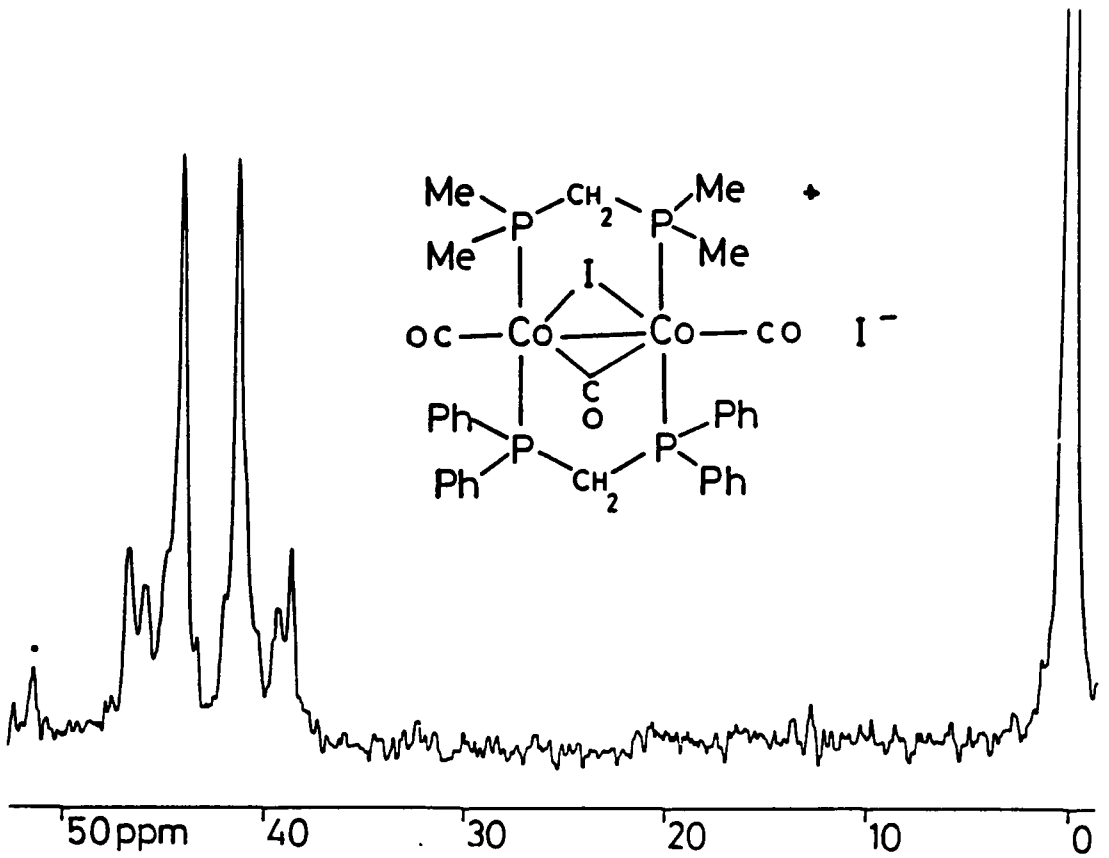

Figure 23. The ^{31}P NMR spectra for $Co_2(CO)_3(\mu\text{-}I)(DMM)(DPM)^+$: The solvent is $CDCl_3$, the internal chemical shift reference is 85% H_3PO_4. The complex multiplet centered around 42 ppm shows an approximate AA'BB' pattern. The small peak designated with an asterisk is $Co_2(CO)_3DPM_2I_2$.

In Figure 23 is shown the ^{31}P NMR spectrum of **9** at ambient temperature. This compound exhibits a complex but very symmetrical splitting pattern in this spectrum. This corresponds approximately to an AA′ BB′ pattern where coupling between phosphorus nuclei must occur through the cobalt atoms. Because of the broadening effect of the quadrupolar ^{59}Co nuclei, all of the expected transitions for an AA′ BB′ pattern are not seen. The main point to be derived from Figure 23 is that a dynamic process is not occuring in **9** to exchange carbonyls.

The ^{13}C NMR data for **8** and **9** support this claim. Table VII shows the ^{13}C NMR data for the "A-Frame" molecules **8** and **9**. The spectrum of compound **8** shows bridging and terminal carbonyl resonances at 199.35 ppm and 239.46 ppm respectively, with an expected ratio of 1:2. The spectrum of compound **9** shows bridging and terminal carbonyl resonances with a ratio of 1:2 also. The observance of bridging and terminal carbonyl resonances proves conclusively that a dynamic process is not occurring in these molecules. This may be due to the fact that there are no empty coordination sites available for the carbonyl ligands to utilize in a fluxional process. Evidence to support this fact is shown by the crystal structure of compound **9**, which is coordinatively saturated around the cobalt atoms.

It was realized that fluxional behavior of these complexes was not important because of the extreme rigidity of these Cobalt "A-Frame" complexes. Of more importance was the reactivity of these cobalt dimers compared to the rhodium, iridium dimers, etc., because of the completely different reactivity exhibited by the cobalt dimers.

Solution Chemistry of $Co_2(CO)_3(DPM)_2I_2$, 8

Complex **8** is quite unreactive in solution to substitution by a number of reagents such as acetylenes, CO, H_2, phosphines, and alkenes. This is shown in the schematic below.

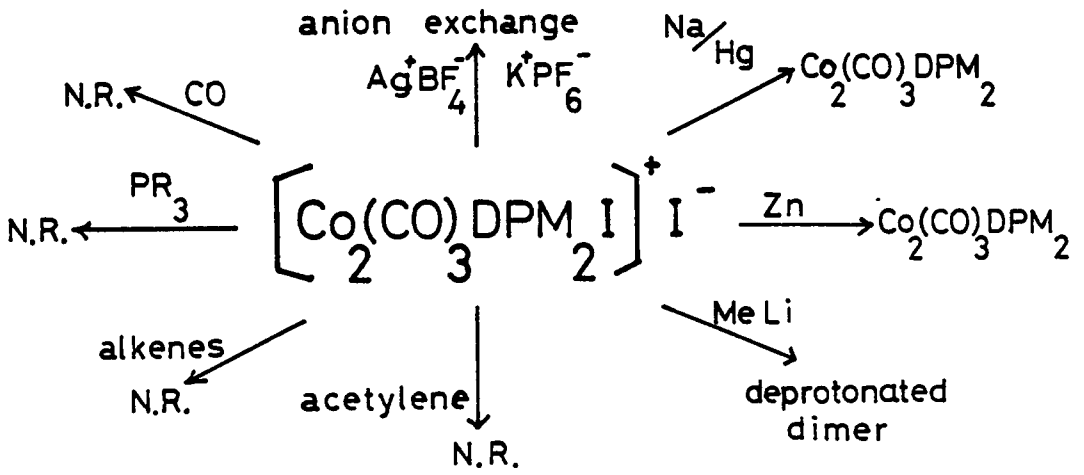

The reactions were performed with a stoichiometry of 1:1 at ambient temperature and only the starting material **8** was retrieved from the mixtures. Carbon monoxide gas was bubbled through a CH_2Cl_2 solution of 1 and no reaction was evident. As expected, anion exchange of I^- with the reagents $Ag^+BF_4^-$ and $K^+PF_6^-$ can be accomplished in a straightforward fashion by adding solutions of the salts together. The bridging DPM ligand will, however, undergo deprotonation of its methylene carbon with either n-butyl or methyl lithium to give a soluble neutral complex as seen in eqn. 9.

$Co_2(CO)_3(DPM)_2I_2 + MeLi \rightarrow$

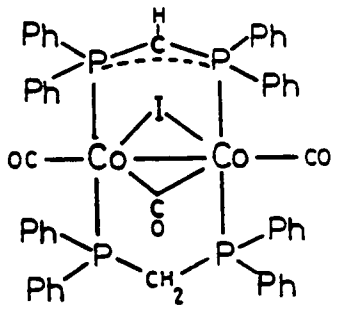

This neutral complex was identified by its characteristic AA'BB' pattern in the ^{31}P NMR spectrum and by its infrared spectrum.

It was imagined that a very novel and possibly important molecule of Co° instead of Co^{1+} could be synthesized by using the cobalt "A-Frame" complexes. A simple reduction using Na/Hg amalgam could be employed in the following reaction as shown schematically below:

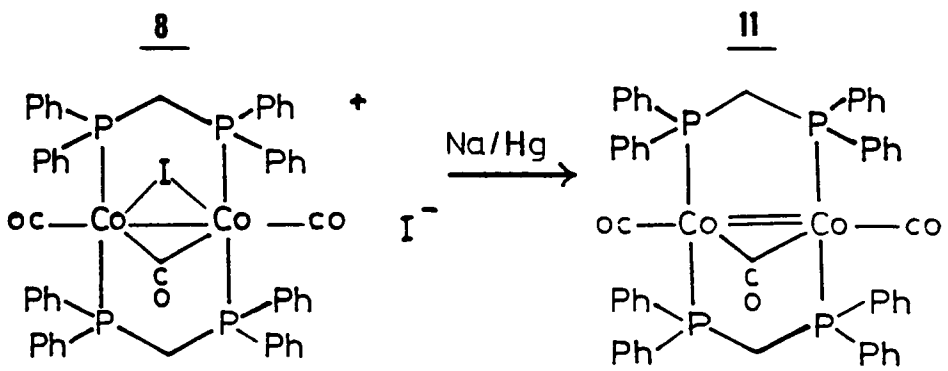

This synthesis was attempted and is described in more detail in the experimental section of this dissertation. Similarly the reduction using a milder reducing agent, Zn, was established.

When **8** and excess Zn (granular or mossy) are stirred in acetonitrile at ambient temperature, an emerald green powder is obtained within a few hours. This powder, which analyzes approximately for $Co_2(CO)_3(DPM)_2$, **11**, is insoluble in

most solvents, and is barely soluble in THF. The powder reacts with halogenated hydrocarbon solvents such as CH_2Cl_2 and $CHCl_3$ to give a number of as yet uncharacterized products (as seen by ^{31}P NMR spectroscopy and solution IR spectroscopy). Furthermore, compound **11** is pyrophoric in air in the solid state showing its great reactivity. It reacts readily with I_2 in THF to give **8** again. Also, compound **11** in a THF slurry will react with CO gas to give the dimer $Co_2(CO)_6$ DPM, the ionic salt [$Co(CO)_3$ DPM$^+$ $Co(CO)_4^-$], and some free DPM (all are seen by ^{31}P NMR spectroscopy and solution IR spectroscopy). This can be seen in the schematic diagram shown below.

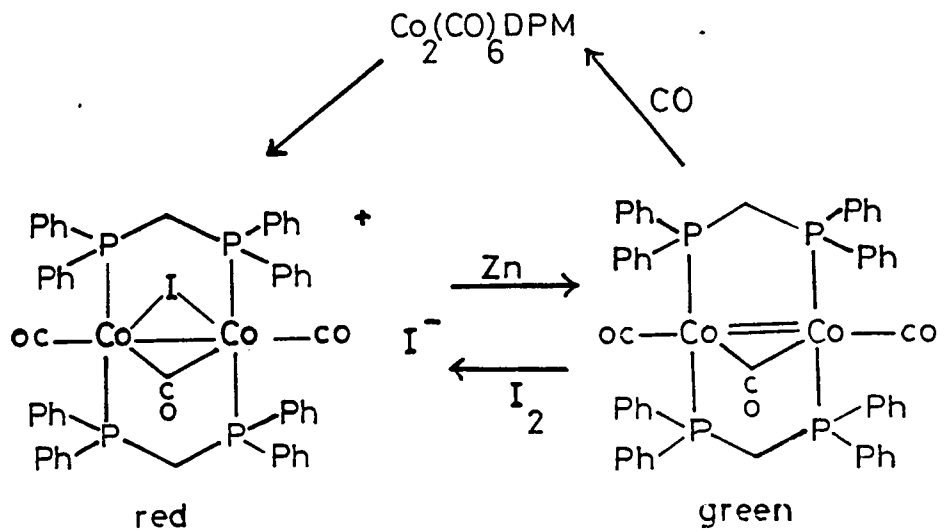

The ^{31}P NMR spectrum of compound **11** in THF solution shows a peak at 36.4 ppm which is upfield of that of compound **8**. The infrared spectrum is very similar to compound **8** but the carbonyl stretching frequencies are shifted to a lower frequency, also indicating more electron density on the cobalt complex. The analogous rhodium complex, $Rh_2(CO)_3(DPM)_2$,[76] has been structurally character-

ized and has a distinctly non "A-frame" structure with DPM ligands which are not in trans postions. The cobalt complex **11** however, is virtually insoluble; whereas, $Rh_2(CO)_3(DPM)_2$ is soluble in acetone and other solvents.

Unfortunately, because of the insolubility of this cobalt dimer, $Co_2(CO)_3DPM_2$, which should have a vacant coordination site, could not be examined in solution for fluxional behavior. The attempt to produce the molecule $Co_2(CO)_2(\mu\text{-}CO)_2DPM_2$ was a failure because the reaction of **11** with carbon monoxide produced predominantly the original dimer **1**. It is important to note that the compound **9** will not undergo a reaction with Zn. Thus the molecule $Co_2(CO)_2(\mu\text{-}CO)(DMM)(DPM)$, the analog of **11**, could not be formed. As far as a study of the fluxional nature of cobalt dimers was concerned, this study showed only that these molecules seem to be extremely rigid.

Attempts to produce Co° dimers with two bridging bis phosphines instead of Co^{+1} dimers were unsuccessful. However, the chemistry of these new type of cobalt compounds is interesting, and potential synthetic applications may be in the future for these compounds.

CHAPTER 5. CONCLUSIONS

This chapter is a discussion of the conclusions that can be drawn from the results obtained in this study on the dynamic behavior of cobalt and rhodium clusters in both solution and the solid state. The goal of this dissertation was to examine the dynamic behavior of the tetranuclear clusters $Co_4(CO)_{12}$, $Rh_4(CO)_{12}$ and their derivatives, by restricting pathways for dynamic processes, but in a manner which would allow carbonyl exchange on the NMR time scale (10^{-6} to 10^{-10} seconds) as a result.

The restrictions were imposed by two methods. The first method was exemplified in Chapter 2. In that chapter, it was shown that the bisphosphine ligands DPM, DMPM, and DMM restrict the carbonyl scrambling pathway in solution which was described by Benfield and Johnson[53] as a polytopol rearrangement. The authors conceded that results on the fluxionality of the tetranuclear clusters that had been obtained, for example $Rh_4(CO)_{12}$, could not disprove the contention that movement of the metal nuclei tetrahedron may be sufficient to scramble carbonyl ligands (as seen by solution NMR spectroscopy).

The second method for restricting carbonyl scrambling was examined in detail in Chapter 3. This method focused on the contention that metal atom movement may play an important role in understanding the fluxional behavior of binary metal carbonyls and possibly of substituted derivatives by studying their solid state ^{13}C NMR spectra.

It seems likely that any movement of the tetrahedron of metal atoms in a tetranuclear complex would be in such a way that all of the metal atoms would maintain the same place relative to each other, so that the metal tetrahedron remains intact. This motion of the entire tetrahedron unit could be described as a wobble as suggested by Johnson,[53] or by a rotational process as postulated in Chapter 3. Furthermore, the work performed by Lauher[64] indicates that another isomer, of T symmetry, can be derived from a parent C_{3v} complex by movement or rotation of the M_4 metal core by about 12° within the carbonyl polyhedron.

All three of the above mentioned mechanisms for metal atom movement have some problems. Johnsons wobble tetrahedron is not well defined, but yet it is appealing because it is easy to imagine a tetrahedron moving in such a way. Johnson also predicted that the ligand cage of carbonyls need not expand if $Rh_4(CO)_{12}$ was the molecule in question.[53] The calculations made by Lauher[64] lend theoretical evidence to the proposition that the ligand cage need not expand in order for the carbonyl ligands to become equivalent. His calculations show that the isomer of T symmetry should be more stable than the isomer of C_{3v} symmetry, and that all of the carbonyl ligands in the isomer of T symmetry are terminally bound and chemically equivalent. Unfortunately, no real examples of a tetranuclear cluster of T symmetry, with carbonyl and phosphine ligands, have been found. Since there are apparent similarities in the proposals made by Johnson and Lauher, then their proposed mechanism can be considered to be virtually the same.

The mechanism postulated in Chapter 3 actually is very similar to the mechanism described by Johnson and Lauher. At temperatures above 30°C in the

solid state, reorientation of the metal tetrahedron must be fast on the NMR time scale in order for carbonyls to become equivalent.

The variable temperature solid state ^{13}C NMR spectra of the binary metal carbonyls shown throughout Chapter 3 indicate that the compounds containing the relatively small nuclei, iron and cobalt, show dynamic processes with smaller activation energies than those of clusters which contain the larger rhodium nucleus. All of these molecules except for $Rh_4(CO)_{12}$ show dynamic behavior as evidenced by their solid state ^{13}C NMR spectra. Since carbonyl ligands cannot move within the crystalline lattice to an extent sufficient to render bridging and terminal carbonyls equivalent, then the dynamic behavior observed for the binary metal carbonyls must be described as metal atom movement within the carbonyl cage. The tetranuclear clusters that contain rhodium show a higher coalescence temperature in their NMR spectra with increasing rhodium content. The cluster $Rh_4(CO)_{12}$ does not exhibit dynamic behavior in the solid state, thus it must be concluded that the rhodium M_4 tetrahedron is too large to move within the carbonyl cage.

Similarly, metal atom movement can be slowed down by using phosphine ligands such as DPM. In both solution (Chapter 1) and in the solid state (Chapter 3), NMR techniques can be used to observe that the ligand DPM slows down the dynamic behavior of the molecule $Co_2(CO)_6$DPM on the NMR time scale.

For the tetranuclear clusters studied in Chapter 2 of this dissertation, the presence of the phosphine ligands may have slightly hampered the dynamic process in solution but it still occurs in roughly the same temperature range (-90°C

to +30°C) as for the molecules $Co_4(CO)_{12}$ and $Rh_4(CO)_{12}$ in solution. From consideration of the postulated fluxional process, as discussed in Chapter 2 for the phosphine substituted tetranuclear clusters, a polytopal expansion mechanism would not rule out the possibility of metal atom movement. However, the $M_4(CO)_9$(tripod) compounds (with M = Co or Rh) do not exhibit fluxionality for all carbonyl ligands, but only for the ones on the apical metal atom.[54] As mentioned in Chapter 2, this data indicates that the fluxional process in solution is due to the dynamic behavior of the metal tetrahedron. Thus, the tripod ligand "locks" the ligand polyhedron onto the basal metal atoms and keeps them from moving enough to exhibit dynamic behavior in solution. It may be that the tripod ligand inhibits fluxionality by simply keeping any of the basal metal atoms from becoming an apical type metal atom, with no bridging carbonyl ligands.

In solution, the carbonyl ligands are able to move and the ligand polyhedron can expand from an icosahedron into a cubooctahedron and this process exchanges carbonyls. However, in the solid state, the expansion of the ligand polyhedron is not allowed and neither is movement of the carbonyl ligands, because of the restraints imposed by the crystal lattice. Thus, the mechanism for dynamic behavior observed in the solid state for metal carbonyls must be described as metal atom movement within a ligand cage.

In general, phosphine ligands force a cluster to have a higher activation energy for the dynamic process, due to superior metal phosphine bonds which are stronger and more rigid than M-CO bonds. This is certainly true in solution, and in the solid state these phosphine ligands may force the metal atoms to be more rigid than their binary metal carbonyl analogues and completely stop the dy-

namic process. This is the case observed for $Co_2(CO)_6DPM$ in the solid state, as discussed in Chapter 3.

It must be noted that the dynamic process occurs at higher temperatures for binary metal carbonyls in the solid than when in solution. Intuitively this makes sense, because it would take less energy to move carbonyls in solution, than it would to move a metal cluster in the solid state.

The cobalt "A-Frame" complexes $Co_2(CO)_3(DPM)I_2$, $Co_2(CO)_3(DMM)(DPM)I_2$, and $Co_2(CO)_3(DPM)_2S$ were synthesized but show no dynamic behavior in solution. The crystal structure of $Co_2(CO)_3(DMM)(DPM)I_2$ shows that the "A-Frame" complex is coordinatively saturated around the cobalt atoms. Thus, these molecules are relatively inert, and show no evidence of carbonyl scrambling.

APPENDIX

Table I. Crystal Data for Compound 9

C33 H36 Co2 I2 O3 P4

F.W. 976.22 F(000) = 1912

Crystal dimensions: 0.10 x 0.20 x 0.25 mm

Peak width at half-height = 0.30°

Mo Kα radiation (λ = 0.71073 A)

Temperature = 23 ± 1°

Monoclinic space group P2-1/n

a = 18.956 (3) A b = 15.881 (6) A c = 21.393 (5) A

β = 97.20 (2) °

V = 3692.8 A³

Z = 4 ρ = 1.76 g/cm³

μ = 28.3 cm-1

Instrument:	Enraf-Nonius CAD4 diffractometer
Monochromator:	Graphite crystal, incident beam
Attenuator:	Zr foil, factor 20.7
Take-off angle:	2.8°
Detector aperture:	2.0 to 2.4 mm horizontal
	2.0 mm vertical
Crystal-detector dist.:	21 cm
Scan type:	w-θ
Scan rate:	4 - 20°/min (in omega)
Scan width, deg:	0.7 + 0.350 tan θ
Maximum 2θ:	45.0°
No. of refl. measured:	5165 total, 4796 unique
Corrections:	Lorentz-polarization
Solution:	Direct methods
Hydrogen atoms:	Not included
Refinement:	Full-matrix least-squares
Minimization function:	Σw(|Fo|-|Fc|)²
Least-squares weights:	4Fo²/σ²(Fo²)
"Ignorance" factor:	0.060
Anomalous dispersion:	All non-hydrogen atoms

Table II. Atomic Positions

Atom	x	y	z
I1	0.46381(9)	0.28320(6)	0.00214(5)
I2	0.15215(7)	0.19174(5)	0.33979(4)
CO1	0.0872(1)	0.0642(1)	0.26376(7)
CO2	0.3054(1)	0.0675(1)	0.32213(7)
P1	0.0032(3)	-0.0006(2)	0.3397(2)
P2	0.2593(3)	0.0078(2)	0.4099(1)
P3	0.1345(3)	0.1364(2)	0.1000(1)
P4	0.3885(3)	0.1323(2)	0.2449(1)
O1	-0.1374(9)	0.0204(7)	0.1872(5)
O2	0.5539(9)	0.0365(6)	0.3764(5)
O3	0.2313(7)	-0.0077(5)	0.2578(4)
C1	-0.046(1)	0.0382(9)	0.2184(6)
C2	0.452(1)	0.0486(8)	0.3532(6)
C3	0.217(1)	-0.0166(7)	0.2721(5)
C4	0.095(1)	0.0052(8)	0.4171(5)
C5	-0.023(1)	-0.1125(9)	0.3252(6)
C6	-0.146(1)	0.0402(9)	0.3569(6)
C7	0.313(1)	-0.1014(9)	0.4227(6)
C8	0.323(1)	0.0622(9)	0.4821(7)
C9	0.275(1)	0.1994(7)	0.1967(5)
C10	0.013(1)	0.2114(7)	0.1516(5)
C11	-0.071(1)	0.1852(9)	0.1015(6)
C12	-0.178(1)	0.2388(10)	0.0825(7)
C13	-0.192(1)	0.3107(9)	0.1145(7)
C14	-0.107(1)	0.3363(9)	0.1646(6)
C15	-0.002(1)	0.2839(8)	0.1831(6)

Table III. Selected Bond Distances (Å)and Angles (deg)

Atom 1	Atom 2	Distance	Atom 1	Atom 2	Atom 3	Angle
I2	Co1	2.639(1)	Co1	I2	Co2	57.80(4)
I2	Co2	2.649(1)	I2	Co1	Co2	61.30(4)
Co1	Co2	2.555(2)	I2	Co1	P1	90.54(9)
Co1	P1	2.219(3)	I2	Co1	P3	91.63(8)
Co1	P3	2.241(3)	I2	Co1	C	133.2(4)
Co1	C1	1.699(11)	I2	Co1	C3	108.5(3)
Co1	C3	1.911(9)	Co2	Co1	P1	95.72(9)
Co2	P2	2.217(3)	Co2	Co1	P3	94.83(8)
Co2	P4	2.236(3)	Co2	Co1	C1	165.5(4)
Co2	C2	1.683(11)	Co2	Co1	C3	47.6(3)
Co2	C3	1.896(9)	P1	Co1	P3	168.9(1)
P1	C4	1.828(10)	P1	Co1	C1	84.2(4)
P1	C5	1.821(12)	P1	Co1	C3	89.6(3)
P1	C6	1.834(11)	P3	Co1	C1	86.4(4)
P2	C7	1.841(12)	P3	Co1	C3	100.0(3)
P2	C8	1.831(12)	C1	Co1	C3	117.9(5)
P3	C9	1.834(10)	I2	Co2	Co1	60.90(4)
P3	C10	1.834(10)	I2	Co2	P2	88.97(8)
P3	C16	1.822(9)	I2	Co2	P4	94.95(8)
P4	C9	1.849(10)	I2	Co2	C2	131.7(4)
P4	C22	1.822(10)	I2	Co2	C3	108.6(3)
P4	C28	1.816(10)	Co1	Co2	P2	96.13(9)
O1	C1	1.166(12)	Co1	Co2	P4	95.19(8)
O2	C2	1.183(11)	Co1	Co2	C2	167.3(4)
O3	C3	1.185(10)	Co1	Co2	C3	48.1(3)
			P2	Co2	P4	168.5(1)
			P2	Co2	C2	84.1(4)
			P2	Co2	C3	91.3(3)
			P4	Co2	C2	85.3(3)
			P4	Co2	C3	97.6(3)
			C2	Co2	C3	119.3(5)
			Co1	P1	C4	114.2(3)
			Co1	P1	C5	113.6(4)
			Co1	P1	C6	116.3(4)
			Co2	P2	C4	114.4(3)
			Co2	P2	C7	115.2(4)
			Co2	P2	C8	114.2(4)
			Co1	P3	C9	113.4(3)
			Co1	P3	C10	111.5(3)
			Co1	P3	C16	117.9(3)
			Co2	P4	C9	111.7(3)
			Co2	P4	C22	112.3(3)
			Co2	P4	C28	116.8(3)
			Co1	C1	O1	180 (1)
			Co2	C2	O2	178.2(9)
			Co1	C3	Co2	84.3(4)
			Co1	C3	O3	137.3(8)
			Co2	C3	O3	138.1(8)
			P1	C4	P2	111.1(5)
			P3	C9	P4	106.4(5)

REFERENCES

1. Adams, R.D.; Cotton, F.A.; Chapter 12 in *"Dynamic Nuclear Magnetic Resonance Spectroscopy"*, Jackman, L.M.; Cotton, F.A.; eds., Academic Press, New York, (1975).
2. Cotton, F.A.; Danti, A.; Waugh, J.S.; Fessenden, R.W.. *J. Chem. Phys.* **1958**, *29*, 1427.
3. Meakin, P.; Jesson, J.P., *J. Am. Chem. Soc.* **1973** , *95* , 1344.
4. Berry, R.S., *J. Chem. Phys.* **(1960)**, *32* , 933.
5. Meakin, P.; Jesson, J.P., *J. Am.Chem. Soc.* **1974**, *96*, 5751.
6. English, A.D.; Ittel, S.D.; Tolman, C.A.; Meakin, P.; Jesson, J.P. *J. Am. Chem. Soc.* **1977**, *99*, 117.
7. Favez, R.; Roulet, R.; Pinkerton, A.A.; Schwarzenbach, D., *Inorg. Chem.* **1980**, *19*, 1356.
8. Domaille, P.J.; Wreford, S.S.; *Inorg. Chem.*, **1980**, 2188.
9. Hanson, B.E.; Ph.D. Thesis., Texas A & M University, 1978.
10. Ichikawa, M.; *J. Catal.* **1979**, *59(1)*, 67.
11. Dorn, H.C.; Hanson, B.E.; Motell, E.; *Inorg. Chim. Acta.*, **1981**, *54*, L71.
12. Hanson, B.E.; Sullivan, M.J.; Davis, R.J.; *J. Am. Chem. Soc.*, **1984**, *106*, 251.
13. Mond, L.; Hirtz, H.; Cowap, M.D., *J. Chem. Soc.*, **1910**, *798*.
14. Falbe, J., *J. Organomet. Chem.*, **1975**, *94*, 213.
15. Evans, G.O.; Pittman, C.U.; McMillan, R.; Beach, R.T.; Jones, R.; *J. Organomet. Chem.*, **1974**, *67*.

16. Fukumuto, T.; Matsumura, Y.; Okwara, R.; *J. Organomet. Chem.*, **1974,** *69,* 37.

17. Chia, L.S.; Chllen, W.R.; Franklin, M.; Manning, A.R. *Inorg. Chem.* **1975,** *14,* 2521.

18. Karsch, H.H.; Schmidbauer, H.;*Z. Naturforsch.*, **1977,** *32b,* 762-767.

19. Cheung, K.K.; La.; T.F.; Mok, K.S.; *J. Chem. Soc. (A),* **1971,** 1644.

20. Schmidbauer, H.; Mandl, J.R., *Angew. Chem. Int. Ed. Engl.*, **1977,** *16,* 640

21. Lee, C.; Hunt, C.T.; Balch, A.L.; *Inorg. Chem.* **1981,** *20,* 2498.

22. Pringle, P.G.; Shaw, B.L.; *J. Chem. Soc., Chem. Commun.*, **1982,** 581.

23. Cowie, M.; Mague, J.T.; Sanger, A.R. J. *Amer. Chem. Soc.*, **1978,** *100,* 11, 3628.

24. Dawkins, G.M.; Green, M.; Jeffery, J.C.; Stone, F.G.A.; *J.C.S. Chem. Commun.*, **1980,** 1120.

25. Sullivan, B.P.; Meyer, T.J.; *Inorg. Chem.*, **1980,** *19,* 2500.

26. Ferguson, G.; Laws, W.J.; Parver, M.; Puddephatt, *Organometallics,* **1983,** *2,* 276.

27. Mays, M.J.; Prest, D.W.; Raithby,P.R. J. *Chem. Commun.*, **1985,** 171.

28. Puddephatt, R.J.; *Chem. Soc. Rev.*, **1983,** 99.

29. Sinclair, R.A.; Burg, A.B; *Inorg. Chem.*, **1968,** *7,* 2160.

30.

    a. Cotton, F.A.; Roth, W. J. *Inorg. Chem.*, **1983,** *22,* 3654.

    b. Cotton, F.A.; Duraj. S. A.; Roth, W.J. *Inorg. Chem.*, **1984,** *23,* 4113.

31. Cotton, F.A.; Dura; S.A.; Falvello, L.R.; Roth, W.J.; *Inorg. Chem.* **1985,** *24,* 4389.

32. Novikova, Z.S.; Prishchenko, A.A.; Lustenko, I.F. *Zh. Obshch. Khim.* **1977,** *47,* 775.

33. Karsch, H.H.Z. Naturforsch, B; *Anorg. Chem.,Org. Chem.* **1983,** *38 B,* 1027.

34.

a. Harrison, W.; Trotter, J.; *J. Chem.Soc. A,* **1971,** 1607.

b. Cullen, W.R.; Crow, J.; Harrison W.; Trotter, J.; *J. Amer. Chem. Soc.,* **1970,** *92,* 6339.

c. Thornhill, D. J.; Manning, A. R.; *J. Chem. Soc., Dalton Trans.,* **1973,** 2086.

35. Bird, P.H.; Fraser, A.R.; Hall, D.N.; *Inorg. Chem.,* **1977,** *16,* 8, 1924.

36. Balch, A.L.; *Homogeneous Catal. Met. Phosphine Complexes,* **1983,** 239.

37. Hanson, B.E.; Fanwick, P.E.; Mancini, J.S.; *Inorg. Chem.,* **1982,** *21,* 3811.

38. Hanson, B.E.; Mancini, J.S.; *Organometallics,* **1983,** *2,* 126.

39. Laws, W.J.; Puddephatt, R.J.; *J. Chem. Soc. Chem. Commun.,* **1983,** 1020.

40. Absi-Halabi, M.; Atwood, J.D.; Forbus, N.P.; Brown, T.L.; *J. Amer. Chem. Soc.,* **1980,** *102,* 6248.

41. Forbus, N.P.; Brown, T.L.; *Inorg. Chem.,* **1982,** *20,* 4343.

42. Shaw, B.L.; *J. Organomet. Chem.,* **1980,** *200,* 307.

43. Puddephatt, R.J.; Thomson, M.A.; Manojlovic-Muir, L.J.; Muir, K.W.; Frew, A.A.; Brown, M.P.; *J. Chem. Soc., Chem. Comm.,* **1981,** 305.

44. Meek, D.W.; Mazanec, T.J.; *Acc. Chem. Res.* **1981,** *14,* 266.

45. Huq, R.; Poe, A.; *J. Organomet. Chem.,* **1982,** *226,* 277.

46. Carre, F.H.; Cotton, F.A.; Frenz, B.A.; *Inorganic Chem.,* **1976,** *15,* 381.

47. Foster, D.F.; Nicholls, B.S.; Smith, A.K.; J. *Organomet. Chem.*, **1982**, *236*, 395.

48. Wilkinson, G.; Stone, F.G.A.; Abel, E.W. eds; *Comprehensive Organometallic Chemistry*, Vol. 5, Pergamon Press Ltd. (**1982**).

49. Evans, J.; Johnson, B.F.G.; Lewis, J.; Matheson, T.W.; *J. Am. Chem. Soc.*, **1975** *97*, 1245.

50.

a. Cotton, F. A.; Kruczynski, Li; Shapiro, B.L.; Johnson, L.F.; J. *Chem. Soc.*, **1972**, *94*, 6191.

b. Evans, J.; Johnson, B.F.G.; Lewis, J.; Norton, J.R.; Cotton, F.A.; J. *Chem. Soc., Chem. Commun.*, **1973**, 807.

51. Darensbourg, D.J.; Incorvia, M.J.; *Inorg. Chem.*, **1981**, *20*, 1914.

52. Cotton, F.A.; *Inorg. Chem.*, **1966**, *5*, 1083.

53. Johnson, B.F.G.; Benfield, R.E.; *J. Chem. Soc. Dalton Trans.*, **1978**, 1554.

54. Bahsown, A.A.; Osborn, J.A.; *Organometallics*, **1982**, *1*, 9, 1114.

55.

a. Yannoni, C.S.; *Acc. Chem. Res.*, **1982**, *15*, 201.

b. Fyfe, C.A.; *"Solid State NMR for Chemists,"* **1983**, CFC Press, Guelph.

c. Andrew, E.R.; *Prog. Nucl. Magn. Reson. Spectrosc.*, **1971**, *8*, 1.

56. Dorn, H.C.; Hanson, B.E.; Motell, E.; J. *Organomet. Chem.*, **1982**, *224*, 181.

57. Vanderhart, D.; Ph.D. Thesis, University of Illinois, 1967.

58. Cotton, F.P.; Hanson, B.E.; *Inorg. Chem.*, **1978**, *17*, 3237.

59. Wei, C.H.; Dahl, L.F.; *J. Am. Chem. Soc.*, **1969**, *91*, 1351.

60. Desiderato, R.; Dobson, G.R.; *J. Chem. Ed.*, **1982**, *59*, 752.

61. Sumner, G.F.; Klug, H.P.; Alexander, L.E. *Acta Crystallogr.* **1964**, *17*, 732.

62. Gleeson, J.W.; Vaughan, R.W. *J. Chem. Phys.* **1983**, *78*, 5384.

63. Wei, C.H.; Wilkes, G.R.; Dahl, L.F.; *J. Am. Chem. Soc.*, **1967**, *89*, 4792. Lauher, J.W.; *J. Am. Chem. Soc.*, **1986**, *108*, 1521.

64. Hanson, B.E.; Fanwick, P.E.; Mancini, J.; *Inorg. Chem.*, **1982**, *21*, 3811.

65. Puddephatt, R.J.; *Chem. Soc. Rev.*, **1983**, 99.

66. Barder, T.J.; Cotton, F.A.; Lewis, D.; et al.; *J. Am. Chem. Soc.*, **1984**, *106*, 2882.

67. Abbott, E.H.; Bose, K.S.; Cotton, F.A.; Hall, W.T.; Sekutowski, J.C.; *Inorg. Chem.*, **1978**, *17*, 3240.

68. Kubiak, C.P.;Eisenberg, R.; *J. Am. Chem. Soc.*, **1977**, *99*, 6129.

69. Cowie, M.; Dwight, S.R.; *Inorg. Chem.*, **1979**, *18*, 2700.

70. Cooper, S.J.; Brown, M.P.; Puddephatt, R.J.; *Inorg. Chem.*, **1982**:, *20*, 1374.

71.

a. Cowie, M.; Mague, J.T.; Sanger, A.R.; *J. Am. Chem. Soc.*, **1978**, *100*, 3628.

b. Kullberg, M.L.; Kubiak, C.P.; C_1 *Mol. Chem.*, **1984** ,*1*, 171.

72.

a. Kullberg, M.L.; Lemke, F.R.; Powell, D.R.; Kubiak, C.P.; *Inorg. Chem.*, **1985**, *24*, 3589.

b. McLennon, A.J.; Puddephatt, R.J.; *Organometallics*, **1985**, *4*, 485.

73. Lisic, E.C.; Hanson, B.E.; *Inorg. Chem.*, **1986**, *25*, 812.

74. King, R.B.; Gimeno, J.; Lotz, T.J.; *Inorg. Chem.*, **1978**, *17*, 2401.

75. Sumner, G.F., Klug, H.P.; Alexander, L.E.; *Acta Cryst.* **1964**, *17*, 732.

76. Leang, P.C.; Coppens, P.; *Acta Cryst. B.*, **1983**, *39*, 535.

77. Woodcock, C.; Eisenberg, R.; *Inorg. Chem.*, **1985**, *24*, 1285.

The vita has been removed from the scanned document